Spring 4-12-2018

EVALUATING THE EFFECTS OF CATASTROPHIC WILDFIRE ON WATER QUALITY, WHOLE-STREAM METABOLISM AND FISH COMMUNITIES

Justin K. Reale

Biology

Justin K. Reale

Candidate

Biology

Department

This dissertation is approved, and it is acceptable in quality and form for publication:

Approved by the Dissertation Committee:

Dr. Clifford N. Dahm, Chairperson

Dr. David J. Van Horn, Co-Chairperson

Dr. Thomas F. Turner

Dr. Ricardo González-Pinźon

EVALUATING THE EFFECTS OF CATASTROPHIC WILDFIRE ON WATER QUALITY, WHOLE-STREAM METABOLISM AND FISH COMMUNITIES

BY

JUSTIN KEVIN REALE

B.S., University of New Mexico, 2009

M.S., University of New Mexico, 2016

DISSERTATION

Submitted in Partial Fulfillment of the Requirements for the Degree of

Doctor of Philosophy

Biology

The University of New Mexico Albuquerque, New Mexico

May, 2018

ACKNOWLEGEMENTS

I would like to express my gratitude to my co-advisors, Drs. Dahm and Van Horn, for their mentoring, teaching and support throughout my dissertation. I also thank Drs. Turner and González-Pinźon for their willingness to serve on my committee. I acknowledge Cecilia Horner, Amy Louise, and Susan Bittick, as I would not have been able to complete my dissertation without your support. I would like to thank my friends for providing encouragement and support throughout this endeavor. To my family, Jamie, Aiden, Kevin, Sue and Chelsea, thank you for your love, encouragement, patience, and understanding.

EVALUATING THE EFFECTS OF CATASTROPHIC WILDFIRE ON WATER QUALITY, WHOLE-STREAM METABOLISM AND FISH COMMUNITIES

by

Justin Kevin Reale

B.S., University of New Mexico, 2009
M.S., University of New Mexico, 2016
Ph.D., University of New Mexico, 2018

ABSTRACT

This dissertation investigated the initial and multi-year effects of a catastrophic wildfire (Las Conchas fire in 2011) on adjacent and downstream aquatic ecosystems in comparison to pre-fire conditions. Specifically, the research looked at 1) multi-year water quality responses along the river continuum using data collected before, immediately after and for multiple years post-fire, 2) differential water quality and whole-stream metabolism responses of paired headwater catchments over multiple years after disturbance, and 3) fish communities at two sites on a larger river downstream of the extensive region impacted by the catastrophic wildfire. Overall, the research in this dissertation highlights the importance of long-term ecological data collection using advanced instrumentation that can be used to evaluate the effects of a changing climate and climate-mediated disturbances on water resources. Secondly, these studies emphasize the need to collect water quality and biological data at temporal and spatial scales that more effectively capture the hydrology and water quality dynamics of landscape-scale disturbances that are becoming more common and more destructive with climate change and growing human impingement on forested lands. Thirdly, this research highlights the importance of evaluating streamflow pathways, geomorphology, physiochemical properties with biogeochemical processes, and watershed-specific hydrologic connections within their landscapes prior to and following landscape-scale disturbance.

<h1 style="text-align:center">Table of Contents</h1>

Introduction

Watershed characteristics and processes control the structure and function of stream ecosystems. Landscape-scale disturbances within a watershed often alter local hydrologic and geomorphic characteristics, impacting physiochemical and biogeochemical characteristics and processes in adjacent streams. These effects can also propagate from the source, transported by hydrologic networks, impacting lotic ecosystems tens to hundreds of kilometers downstream of the initial disturbance. This dissertation investigated the initial and multi-year effects of a catastrophic wildfire (Las Conchas fire in 2011) on adjacent and downstream aquatic ecosystems in comparison to pre-fire conditions. Specifically, the research looked at 1) multi-year water quality responses along the river continuum using data collected before, immediately after and for multiple years post-fire, 2) differential water quality and whole-stream metabolism responses of paired headwater catchments over multiple years after disturbance, and 3) fish communities at two sites on a larger river downstream of the extensive region impacted by the catastrophic wildfire.

To further the understanding of the linkages among wildfire, streamflow pathways, and water chemistry, a network of water-quality sensors and streamflow gages were used to assess initial and long-term effects of wildfire along a river continuum. The water quality of a 3rd-order (East Fork Jemez River) and a 7th-order (Rio Grande at U.S. 550) stream in a single watershed for 5 monsoon seasons (i.e., June through September) before, during, and after a catastrophic wildfire was evaluated. The wildfire had significant and sustained long-term effects on both streams. In the 3rd-order stream, variability in dissolved O_2 (DO) increased after the fire with prominent DO sags. Precipitation trends were similar to pre-fire conditions, but episodic storm events resulted in significant increases in stream discharge that led to elevated turbidity and specific conductance (SC) following the fire. In the 7th-order stream, the wildfire led to elevated SC and greater variability of the DO signal with strong sags when fire scar material was in transport, in comparison to the pre-fire records. Water-quality data from a 2nd-order (Jaramillo Creek), 3rd-order (East Fork Jemez River), 4th –

1

order (Jemez River near Jemez Springs), and 7th order (Rio Grande at U.S. 550) along the river continuum over a four-month period before, during, and after the wildfire were also evaluated. Overland transport and debris-flow events in the 2nd- and 3rd-order streams resulted in elevated particles (e.g., soil, sediment, rock, ash, charcoal, and plant biomass) and solutes in transport that elevated turbidity and SC, and a dampened DO signal likely due to reduced stream metabolic rates (i.e., gross primary productivity and ecosystem respiration). Less pronounced post-fire effects in the 4th-order stream, possibly because of groundwater contributions and a higher stream gradient with a pool–riffle geomorphology increasing reaeration, were observed. Strong SC spikes, and strong DO decreases likely due to intensified chemical oxygen demand and/or biological oxygen demand, were documented in the 7th-order stream. The turbidity effects on the 7th order stream could not be assessed due to concentrations exceeding the sensor's maximum detection limit (i.e., 4000 NTU) prior to and following the wildfire. These findings determined that streamflow pathways, channel geomorphology, physiochemical properties, and biogeochemical processes all play a central role in the post-fire water quality responses along the river continuum. These findings also highlight the importance of collecting water-quality measurements at temporal and spatial scales that effectively capture the variable hydrological dynamics of the study sites.

Post-fire effects on hydrologic and geomorphic processes are known to alter the sediment loads and water quality of burned catchments and downstream riverine ecosystems. However, the lack of high-frequency and long-term data prior to and following a catastrophic wildfire limits our understanding of how ecosystem processes respond and recover over time. Nine years of high-frequency water quality parameters collected during the growing season before, immediately after, and for multiple years post-fire, combined with streamflow and meteorological records were analyzed. In addition, the variability of water quality parameters over time both pre-fire and post-fire were assessed for their effects on gross primary productivity (GPP) and ecosystem respiration (ER) in two nearly identical and paired headwater streams. Data from before (3 years of data) and after (6 years of data) the catastrophic wildfire were

analyzed. Pre-fire, a positive correlation between GPP and ER (r^2 >0.4) in the low-turbidity (< 10 NTU) streams was observed. Immediately following the wildfire, both streams had elevated turbidity (3 to 25x pre-fire) and specific conductance (2x pre-fire), > 20% reduction in GPP, < 10% reduction in ER, and positive correlations between GPP and ER (r^2 >0.6). This study found that the shorter-term (1 to 3 years post-fire) turbidity, GPP and ER estimates were different between the two streams, while the longer-term (4 to 5 years post-fire) responses showed that both systems had returned to near pre-fire conditions. To link our results with catchment hydrology, watershed, stream, and wildfire characteristics were analyzed. Paradoxically, the results suggest that the water quality and ecosystem responses (via metabolism) to the wildfire of these nearly identical streams were different and likely controlled by watershed-specific hydrologic connections (i.e., stream gradient and watershed slope) with their post-fire landscapes (i.e., burn severity and proximity to the burn scar). This variability resulted in a differential response in turbidity, which was found to negatively impact GPP and ER post-fire. Thus, accounting for catchment specificity remains a relevant, open challenge for predicting watershed-scale effects of wildfire disturbances on aquatic ecosystems.

The effects of wildfire on coldwater fish communities in headwater streams within, or in close proximity to the burned areas are well known; however, few studies have evaluated the effects of a catastrophic wildfire on downstream fish assemblages. Long-term fish community survey data with supporting high-frequency water quantity and quality data were analyzed prior to and following the Las Conchas fire at two sites on the Rio Grande (i.e., 7th order) that were > 20 km downstream of a major wildfire. The effects of a >1000-year rain event and subsequent flood (during year 3 post-fire) on the fish community in a post-fire environment was also evaluated. Prior to the fire, moderate between-site overlap in commonly detected and abundant species was observed. There was also considerable seasonal and interannual variability in the fish community at both sites. Small episodic DO sags were documented prior to the fire, although concentrations remained greater than 5.5 mg L^{-1} throughout the year. During the first three years post-fire, we observed multiple severe DO sags (< 3 mg L^{-1}) in both

reaches. A reduction in total fish abundance, diversity, and evenness, was observed post-fire in the upstream community. In contrast, the community at the downstream site appeared to be generally unaffected by the effects from the fire. Following a major flood event in 2013, a further reduction in total and species-specific fish abundance was observed at the upstream site. While total and species-specific abundance, diversity and evenness remained unchanged at the downstream site immediately following the large flood. At the upstream site, two native cyprinids, which were commonly collected both pre- and post-fire, were absent during each of the first three surveys after the 2013 flood event, and only a single individual of each species was collected in the fourth survey following the flood event. In contrast, a non-native catastomid was detected in each of the four surveys immediately after the flood at the upstream site, and this species exhibited similar seasonal trends pre- and post-fire years. Consistent with previous studies, the differential post-fire and post-flood response at the two sites with similar community composition and flow regime can be attributed to 1) the proximity and quantity of fire-impacted watersheds upstream and 2) non-natives' tolerance to harsh abiotic conditions, along with habitat generalist classification. These results highlight the need to evaluate watershed-specific hydrologic, water quality, and biotic responses to fully assess the impacts of wildfire on downstream aquatic ecosystems.

Forested watersheds throughout the western United States are currently experiencing warmer temperatures, larger spring and fall vapor pressure deficits, less snow and more rainfall, and extended fire seasons. Wildfire activity has increased during each decade since the 1970s. These trends are forecast to grow worse in the coming decades given forecasted increases in air temperature and aridity. Catastrophic forest fires with higher intensities, larger areas burned, and longer durations are likely future outcomes. This investigation shows how a large and high intensity wildfire impacts water quality, ecosystem processes, and biotic communities in the stream and river network affected by a large and high-intensity fire. These findings also demonstrate the importance of collecting long-term chemical and ecological data at time scales that effectively capture the ecohydrological dynamics of the watershed prior to and following major watershed-scale disturbances.

THE EFFECTS OF CATASTROPHIC WILDFIRE ON WATER QUALITY ALONG A RIVER CONTINUUM

Authors: Justin K. Reale [1,2,4], David J. Van Horn [1,5], Katherine E. Condon [3,6], Clifford N. Dahm[1,7]

[1] Department of Biology, University of New Mexico, Albuquerque, New Mexico 87131 USA
[2] US Army Corps of Engineers, Albuquerque, New Mexico 87109 USA
[3] Valles Caldera National Preserve, Jemez Springs, New Mexico 87025 USA

E-mail addresses: [4]justin.k.reale@usace.army.mil; [5]vanhorn@unm.edu; [6]kcondon@vallescaldera.gov; [7]cdahm@sevilleta.unm.edu

Abstract

To further our understanding of the linkages among wildfire, stream flow pathways, and water chemistry, we used a network of water-quality sensors and streamflow gages to assess initial and long-term effects of wildfire along a river continuum. We assessed pre- and postfire water quality of a 2nd- and a 4th-order stream in a single watershed for 5 monsoon seasons before, during, and after a catastrophic wildfire. Our findings documented that fire had significant and sustained long-term effects on both streams. In the 2nd-order stream, variability in dissolved O_2 (DO) increased after the fire. Daily total precipitation was unchanged, but episodic storm events resulted in significant increases in stream discharge that led to elevated turbidity and specific conductance (SC). In the 4th-order stream, fire led to minimal measurable effects on turbidity, elevated SC, and greater variability of the DO signal. We also assessed water-quality data from 4 sites along the river continuum for a 4-mo period before, during, and after the wildfire. Large overland and debris-flow events in the 1st- and 2nd-order streams resulted in elevated particles (e.g., soil, sediment, rock, ash, plant biomass) and solutes in transport that elevated turbidity and SC and

dampened the DO signal. We documented less severe post-fire effects in the 3rd-order stream probably because of groundwater contributions and a higher stream gradient with a pool–riffle geomorphology. We observed nominal changes in turbidity, strong SC spikes, and strong DO decreases in the 4th-order stream. Streamflow pathways, geomorphology, physiochemical properties, and biogeochemical processes play a central role in the postfire water-quality response along the river continuum. Our findings highlight the importance of collecting water-quality measurements at temporal and spatial scales that effectively capture hydrological dynamics.

Introduction

Forests in the western USA have a 'fire deficit' linked to synergistic effects of fire suppression, landuse change, and ongoing climate change (Marlon et al. 2012). The combination of elevated winter temperature and associated reduced spring snow accumulation (Cayan et al. 2001, Mote et al. 2005), reduced winter precipitation minus evaporation (Seager et al. 2007), greater frequency and duration of droughts (Seager et al. 2007), earlier spring snowmelt (Cayan et al. 2001, Stewart et al. 2004), and greater vapor-pressure deficit in the warm season (Williams et al. 2012) has amplified the stress on western US forests and has led to an increase in fire frequency and intensity in the southwestern USA (Westerling et al. 2006, Allen et al. 2010). Widespread and high-intensity wildfires cause considerable hydrologic and geomorphic changes in affected watersheds (DeBano 2000, Shakesby and Doerr 2006) including extreme floods and debris flows (Neary et al. 2002, Pausas et al. 2009) with serious implications for water quality, drinking water sources (Writer and Murphy 2012, Bladon et al. 2014), and aquatic ecosystems (Bisson et al. 2003, Romme et al. 2011).

Specific wildfire-induced water-quality effects are numerous. Increased sediment loading from fire negatively affects stream and river channels (Malmon et al. 2007, Smith et al. 2011, Goode et al. 2012, Moody et al. 2013) by elevating in-stream turbidity levels (Rhoades et al. 2011, Oliver et al. 2012, Sherson et al. 2015). Ash inputs

6

and elevated erosion also increase the transport of major ions and elevates postfire specific conductance (SC) values (Earl and Blinn 2003, Lyon and O'Connor 2008, Dahm et al. 2015) and in-stream nutrients (Spencer and Hauer 1991, Oliver et al. 2012, Miller et al. 2013, Sherson et al. 2015). Decreases in dissolved O_2 (DO) to hypoxia (<2 mg/L) also have been observed (Verkaik et al. 2013, Dahm et al. 2015, Sherson et al. 2015).

Previous investigators have used discrete or event-driven sampling methods to document the negative effect of wildfire on water quality (Townsend and Douglas 2000, Earl and Blinn 2003, Rhoades et al. 2011, Oliver et al. 2012). Relying on discrete samples, even at weekly intervals, does not always provide the temporal resolution to understand the linkage between catchment hydrology and stream water chemistry (Kirchner et al. 2004, Johnson et al. 2007). High-frequency and high-resolution data are needed to improve our understanding of highly dynamic and fast changing ecohydrological processes (Kirchner et al. 2004). Data collection also must be spatially distributed, long-term, and real-time to capture the ecohydrological dynamics and large-scale implications effectively (Krause et al. 2015). Establishment and maintenance of in situ, long-term, continuous water-quality monitoring networks before and after fire events is economically and logistically difficult but is a crucial step for assessing post-wildfire effects on stream chemistry (Smith et al. 2011). A few investigators (Lyon and O'Connor 2008, Dahm et al. 2015, Sherson et al. 2015) have used continuously deployed water-quality and nutrient sensors to capture the effects of wildfire on aquatic systems, but these investigators focused on the initial response within a single stream order.

The River Continuum Concept (RCC; (Vannote et al. 1980) presents a gradient of physical variables from headwater to terminus, and has been used to predict and compare biological aspects of lotic systems. We used this framework to analyze data from a network of continuously deployed, multiparameter water-quality sensors (sondes) in the Jemez Mountains and Rio Grande in New Mexico. This network lies within and downstream of major catchments burned by the Las Conchas (LC; 2011) and Thompson Ridge (2013) fires. Our goals were to use continuous water quality and quantity data to: 1) assess the pre- and postfire water quality of a 2nd- and a 4th-order

stream in a single watershed for 5 summer monsoon seasons before, during, and after a catastrophic wildfire; and 2) investigate the water-quality response (turbidity, specific conductance (SC) and dissolved O_2 [DO]) along the river continuum (1st- to 4th-order streams) for a 4-mo period that included a catastrophic wildfire.

Methods

Watershed and site descriptions

We worked in headwater streams of the Jemez Mountains (Fig. 1A–C). We focused on Jaramillo Creek (JC; 1st order; Fig. S1A), and the East Fork Jemez River (EFJR; 2nd order, Fig. S1B) in the Valles Caldera National Preserve (VCNP; Fig. 1C). JC (Fig. S1A) is a major tributary to the EFJR (Van Horn et al. 2012). The Jemez River is a tributary of the Middle Rio Grande (MRG; the Rio Grande from the US Geological Survey streamflow gage at Otowi (08313000) above Cochiti Dam to Elephant Butte Reservoir) in central New Mexico (Fig. 1A, B). The Jemez River enters the Rio Grande 6.4 km north of the US 550 bridge in the town of Bernalillo, New Mexico (Fig 1B, S1D). Jemez Canyon Dam is 1.6 km upstream of the confluence and has been operated as a pass-through facility since 2002 (U.S. Army Corps of Engineers 2009) (Fig. 1B).

The Jemez Mountains are semi-arid and seasonally snow-covered. Approximately ½ of the regional precipitation occurs from October to April in the form of rain and snowfall (Bowen 1996). The remainder occurs as rainfall associated with the North American monsoon, during the primary monsoon (July, August) and transition (June, September) months. The large elevation gradient results in high variability in the vegetation community, which includes Engelmann spruce (*Picea engelmannii*) and corkbark fir (*Abies lasiocarpa* var. *arizonica*) above 3040 m asl; Douglas fir (*Pseudotsuga menziesii*), white fir (*Abies concolor*) and blue spruce *(Picea pungens),* and scattered aspen stands (*Populus tremuloides*) between 3040 and 2740 m; ponderosa pine (*Pinus ponderosa*) and Gambel oak (*Quercus gambelii*) below 2740 m; and montane wet meadows and wetlands of the Valles Caldera (Muldavin et al. 2006). The soils in the VCNP are generally classified as forest (Andisols, Alfisol, and Inceptisol

soil orders) and grassland (Mollisols) soils (Muldavin and Tonne 2003).

The JC and EFJR sites were within an expansive, high-elevation (>2590 m) meadow valley with minimal overstory vegetation (Sherson et al. 2015) in the 1.25 Ma-year-old Valles Caldera (Goff et al. 2006). The JC sonde is ~5.4 km upstream of the confluence with the EFJR (Fig. 1C). Subsurface flow and groundwater contribute most of the stream water to the EFJR except during intense monsoonal thunderstorms when contributions from near-surface runoff occur (Liu et al. 2008). Stream discharge data for JC were obtained from the Catalina-Jemez Critical Zone Observatory (CZO) (Broxton et al. 2009), ~7.3 km upstream of the sonde. The EFJR sonde is ~1.0 km upstream of the VCNP stream gage. The Jemez River (JR; 3rd order) sonde is upstream of the confluence with the Rio Guadalupe in the town of Jemez Springs, New Mexico (Figs 1B, S1C). Surface-water inputs and shallow and deep groundwater inputs contribute surface water flow in this river reach (Trainer et al. 2000). The US Geological Survey (USGS) stream gage on the JR (08324000) is ~14.6 km downstream of the sonde and 1.9 km downstream of the confluence with the Rio Guadalupe (Fig. 1B).

Within the mainstem of the Rio Grande, we focused on the sonde at the US 550 Bridge (US 550; 4th order), in Bernalillo, New Mexico (Fig. 1B). We selected this site because it is upstream of major urban stormwater and wastewater point-source discharges and below tributaries affected by recent wildfires. We used the USGS stream gage at San Felipe (08319000), which is 20.1 km upstream of US 550, to document specific flow events. Perennial tributaries upstream of Cochiti Dam (Fig. 1B) are the major sources of surface-water flow (Ortiz and Lange 1996) except during intense rainfall or heavy snowmelt (Moore and Anderholm 2002). The MRG is considered a predominantly losing stream (i.e., a stream that loses surface water to the saturated zone) (McAda and Barroll 2002). Discharge downstream of Cochiti Dam is predominantly from controlled releases, and ephemeral and intermittent streams downstream of the dam provide minimal surface-water inputs except during periods of intense summer monsoonal rainfall (often flowing for ≤1 d/event) (Moore and Anderholm 2002). Despite the infrequency of surface-water inflow, these ephemeral and intermittent systems contribute large amounts of suspended sediment, turbidity,

9

solutes, and nutrients to the Rio Grande (Healy 1997, Moore and Anderholm 2002, Dahm et al. 2015). The MRG is a naturally turbid river, except during periods when clear-water flow from Cochiti Dam is the only contributing source of surface water to the system (e.g., during winter base flow) (Dahm et al. 2013). We obtained stream order for study reaches from the USGS National Hydrography Dataset, which uses Strahler stream order (Strahler 1952).

Wildfire descriptions

The Las Conchas (LC) fire began on 26 June 2011 and was 100% contained on 3 August 2011. During this period, the fire burned ~63,370 ha of mixed conifer and ponderosa pine forest, pinyon-juniper woodland, high elevation montane grassland, and meadows in the Jemez Mountains (Fig. 1B). At that time, the fire was the largest forest fire recorded in the history of New Mexico. The US Forest Service's Burned Area Emergency Response team developed a soil burn-severity map for the fire. Soil burn severity is indicative of the degree of impact on soil and ground properties that may affect infiltration, runoff, and erosion potential (Parsons 2002), and the maps are used to prioritize treatments and protect at-risk resources (Bobbe et al. 2001). The maps are based on pre- and postfire satellite imagery comparisons and field surveys (vegetation, ground cover, water repellency, and soil characteristics), and areas on the maps are grouped into unburned, low, moderate, and high severity categories (Parsons et al. 2010). The burn severity of the LC fire was ~20% high, 26% moderate, 39% low, and 15% unburned (Fig. 1C). We used Hydrologic Unit Codes (HUC) subunits in combination with the LC burn perimeter to calculate % area burned in ArcGIS (ArcGIS Desktop: Release 10. Environmental Systems Research Institute, Redlands, California). The LC fire burned 31% of the JC catchment and 36% of the EFJR catchment. The Thompson Ridge fire began on 31 May 2013 and was declared 100% contained on 1 July 2013. This fire burned 9698 ha of grassland, Ponderosa pine forest, and mixed conifer forest near and within the VCNP (Fig. 1B). The burn severity of the Thompson Ridge fire was 3% high, 23% moderate, and 74% low/unburned.

Dahm et al. (2015) identified the Peralta Creek watershed (of which ~7252 ha

[62% burnt]) as a major contributor of water-quality impacts to the MRG downstream of Cochiti during July and August 2011. This tributary is an ungaged ephemeral stream that enters the Rio Grande below Cochiti Dam (Fig 1B). Cochiti Reservoir and its controlled hypolimnetic releases significantly buffered the monsoon flood pulses and water-quality excursions immediately after the LC fire, with the exception of 2 water-quality excursions (elevated SC and turbidity and ~1.5 mg/L decrease in DO) observed at the USGS continuous streamflow and sonde (08317400) immediately downstream of the dam (Dahm et al. 2015). Sherson et al. (2015) also documented postfire water-quality effects in the headwater streams of the Jemez during the 2011 monsoon season with a focus on EFJR.

Continuous measurements

Water-quality data (turbidity, DO, and SC) were collected at 15-min increments by with multiparameter sonde models: Yellow Springs Instruments (YSI) 6920 (YSI Inc./Xylem Inc., Yellow Springs, Ohio), YSI EXO 1, and In-Situ 9500 troll (In-Situ Inc., Fort Collins, Colorado). The range, resolution, and accuracy of each probe are provided in Table S1. The maximum detection limit (MDL) for the turbidity probes deployed varies greatly (Table S1) among the YSI 6920 (1000 NTU), 9500 Troll (2000 NTU), and YSI EXO (4000 NTU) and we took this variability into consideration during the analyses. We made site visits at 2- to 4-wk intervals to clean and calibrate the sondes following USGS standard operating procedures (Wagner et al. 2006). We calibrated probes with laboratory-grade conductivity, pH, and turbidity standards. We calibrated DO in water-saturated air or air-saturated water. We recorded detailed field information during each site visit (site and river conditions, observed probe/sonde burial or fouling, pre- and post-cleaning values, pre- and post-calibration values, and values from a laboratory-calibrated comparison sonde). Data gaps in the water-quality records were caused by multiple factors (e.g., a sonde was not deployed, probe was buried/out of the water, probe malfunction, probe fouling). Gaps exist in the long-term continuous records, but these methods still provide a much greater temporal resolution and completeness than traditional periodic grab or event sampling.

We compiled and validated water-quality data with Aquarius Workstation 3.3 (Aquatic Informatics, Vancouver, British Columbia). We flagged suspect data, and documented the possible causes of low-quality data (i.e., instrument fouling, exposure to air, burial, probe or wiper malfunction, low voltage). We used data collected in the field (see above) to correct sonde data for fouling drift and calibration drift. Suspect data that could not be corrected were removed from the record. We used data from colocated (i.e., deployed <50 m apart in similar flow conditions) sondes maintained by the VCNP (EFJR) and USGS (Rio Grande at US 550) to fill data gaps in the water-quality record and to provide additional data validation.

We used stream discharge estimates from the USGS (JR near Jemez Springs and Rio Grande at San Felipe), VCNP (EFJR), and CZO (JC). All stations were equipped with a pressure transducer (HOBO 30-Foot Depth Water Level Data Logger; Onset Computer Corporation, Bourne, Massachusetts) that collected data at 10- to 30-min increments in the bottom of a stilling well to infer water levels (corrected for barometric pressure and temperature). Rating curves were developed and periodically updated using direct streamflow measurements by the USGS (2015) and VCNP (Condon and Gregory Unpublished). Water levels at JC were used in conjunction with an in-stream flume to estimate discharge at this station (Broxton and Troch Unpublished). We obtained daily total precipitation data from the weather station at the VCNP headquarters (VCNP HQ; Western Regional Climate Center 2014),) which is ~2.5 km upstream of the EFJR sonde.

Data analysis

To document the long-term water quality along the river continuum, we conducted an analysis for the EFJR and US 550 during the monsoon seasons before, during, and after the LC fire. We selected 2 prefire years with the most complete water-quality records for all water-quality variables for the EFJR (2008 and 2009) and US 550 (2007 and 2008). The 2010 data were excluded because of incomplete water-quality records for all variables. We calculated summary statistics for the time-series data for each water-quality variable at each station (Table 1). We generated pre- and postfire histograms for each variable at each station using the percent-of-total (POT)

measurements because of the variability in pre- and postfire sample sizes (see Table 1). We used a 2-sample Kolmogrov–Smirnov (KS) test implemented in RStudio (version 0.98.501; RStudio, Boston, Massachusetts) to perform a nonparametric value-distribution analysis (Corder and Foreman 2014) to assess whether the pre- and postfire data came from the same distribution. The 2-sample KS test is a powerful, nonparametric method that evaluates the divergence between the cumulative distribution functions of the 2-sample data vectors over the range of x in each data set (Young 1977). We evaluated the null hypotheses at $\alpha = 0.05$.

We removed missing values before running the KS test (sample sizes for each sample are provided in Table 1). To normalize for variations in the turbidity probe MDL, we set all values >1200 NTU to 1200 NTU based on observations that the YSI 6920 probe recorded reliable data up to 1200 NTU when deployed with other probes with greater MDLs (Table S1). We used the validated 15-min record for turbidity, SC, and DO analyses. We also calculated the DO daily (0000–2345 h) minimum and maximum because we were interested in both daily high and low values and potential effects of nutrient fertilization (Table 1).

We used the KS test to evaluate the effects of wildfire on hydrologic flow paths and discharge. We conducted a POT analysis of daily precipitation at the VCNP HQ station and instantaneous stream flow at the EFJR stream gage to compare pre- and postfire daily precipitation and instantaneous discharge. We did not analyze precipitation and discharge data on the Rio Grande because we were interested in fire-related changes in discharge and flow path contributions in the affected headwaters that then propagated to lower reaches.

Results

Precipitation and discharge in a 2nd-order system affected by wildfire

We used the EFJR to assess changes in precipitation and discharge during the monsoon seasons before and after the LC fire. Greater than 80% of the monsoonal

precipitation events at the VCNP HQ station before and after the LC fire fell into the 0 to 5 mm/d bin, with similar distributions and variability observed during both periods (Figs S2A, S3). Pre- and postfire means were 2.31 and 2.96 mm/d, respectively (Table 1), with maximum values of 48.26 and 56.13 mm/d, respectively (Table 1). The null hypothesis was not rejected (Table 2).

Minimal change occurred in baseflow discharge pre- and postfire (Table 1) on the EFJR (0.04 m^3/s and 0.017 m^3/s decrease in the median and mean, respectively), and >80% of the stream discharge values fell into the 0 to 0.25 m^3/s bin for both periods (Fig. S2B). However, post-fire precipitation events (Fig. S3) increased the magnitude of discharge (Fig. S4) resulting in a histogram that was right skewed (Fig. S2B). The pre- and postfire maximum discharge values were 0.492 and 3.620 m^3/s, respectively (Table 1). The null hypothesis was rejected (Table 2).

Water quality in a 2nd-order and a 4th-order system affected by wildfire

We selected the EFJR (2nd order) and US 550 (4th order) to assess water quality (turbidity, SC and DO) during the monsoon seasons before, during, and after the LC fire. The EFJR showed dramatic increases in turbidity after the fire. Before the fire, >90% of all turbidity values were <50 NTU and no values were >100 NTU (Fig. 2A). After the fire, 15% of all values were >150 NTU, and 5% were >400 NTU. The median turbidity decreased by 3.4 NTU postfire, whereas the mean turbidity increased by 22.5 NTU postfire (Table 1). During monsoonal thunderstorms before the fire, turbidity peaked between 15 and 150 NTU, whereas turbidity during thunderstorms peaked between 250 and 1200 NTU after the fire (Fig. S5). The null hypothesis was rejected (Table 2).

US 550 showed minimal, but statistically significant (Table 2) changes in turbidity after the fire. Before the fire, turbidity at this site regularly exceeded 200 NTU, and 7% of the total values were >1150 NTU (Fig. 2B). Postfire values regularly exceeded 200 NTU, and 11% of the total values were >1150 NTU. In 2013, an EXO turbidity probe detected turbidity >4000 NTU MDL during postfire monsoon storm pulses at this site. The median pre- and postfire turbidity increased only 30 NTU postfire (Table 1). During pre- and postfire monsoonal thunderstorms upstream of US

550, turbidity regularly exceeded 1200 NTU (Fig. S6). The null hypothesis was rejected (Table 2).

The EFJR showed clear increases in SC after the fire (Table 1), resulting in a histogram that was right skewed (Fig. 3A). The median and mean SC showed minimal variation with only 0.033 and 0.046 mS/cm increases postfire, respectively (Table 1). During prefire monsoonal thunderstorms, SC increased to a maximum of 0.15 mS/cm, in pulses that were infrequent and dissipated within hours (Fig. S7). During postfire events, SC pulses peaked between 0.150 and 0.350 mS/cm, with durations from hours to weeks (Fig. S7). The null hypothesis was rejected (Table 2).

US 550 also showed clear increases in SC after the fire (Table 1), and the distribution shifted to the right (Fig. 3B). The median and mean SC showed minimal variation with only 0.005 and 0.023 mS/cm increases postfire, respectively (Table 1). SC peaks also increased. Prefire peaks from monsoonal thunderstorms were between 0.500 and 1.130 mS/cm, and postfire peaks were between 0.500 and 3.740 mS/cm (Fig. S8). The null hypothesis was rejected (Table 2).

The DO signal at EFJR changed strongly after the fire. Postfire, the minimum, median, and mean decreased, whereas the daily maximum increased (Table 1) and the interquartile range (IQR) expanded in both directions (Table 1). POT analysis documented a positive and negative expansion of the DO distribution (Fig. 4A), positive and negative expansion of the daily DO maximum distribution (Fig. S9A), and a negative expansion of the daily DO minimum distribution (Fig. S10A). The DO time series (Fig. S11) showed a strong prefire diel signal that expanded in both directions (i.e., lower daily minimum and higher daily maximum) postfire. During postfire discharge events (Fig. S4), DO maxima were severely reduced, whereas DO minima were only minimally reduced (Fig. S11). This signal dampening also was observed prefire after changes in discharge, but was less frequent and less severe (Fig. S11).

The DO signal and distribution also changed postfire at US 550. Change in the median was minimal (0.1 mg/L), and the mean did not change (Table 1). However, the DO minimum was lower and the maximum was greater after than before the fire (Table 1). POT analysis showed positive and negative expansions of: 1) the DO signal

15

distribution (Fig. 4B), 2) the daily DO maximum distribution (Fig. S9B), and 3) the daily DO minimum distribution (Fig. S10B). Before the fire, the DO signal (Fig. S12) was fairly stable throughout the monsoon season, with small daily variability. During postfire discharge events (Fig. S13) the DO minima were substantially lower (Fig. S12). The null hypotheses for the DO signal, daily minimum DO, and daily maximum DO at the EFJR and DO at the Rio Grande at US 550 were rejected (Table 2).

Initial postfire response along the river continuum

We selected JC, EFJR, JR, and US 550 data to assess the initial response during the monsoon season before, during, and after the LC fire. Approximately 1 mo after the onset of the LC fire, monsoon precipitation events resulted in changes in discharge along the continuum (Fig. 5A). The postfire discharge events coincided with turbidity >1000 NTU at all stations along the river continuum (Fig. 5B). In August 2011, turbidity measurements on the Rio Grande at US 550 during water-quality excursions were >1200 NTU then immediately dropped to 0 NTU, while SC (Fig. 5C) increased and DO decreased (Fig. 5D). The failure to detect turbidity at US 550 during some of these events (because of instrumental issues; see below) was not seen in the headwater streams.

SC initially decreased during fire-related pulses followed by strong increases in maximum values to 0.33, 0.33, 0.92, and 2.34 mS/cm at the JC, EFJR, JR. and US 550 sites, respectively (Fig. 5C). The diurnal variability of the DO signal during fire-affected discharge events was almost completely absent from JC and EFJR (Fig. 5D). Multiple DO depressions (<4 mg/L) were observed at JR and EFJR during this period with depressions to 0.14 and 0.96 mg/L, respectively (Fig. 5D). The DO signal at JR was depressed during discharge events, but did not drop <6.9 mg/L (Fig. 5D). The diurnal DO signal at US 550 was completely absent during this period, and 10 DO depressions (<4 mg/L) occurred in July and August (Fig. 5D).

Discussion

Fire effects on 2ⁿᵈ- and 4ᵗʰ-order streams

Erosive overland flow responsible for large sediment inputs to streams is observed rarely in undisturbed grassland and forested catchments (Shakesby and Doerr 2006). Before the fire, the EFJR fit this pattern, and subsurface flow and groundwater contributed most of the water during the monsoon season with negligible contributions from near-surface or overland flow during summer baseflow periods (Liu et al. 2008). The single prefire exception was during heavy (20–40 m/d) and continuous rainfall when near-surface water contributed to the EFJR (Liu et al. 2008) as a result of saturated overland flow. Wildfire removes forest litter that promotes water storage (Shakesby and Doerr 2006), reduces or halts transpiration (Loaiciga et al. 2001), and induces or enhances pre-existing water repellency of soils by altering physical and chemical properties of the soil (Shakesby and Doerr 2006). The daily total precipitation POT analysis (Fig. S2A, Table 2) showed statistically similar pre- and postfire daily precipitation distributions. However, analysis of the discharge record at the EFJR (Fig. S2B, Table 2) confirmed a significant increase in postfire discharge (Fig. S4) during episodic monsoonal precipitation events (Fig. S3). These results suggest that fire decreased water storage capacity and increased surface runoff in the EFJR watershed.

The historical median turbidity of the EFJR was very low (7.4 NTU; Table 1), supporting the importance of subsurface inputs (Liu et al. 2008). Prefire precipitation events (Fig. S13) led to minimal increases in discharge (Fig. S4) and small (rarely >100 NTU; Fig. S5) turbidity spikes that were infrequent and dissipated within hours. Postfire baseflow values remained low (median turbidity decreased by 3 NTU), but postfire precipitation events of intensities similar to those observed prefire led to a greater discharge response (frequently >1000 NTU; Fig. S5) and larger turbidity spikes lasting hours to weeks; Fig. S5). These results confirm that overland flow and associated erosion significantly affected postfire water quality. Pelletier and Orem (2014) used pre- and postfire LiDAR (light detection and ranging) data to document significant post-

17

LC-fire sediment transport in the VCNP. They identified rill formation as an important hillslope erosion mechanism and reported transport of boulders up to 1 m in diameter, confirming our in-stream water-quality observations. Fire-related impacts on water clarity have been observed in other streams (Smith et al. 2011). In some 1st- through 3rd-order streams, elevated turbidity lasted for up to 5 y after fire (Nyman et al. 2011, Rhoades et al. 2011). Rhoades et al. (2011) also documented that turbidity and NO_3^- concentration increased linearly with the percentage of basin that was burned or was burned at high severity. Identifying the mechanism for the observed increase in overland flow is beyond the scope of our study. However, our analyses documented an increase in turbidity in VCNP headwater streams that was independent of precipitation severity. Elevated turbidity probably was caused by increased frequency, magnitude, and duration of overland flow, and subsequent sediment, charcoal, and ash mobilization.

Despite flood and sediment control in the MRG, both pre- and postfire turbidity often were >1200 NTU during monsoonal thunderstorms (Fig. 2B, Fig. S6). Many studies of fire effects on streams have been focused on total suspended sediment (TSS) rather than on turbidity because TSS is transferable among watersheds (Smith et al. 2011). However, this preference has resulted in few studies documenting the postfire turbidity regime in large river systems. Leak et al. (2003) documented postfire debris-flow pulses with a maximum turbidity of 129,000 NTU in the Buckland River, Victoria, Australia. This event propagated into the Ovens River >150 km downstream from the source, resulting in a maximum of 2370 NTU 12 d after the initial pulse in the Buckland River (Leak et al. 2003, Lyon and O'Connor 2008). High background turbidity and values >4000 NTU MDL prevented us from assessing whether maximum turbidity values changed significantly in the Rio Grande at US 550 after the fires. Black C (ash and charcoal) events that eliminated all light scattering and resulted in instrument measurements of 0 NTU also were a limitation when using continuously deployed turbidity sensors to document post-fire effects on water quality. Dahm et al. (2015) simulated these conditions in the laboratory with ash and charcoal (black C). These substances absorbed all light emitted from the probe and simulated conditions of no

particle-related light scatter, resulting in instrument measurements of 0 NTU. It is unclear why this phenomenon was documented at US 550 but not in the headwater systems in spite of observed debris flow events in the VCNP (Dahm et al. 2015). This discrepancy might be attributable to differences in the size distribution of suspended material (Landers and Sturm 2013), heterogeneity of the types of suspended sediment between stream orders (Lenzi and Marchi 2000), or the size and shape of the particles (Bisantino et al. 2011), all of which influence the sensitivity and accuracy of the optical turbidity measurement. We identified the benefit of in situ turbidity measurements to assess impacts on water clarity and the limitations of such measurements in systems that are highly turbid prior to disturbance, such as wildfire.

The effects of wildfire on total dissolved solids (TDS) and SC have rarely been studied (Neary et al. 2002). The few investigators who explored postfire SC found mixed results. Some investigators observed elevated postfire SC (Earl and Blinn 2003, Lyon and O'Connor 2008, Dahm et al. 2015) including an ~2× increase in SC from baseline values. SC also was positively correlated with sediment loss during rainfall over an artificial burn (Badia and Marti 2008). However, Hall and Lombardozzi (2008) used discrete sampling and showed statistically nonsignificant changes in SC after forest fire. We found long-term fire-induced changes in SC in both the 2nd- and 4th-order streams over a 3-y period (Fig. 3A, B). Salinization has been identified as the greatest water-quality concern for the Rio Grande and may limit agricultural and municipal use in the future (Moyer et al. 2013). Our findings suggest that more frequent and severe wildfires probably will accelerate the concentration and load of TDS in the MRG, but other sources (e.g., saline groundwater discharge, mineral dissolution, agricultural returns, and wastewater treatment plant effluent (Moyer et al. 2013) probably will continue to dominate the salinity budget.

The prefire SC record for the EFJR was quite stable with only small depressions and spikes during precipitation events (Fig.S7). Liu et al. (2008) hypothesized that strong seasonal evapotranspiration in the VCNP decreases soil moisture and increases water retention time, both of which reduce the magnitude of near-surface runoff during short duration, high intensity monsoonal thunderstorm events. These factors

minimized prefire SC spikes in the EFJR (Fig.S7) and resulted in minimal variation in SC values (Fig. 3A). The postfire EFJR SC spikes increased in magnitude, frequency, and duration (Fig. 3A, Fig.S7). These changes can be attributed to synergistic effects of altered soil properties, input of ash and charcoal from combusted organic matter, and postfire changes in hydrologic flow paths including increased overland flow. Furthermore, elevated Ca^{2+}, Mg^{2+}, K^+, and SO_4^{2-} have been observed in postfire surface soils (Khanna et al. 1994, Certini 2005) and combusted plant matter can leach Na^+, SO_4^{2-}, and Cl^- when wetted (Murphy et al. 2006). Both mechanisms probably increase the availability of ions that are easily dissolved in water and transported to streams near the fire scars. As a result, ephemeral and intermittent tributaries of the MRG that were affected by the LC fire are contributing higher concentrations of dissolved ions to the Rio Grande.

The wide range of prefire daily summertime DO values in the EFJR (Fig. 4A, Fig. S11) show that this system had high rates of primary production and ecosystem respiration before the fire. Whole-stream metabolism modeling estimates spanning 6 y confirmed that the EFJR is a very productive ecosystem (Shafer 2013). Gross primary production (GPP) and community respiration (CR) rates are among the highest reported in the literature for open-canopied streams (Shafer 2013). The RCC predicts that autotrophic production should be low in headwater streams (Vannote et al. 1980, Webster 2007), but low GPP clearly is not the case in open-canopied systems, such as the EFJR or those in other grassland ecosystems (Young and Huryn 1996). Hydrologic stability (i.e., periods that lack flooding) can increase GPP (Leggieri et al. 2013). Episodic storm events resulting elevated turbidity and reduced light penetration can decrease GPP for short periods (Hall et al. 2015). The postfire expansion of the IQR and DO maximum and minimum values in the EJFR (Fig. 4A, Fig. S11) indicate that the fire had a large effect on this important water-quality variable via physical and biogeochemical mechanisms that both increased and decreased DO values. The DO signal, which typically exhibits high diurnal variability (Fig. S11), was suppressed during postfire river stage increases (Fig. S4). The stage increases are caused by large overland flow events documented by elevated turbidity (Fig. S5) and SC (Fig.S7) after

precipitation events (Fig. S3) within the burn scar. The loss of the diurnal pattern is probably a result of light limitation from high sediment loads and increased metabolism from dissolved and particulate organic matter in transport (Figs S5, S7). However, these limited DO depressions were not responsible for observed changes in the postfire distributions of DO values (Fig. 3A), which arose from consistently higher daytime and lower nighttime DO concentrations throughout the summer seasons after the fire (Fig. S11). Our findings suggest that wildfire can alter rates of primary production and ecosystem respiration in headwater streams.

Wildfires have increased nutrient supply in the EFJR (Sherson et al. 2015) and other streams (Bayley et al. 1992, Earl and Blinn 2003, Betts and Jones 2009). This creates a fertilization effect that directly stimulates in-stream primary production in nutrient-limited systems (Betts and Jones 2009). Elevated community respiration results from multiple factors including increased fire-related organic-matter resources, reduced nutrient limitation, and stimulation of autochthonous supplies including the biomass of benthic algae and aquatic macrophytes and labile exudates (Bertilsson and Jones 2003) related to the increase in primary production. Our results suggest a fertilization effect is occurring at the EFJR, and has yet to subside 3 y post-fire.

Prefire DO concentrations at US 550 showed much smaller diurnal variability with much of the variability controlled by abiotic factors such as temperature. The absence of a strong autotrophic signal differs from the prediction for mid-size rivers made in the RCC (Vannote et al. 1980). Authors of a meta-analysis of metabolism data from 30 US streams and rivers also found that streams in deserts and with larger watersheds generally have higher metabolic values (Lamberti and Steinman 1997), but this was not the case in the Rio Grande. Low available nutrient levels in the Rio Grande above Albuquerque (Passell et al. 2005) and light limitation from high sediment loads even at baseflow conditions probably are responsible for the weak diurnal primary production signal at this site. The small postfire increase in the frequency of DO values >8.5 mg/L and in the IQR of DO concentrations at US 550 (Fig. 4B) suggests that the fire did produce a small fertilization effect during baseflow conditions. However, the major fire-related effects occurred during discrete discharge pulses from fire-affected and

intermittent tributaries entering the Rio Grande below Cochiti Dam. These episodic pulses periodically drove DO levels to 0 mg/L in 2011 (Dahm et al. 2015) and <3 mg/L in 2012 and 2013 (Fig. S12). The MRG is listed in the State of New Mexico Clean Water Act (2000) as an impaired waterbody for DO. Our results document additional DO impairment from the recent wildfires.

Together, DO data from the EFJR and US 550 suggest large differences in biologically driven water-quality responses to fire along the river continuum. The high benthic surface area:water volume ratio in headwater streams (Battin et al. 2008) promotes strong biological control of DO concentrations, and fire-related nutrient fertilization increases both GPP and CR during baseflow conditions in EFJR. However, the main impact on DO concentrations during storm discharge events were reductions in the daily maximum DO. This effect can be attributed to the large quantities of fire-related material in transport and elevated turbidity. As a result, primary production was suppressed resulting in DO values comparable to typical nighttime concentrations when respiration pathways dominate. DO at US 550 during summer baseflow changed minimally after the fire, largely because of the strong abiotic controls (temperature and light limitation) and limited biological controls regulating the DO signal, both pre- and postfire at US 550 (Van Horn and Reale Unpublished). Large storm pulses of fire-scar-derived material were sufficient to lower DO concentrations strongly at US 550 up to 3 y after the fire. In summary, we found that pre- and postfire abiotic and biotic processes, influence the response of DO to fire-related effects and should be taken into consideration when assessing postfire DO effects on streams along the river continuum.

Initial postfire water-quality responses along the river continuum

Overbanking was observed in many streams in the VCNP during the initial postfire pulses (Sherson et al. 2015), and ash, sediment, black C, and debris-laden floods occurred throughout the basin after the fire in 2011 (Dahm et al. 2015). (Vannote et al. 1980) did not discuss changes in turbidity of streams and rivers along the river continuum except to say that that turbidity will limit primary production in large rivers. Webster (2007) showed that as the distance from headwaters increases, so do seston

22

(suspended particles in transport) levels, a result suggesting elevated TSS and turbidity along the river continuum. Rhoades et al. (2011) documented elevated turbidity in 1st- through 3rd-order streams after wildfire, but they compared streams in burned and unburned basins collectively so differential effects on various stream orders cannot be assessed. We observed turbidity events that were >1000 NTU in 1st- through 4th-order streams immediately after the LC fire (Fig. 5B). However, the magnitude above 'normal' prefire turbidity values decreased in a downstream direction, suggesting that the fire-related turbidity response is strongest in headwater streams (JC and EFJR) and less strong in higher-order systems (JR and US 550).

Ash inputs and elevated erosion can increase transport of major ions as evidenced by elevated SC after wildfires (Earl and Blinn 2003, Lyon and O'Connor 2008, Dahm et al. 2015), but such changes have not been assessed along a river continuum. Postfire precipitation events in headwater streams (JC and EFJR) resulted in significant increases in SC, with gradual descending limbs that sometimes lasted weeks to months before returning to prefire levels (Fig. 5A). Initial SC spikes corresponded with elevated turbidity and were probably caused by increased overland flow that mobilized ash, charcoal, plant leachate, and sediment into the stream as suggested by Earl and Blinn (2003), who documented an immediate increase in SC after addition of ash to a 1st-order stream. We hypothesize that the gradual descending limbs for SC after fire in low-order streams are a consequence of ions leaching from deposited ash and sediment. The SC response at JC was noticeably larger than at the EFJR, possibly because of differences in stream discharge between the stream orders. JC discharge is approximately an order of magnitude less than discharge in the EFJR during baseflow (subsurface and groundwater inputs) and during storm events (near-surface and overland flows) (Fig. 5A). Therefore, the conductivity dilution factor probably is greater on the EFJR than JC, which results in a stronger initial response and a more gradual and longer-duration descending limb in SC. The proportions of the JC and EFJR basins burned by the LC fire were similar, and we suggest that fire affected these basins similarly but that the lower discharge from JC led to higher SC concentrations in JC than in EFJR.

The SC response at JR during postfire precipitation events consisted of an initial

dilution followed by a gradual increase and decrease in concentration (Fig. 5C). This response probably was caused by mineralized geothermal inputs to JR (Trainer et al. 2000). These additions overwhelmed the postfire SC response observed higher in the Jemez catchment. The postfire SC response at US 550 consisted of high-intensity, short-duration spikes that quickly returned to prepulse values (Fig. 5C). We suggest this effect was caused by the high-intensity, short-duration pulses from ephemeral tributaries affected by wildfire, which were quickly diluted by releases from Cochiti Dam. Dahm et al. (2015) documented minimal variation (0.05 mS/cm) downstream of Cochiti and considerable and short-lived increases at US 550 (0.30 mS/cm) during the 2011 monsoon season, suggesting these ephemeral inputs are the sources of elevated SC.

Single-site, postfire DO depressions have been measured previously using continuously deployed water-quality probes (Lyon and O'Connor 2008, Dahm et al. 2015, Sherson et al. 2015). However, wildfire effects on DO along a river continuum have not been assessed. Strong prefire diurnal DO variability in the headwater systems (JC and the EFJR) was suppressed after the fire, probably because of light limitation from high sediment loads and possible scour of the primary producers (Fig. 5D). Strong diel variability returned more quickly on the EFJR than JC. This difference in recovery can be attributed to faster recovery of the primary producers. The higher-order systems (JC and US 550) had lower diurnal variability in the prefire DO signal, but these sites responded differently postfire. The JR DO signal decreased 1 to 2 mg/L immediately during flow events, but these depressions rebounded quickly to prepulse values. JR has a large stream surface area:volume ratio, higher stream gradient and streambed roughness, and a pool and riffle bed morphometry (New Mexico Environmental Department 2005), all of which create significant turbulence and reaeration that can buffer the DO signal during postfire discharge events. The fire-related depressions were much more severe at US 550 than at the low-order streams, with 10 large DO depressions (<4 mg/L) in July and August (Fig. 5D). Dahm et al. (2015) hypothesized that DO depressions on the MRG could be attributed to intensified biological and chemical O_2 demand stimulated by the input of fire-related organic matter, chemically reduced compounds, and black C. US 550 has a deep and narrow channel configuration,

an incised thalweg, and lower gradient (Ortiz 2004). These factors reduce atmospheric reaeration and extend residence times. Thus, biological and chemical O_2 demand can reduce DO levels when large quantities of fire-scar materials are present.

Conclusions

Discrete samples, even at weekly intervals, provide insufficient temporal resolution to fully describe and understand the linkages between catchment hydrology and stream water chemistry (Kirchner et al. 2004), especially when studying episodic disturbance events like forest fires and assessing long-term trends (Johnson et al. 2007). In addition to high-resolution data, spatially distributed, long-term, and real-time data are needed to assess the dynamic, fast changing, and nonlinear behavior of aquatic systems at the watershed level (Krause et al. 2015). Our findings highlight the importance of collecting water-quality data at time scales that effectively capture the ecohydrological dynamics of the watershed. Establishment of long-term, continuous, water-quality monitoring networks has been proposed as a crucial next step for assessing postwildfire impacts on stream chemistry (Smith et al. 2011). Our study fills this data gap by documenting long-term, pre- and postfire water-quality trends in a 2nd- and 4th-order stream during the summer monsoonal thunderstorm season. We also assessed the initial effects of wildfire along a river continuum (1st- through 4th-order streams) using continuous records. Streamflow pathways, physiochemical and biogeochemical processes, and geomorphology play central roles in the initial and long-term postfire water-quality responses along a river continuum.

Acknowledgements

Figures

Fig. 1. Maps showing the Rio Grande River and the location of the Las Conchas (LC) forest fire in north central New Mexico (A), streamflow gages, water-quality sondes, streams of interest, perimeter of the LC and Thompson Ridge fires, key landmarks, and the major hydrologic unit codes (HUCs) for this section of the Rio Grande (B), and the burn severity map for the LC fire in relation to monitoring locations (C).

27
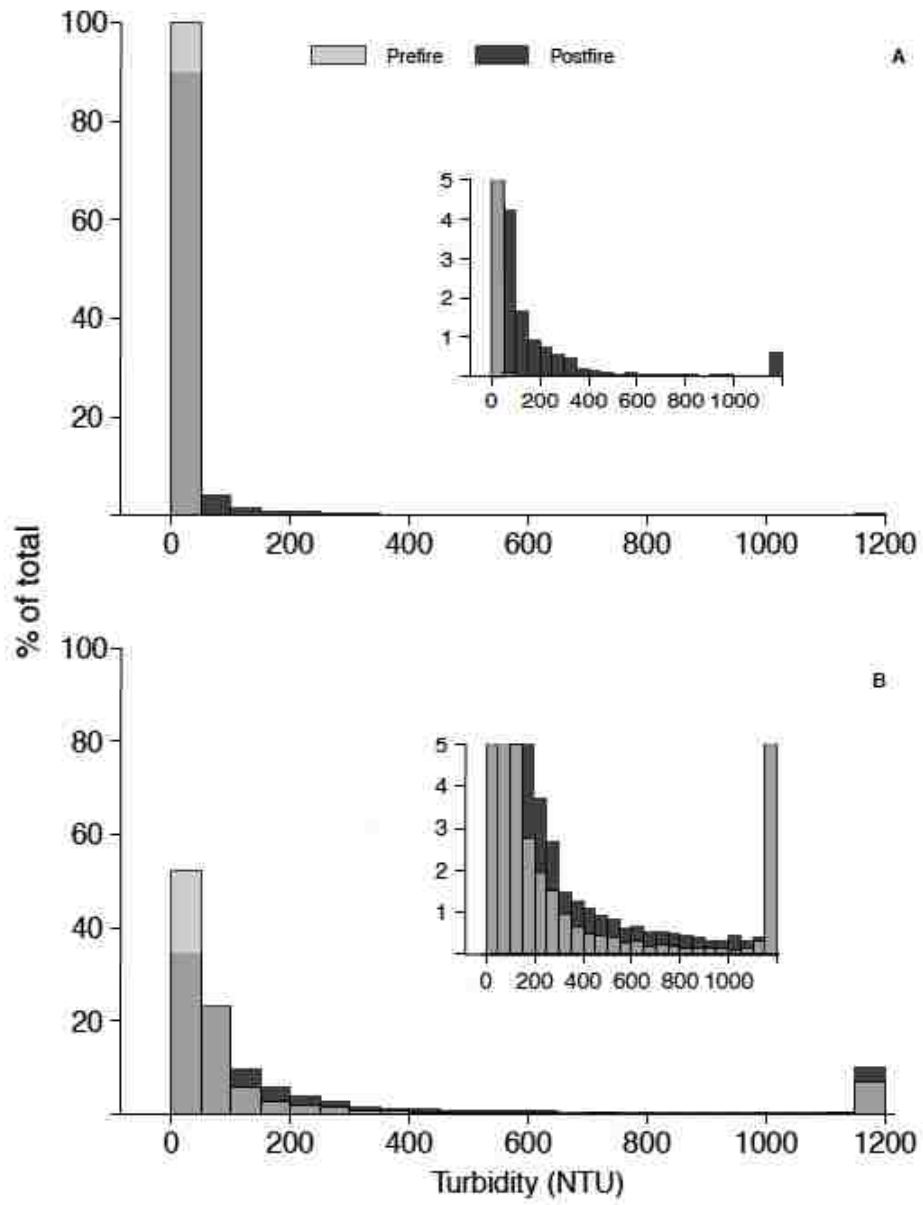
Fig. 2. Distribution of pre- and post-fire turbidity (15-min increments) values at East Fork Jemez River (A) and the Rio Grande (RG) at the US 550 bridge (B). See Table 1 for monsoon seasons analyzed for each location. Insets are magnified views of 0 to 5% of total.
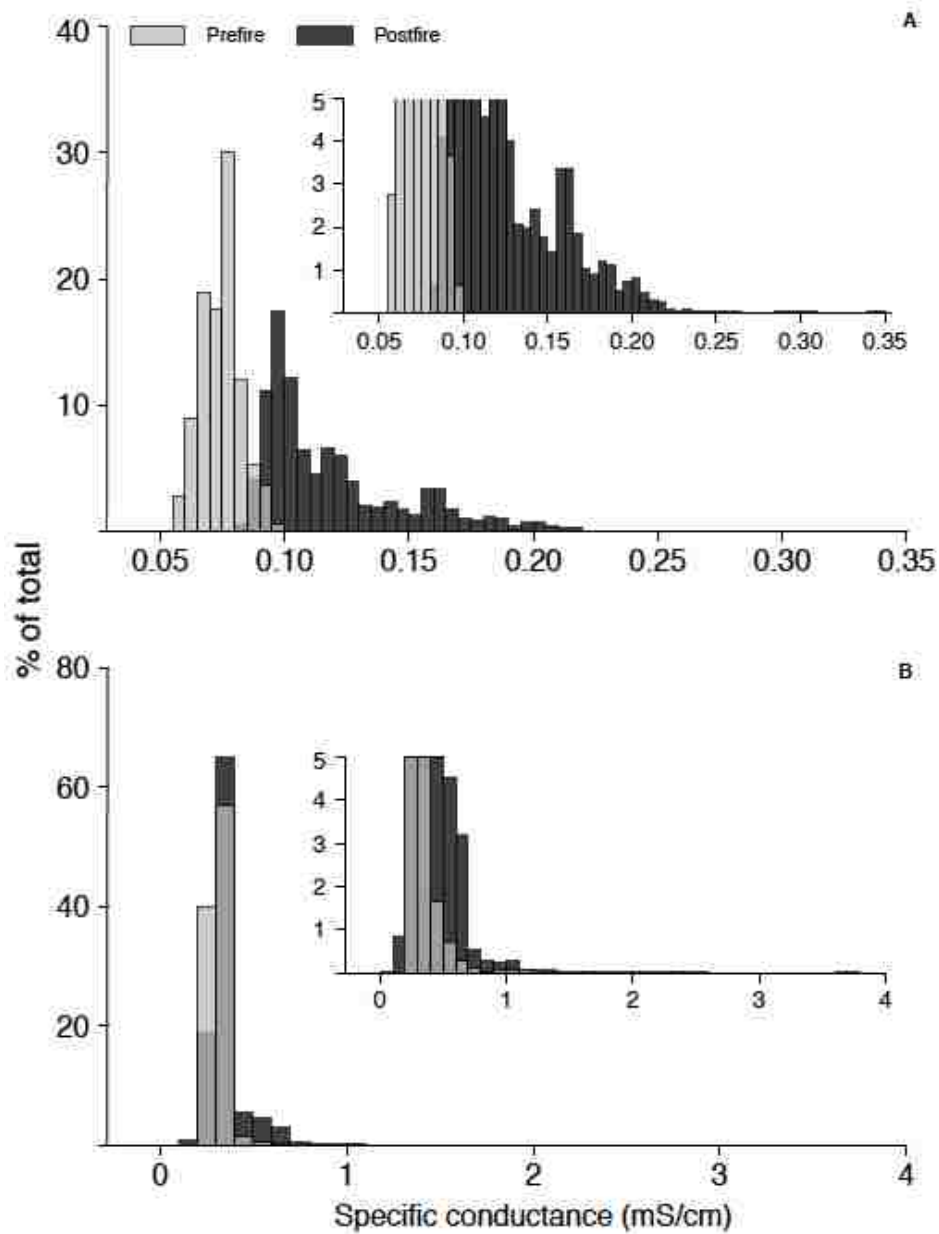
Fig. 3. Distribution of pre- and postfire specific conductance (15-min increments) measurements at East Fork Jemez River (A) and the Rio Grande (RG) at the US 550 bridge (B). See Table 1 for specific monsoon seasons analyzed for each location. Insets are magnified views of 0 to 5% of total.
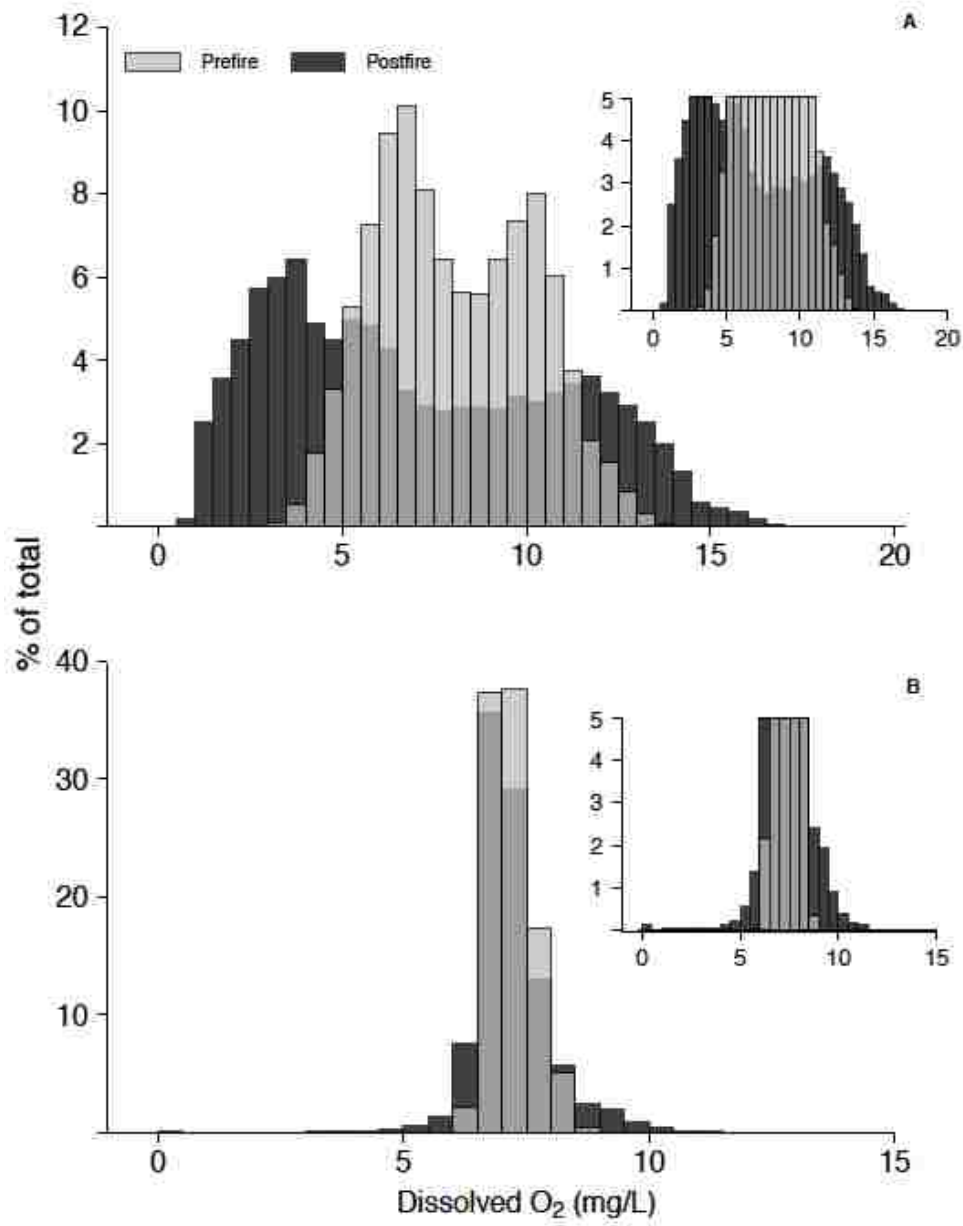
Fig 4. Distribution of pre- and postfire dissolved O_2 (15-min increments) measurements at East Fork Jemez River (A) and the Rio Grande (RG) at the US 550 bridge (B). See Table 1 for specific monsoon seasons analyzed for each location. Insets are magnified views of 0 to 5% of total.
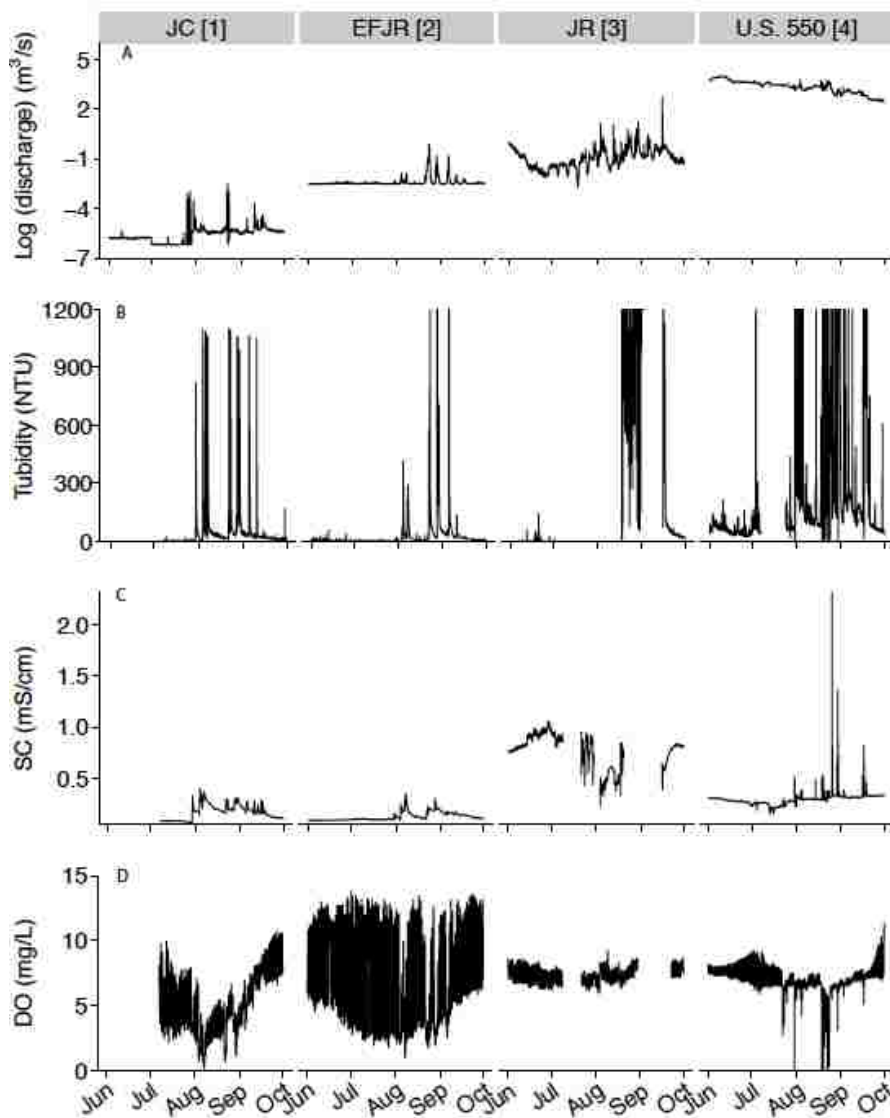
Fig. 5. Log (stream discharge) (A), turbidity (B), specific conductance (SC) (C), and dissolved O₂ (DO) (D) measurements (15-min increments) along the river continuum during the 2011 monsoon season. Stations include Jaramillo Creek (JC), East Fork Jemez River (EFJR), Jemez River (JR), and Rio Grande (RG) at the US 550 bridge (US 550). Turbidity values >1200 NTU were changed to 1200 NTU because of varying maximum detection limits of the deployed probes. The LC fire began on 26 June 2011. Stream order is in brackets.

Tables

Station	Parameter	Condition	Years assessed	Min	1st quart	Median	Mean	3rd quart	Max	n (total)
VCNP HQ	Daily precipitation	Prefire	08, 09, 11	0	0	0	2.31	1.52	48.3	269
VCNP HQ	Daily precipitation	Postfire	11, 12, 13	0	0	0	2.96	2.03	56.1	341
EFJR	Discharge	Prefire	08, 09, 11	0.080	0.088	0.105	0.115	0.134	0.492	23,907
EFJR	Discharge	Postfire	11, 12, 13	0.004	0.039	0.061	0.132	0.084	3.620	26,786
EFJR	Turbidity	Prefire	08, 09, 11	1.7	5.7	7.4	8.6	9.7	87.1	25,321
EFJR	Turbidity	Postfire	11, 12, 13	0	2	4	31.08	16.4	1200	31,019
US 550	Turbidity	Prefire	07, 08, 11	16.4	36.8	48.3	169.4	96.4	1200	19,713
US 550	Turbidity	Postfire	11, 12, 13	0	42	79.4	256.5	237	1200	49,554
EFJR	SC	Prefire	08, 09, 11	0.057	0.069	0.076	0.075	0.080	0.146	25,350
EFJR	SC	Postfire	11, 12, 13	0.081	0.098	0.109	0.121	0.134	0.348	32,105
US 550	SC	Prefire	07, 08, 11	0.252	0.289	0.314	0.320	0.34	1.13	19,818
US 550	SC	Postfire	11, 12, 13	0.005	0.297	0.319	0.343	0.35	3.74	27,153
EFJR	DO	Prefire	08, 09, 11	2.8	6.4	8.1	8.3	10.1	16.4	21,657
EFJR	DO	Postfire	11, 12, 13	0.9	3.5	6.1	6.9	10.2	17.3	32,589
US 550	DO	Prefire	07, 08, 11	5.3	6.9	7.2	7.2	7.5	8.7	20,236
US 550	DO	Postfire	11, 12, 13	0.0	6.8	7.1	7.2	7.5	11.5	52,812
EFJR	DO daily max	Prefire	08, 09, 11	5.0	10.3	11.7	11.8	12.9	16.4	230
EFJR	DO daily max	Postfire	11, 12, 13	1.5	11.5	12.8	12.1	14.0	17.3	341
US 550	DO daily max	Prefire	07, 08, 11	6.9	7.3	7.6	7.6	7.9	8.7	212
US 550	DO daily max	Postfire	11, 12, 13	5.6	7.3	7.6	7.8	8.2	11.5	552
EFJR	DO daily min	Prefire	08, 09, 11	2.8	4.8	5.5	5.5	6.2	8.1	230
EFJR	DO daily min	Postfire	11, 12, 13	0.9	1.9	2.6	2.9	3.5	6.4	341
US 550	DO daily min	Prefire	07, 08, 11	5.3	6.7	6.8	6.9	7.1	7.6	212
US 550	DO daily min	Postfire	11, 12, 13	0.0	6.5	6.7	6.6	7.0	9.8	552

Table 1. Summary table of the long-term pre- and postfire turbidity, specific conductance (SC), dissolved O_2 (DO), and daily DO maximum (max) and minimum (min) (0000–2345 h) comparison for the sondes at Valles Caldera National Preserve Headquarters (VCNP HQ), the East Fork Jemez River (EFJR) and the Rio Grande at US 550 bridge. *n* = the total sample size, quart = quartile. Years are given as the last 2 digits of 2008, 2009, 2011, 2012, 2013.

Station	Variable	D	$D_{critical}$	p	H_0 rejected?
VCNP HQ	Daily precipitation	0.06	0.11	0.6	No
EFJR	Discharge	0.49	0.01	<0.001	Yes
EFJR	Turbidity	0.43	0.01	<0.001	Yes
US 550	Turbidity	0.21	0.01	<0.001	Yes
EFJR	SC	0.91	0.01	<0.001	Yes
US 550	SC	0.22	0.01	<0.001	Yes
EFJR	DO	0.33	0.01	<0.001	Yes
US 550	DO	0.10	0.01	<0.001	Yes
EFJR	DO daily max	0.24	0.12	<0.001	Yes
US 550	DO daily max	0.13	0.11	0.013	Yes
EFJR	DO daily min	0.76	0.12	<0.001	Yes
US 550	DO daily min	0.15	0.11	0.002	Yes

Table 2. Summary table of the 2-sample Kolmogorov–Smirnov (KS) tests comparing pre- and postfire daily precipitation, discharge, turbidity, specific conductance (SC), dissolved O_2 (DO), DO daily maximum (max) and minimum (min) (0000–2345 h) at Valles Caldera National Preserve Headquarters (VCNP HQ), the East Fork Jemez River (EFJR) and the Rio Grande at US 550 bridge. $D_{critical}$ $\alpha = 0.05$.

Supplemental figures and tables

Accessible via: https://www.journals.uchicago.edu/doi/suppl/10.1086/684001

References

Allen, C. D., Macalady, A. K., Chenchouni, H., Bachelet, D., McDowell, N., Vennetier, M., Kitzberger, T., Rigling, A., Breshears, D. D., Hogg, E. H., Gonzalez, P., Fensham, R., Zhang, Z., Castro, J., Demidova, N., Lim, J. H., Allard, G., Running, S. W., Semerci, A., and Cobb, N. 2010. A global overview of drought and heat-induced tree mortality reveals emerging climate change risks for forests. Forest Ecology and Management 259:660-684.

Badia, D., and Marti, C. 2008. Fire and rainfall energy effects on soil erosion and runoff generation in semi-arid forested lands. Arid Land Research and Management 22:93-108.

Battin, T. J., Kaplan, L. A., Findlay, S., Hopkinson, C. S., Marti, E., Packman, A. I., Newbold, J. D., and Sabater, F. 2008. Biophysical controls on organic carbon fluxes in fluvial networks. Nature Geoscience 1:95-100.

Bayley, S., Schindler, D., Beaty, K., Parker, B., and Stainton, M. 1992. Effects of multiple fires on nutrient yields from streams draining boreal forest and fen watersheds: nitrogen and phosphorus. Canadian Journal of Fisheries and Aquatic Sciences 49:584-596.

Bertilsson, S., and Jones, J. B. J. 2003. Supply of dissolved organic matter to aquatic ecosystems: autochthonous sources. Pages 3-19 in S. Bertilsson, J. J. Jones, S. E. G. Findlay and R. L. Sinsabaugh (editors). Aquatic Ecosystems: Interactivity of Dissolved Matter. Academic Press, San Diego, California.

Betts, E. F., and Jones, J. B. 2009. Impact of wildfire on stream nutrient chemistry and ecosystem metabolism in boreal forest catchments of interior Alaska. Arctic, Antarctic, and Alpine Research 41:407-417.

Bisantino, T., Gentile, F., and Liuzzi, G. T. 2011. Continuous monitoring of suspended sediment load in semi-arid environments. in S. S. Ginsberg (editor). Sediment Transport. InTech Open Access Publisher.

Bisson, P. A., Rieman, B. E., Luce, C., Hessburg, P. F., Lee, D. C., Kershner, J. L., Reeves, G. H., and Gresswell, R. E. 2003. Fire and aquatic ecosystems of the western USA: current knowledge and key questions. Forest Ecology and Management 178:213-229.

Bladon, K. D., Emelko, M. B., Silins, U., and Stone, M. 2014. Wildfire and the future of water supply. Environmental Science & Technology 48:8936-8943.

Bobbe, T., Finco, M. V., Quayle, B., Lannom, K., Sohlberg, R., and Parsons, A. 2001. Field measurements for the training and validation of burn severity maps from spaceborne, remotely sensed imagery. U.S. Department of Interior, Joint Fire Science Program.

Bowen, B. M. 1996. Rainfall and climate variation over a sloping New Mexico plateau during the North American monsoon. Journal of Climate 9:3432-3442.

Broxton, P. D., and Troch, P. A. Unpublished. Streamflow Calculation-Valles Caldera National Preserve.

Broxton, P. D., Troch, P. A., and Lyon, S. W. 2009. On the role of aspect to quantify water transit times in small mountainous catchments. Water Resources Research 45:W08427.

Cayan, D. R., Dettinger, M. D., Kammerdiener, S. A., Caprio, J. M., and Peterson, D. H. 2001. Changes in the onset of spring in the western United States. Bulletin of the American Meteorological Society 82:399-415.

Certini, G. 2005. Effects of fire on properties of forest soils: a review. Oecologia 143:1-10.

Condon, K. E., and Gregory, A. Unpublished. Streamflow Calculation- East Fork Jemez River.

Corder, G. W., and Foreman, D. I. 2014. Nonparametric statistics: a step-by-step approach. John Wiley & Sons.

Dahm, C. N., Candelaria-Ley, R., Reale, C. S., Reale, J. K., and Van Horn, D. J. 2015. Extreme water quality degradation following a catastrophic forest fire. Freshwater Biology.

Dahm, C. N., Van Horn, D. J., Reale, J. K., Candelaria-Ley, R., and Reale, C. S. 2013. Continuous water quality monitoring of the Rio Grande and Rio Chama. University of New Mexico, Submitted to the U.S. Army Corps of Engineers, Albuquerque, NM.

DeBano, L. F. 2000. The role of fire and soil heating on water repellency in wildland environments: a review. Journal of Hydrology 231-232:195-206.

Earl, S. R., and Blinn, D. W. 2003. Effects of wildfire ash on water chemistry and biota in South-Western USA streams. Freshwater Biology 48:1015-1030.

Goff, F., Gardner, J. N., Reneau, S. L., and Goff, C. J. 2006. Preliminary geologic map of the Redondo Peak quadrangle, Sandoval County, New Mexico. New Mexico Bureau of Geology and Mineral Resources: Socorro, NM.

Goode, J. R., Luce, C. H., and Buffington, J. M. 2012. Enhanced sediment delivery in a changing climate in semi-arid mountain basins: implications for water resource management and aquatic habitat in the northern Rocky Mountains. Geomorphology 139:1-15.

Hall, R. O., Yackulic, C. B., Kennedy, T. A., Yard, M. D., Rosi-Marshall, E. J., Voichick, N., and Behn, K. E. 2015. Turbidity, light, temperature, and hydropeaking control primary productivity in the Colorado River, Grand Canyon. Limnology and Oceanography 60:512-526.

Hall, S. J., and Lombardozzi, D. 2008. Short-term effects of wildfire on montane stream ecosystems in southern Rocky Mountains: one and two years post-burn. Western North American Naturalist 68:453-462.

Healy, D. F. 1997. Water-quality assessment of the Rio Grande Valley, Colorado, New Mexico, and Texas: summary and analysis ofwater-quality data for the basic-fixed-site network, 1993-95. Pages 82. U.S. Geological Survey Water-Resources Investigations Report 97-4212.

Johnson, K. S., Needoba, J. A., Riser, S. C., and Showers, W. J. 2007. Chemical sensor networks for the aquatic environment. Chemical Reviews 107:623-640.

Khanna, P., Raison, R., and Falkiner, R. 1994. Chemical properties of ash derived from eucalyptus litter and its effects on forest soils. Forest Ecology and Management 66:107-125.

Kirchner, J. W., Feng, X. H., Neal, C., and Robson, A. J. 2004. The fine structure of water-quality dynamics: the (high-frequency) wave of the future. Hydrological Processes 18:1353-1359.

Krause, S., Lewandowski, J., Dahm, C. N., and Tockner, K. 2015. Frontiers in real-time ecohydrology–a paradigm shift in understanding complex environmental systems. Ecohydrology.

Lamberti, G. A., and Steinman, A. D. 1997. A comparison of primary production in stream ecosystems. Journal of the North American Benthological Society 16:95-104.

Landers, M. N., and Sturm, T. W. 2013. Hysteresis in suspended sediment to turbidity relations due to changing particle size distributions. Water Resources Research 49:5487-5500.

Leak, M., Passuello, R., and Tyler, B. 2003. I've seen fire. I've seen rain. I've seen muddy waters that I thought would never clear again. Waterworks 6:38-44.

Leggieri, L., Feijoo, C., Giorgi, A., Ferreiro, N., and Acuna, V. 2013. Seasonal weather effects on hydrology drive the metabolism of non-forest lowland streams. Hydrobiologia 716:47-58.

Lenzi, M. A., and Marchi, L. 2000. Suspended sediment load during floods in a small stream of the Dolomites (northeastern Italy). Catena 39:267-282.

Liu, F., Parmenter, R., Brooks, P. D., Conklin, M. H., and Bales, R. C. 2008. Seasonal and interannual variation of streamflow pathways and biogeochemical implications in semi-arid, forested catchments in Valles Caldera, New Mexico. Ecohydrology 1:239-252.

Loaiciga, H. A., Pedreros, D., and Roberts, D. 2001. Wildfire-streamflow interactions in a chaparral watershed. Advances in Environmental Research 5:295-305.

Lyon, J. P., and O'Connor, J. P. 2008. Smoke on the water: can riverine fish populations recover following a catastrophic fire-related sediment slug? Austral Ecology 33:794-806.

Malmon, D. V., Reneau, S. L., Katzman, D., Lavine, A., and Lyman, J. 2007. Suspended sediment transport in an ephemeral stream following wildfire. Journal of Geophysical Research-Earth Surface **112**:15.

Marlon, J. R., Bartlein, P. J., Gavin, D. G., Long, C. J., Anderson, R. S., Briles, C. E., Brown, K. J., Colombaroli, D., Hallett, D. J., and Power, M. J. 2012. Long-term perspective on wildfires in the western USA. Proceedings of the National Academy of Sciences 109:E535-E543.

McAda, D. P., and Barroll, P. 2002. Simulation of ground-water flow in the middle Rio Grande basin between Cochiti and San Acacia, New Mexico. Pages 81. US Department of the Interior, US Geological Survey.

Miller, W. W., Johnson, D. W., Gergans, N., Carroll-Moore, E. M., Walker, R. F., Cody, T. L., and Wone, B. 2013. Update on the effects of a Sierran wildfire on surface runoff water quality. Journal of Environmental Quality 42:1185-1195.

Moody, J. A., Shakesby, R. A., Robichaud, P. R., Cannon, S. H., and Martin, D. A. 2013. Current research issues related to post-wildfire runoff and erosion processes. Earth-Science Reviews 122:10-37.

Moore, S. J., and Anderholm, S. K. 2002. Spatial and temporal variations in streamflow, dissolved solids, nutrients, and suspended sediment in the Rio Grande Valley Study Unit, Colorado, New Mexico, and Texas, 1993-95. US Department of the Interior, US Geological Survey.

Mote, P. W., Hamlet, A. F., Clark, M. P., and Lettenmaier, D. P. 2005. Declining mountain snowpack in western north America. Bulletin of the American Meteorological Society 86:39.

Moyer, D. L., Anderholm, S. K., Hogan, J. F., Phillips, F. M., Hibbs, B. J., Witcher, J. C., Matherne, A. M., and Falk, S. E. 2013. Knowledge and understanding of dissolved solids in the Rio Grande–San Acacia, New Mexico, to Fort Quitman, Texas, and plan for future studies and monitoring. US Geological Survey.

Muldavin, E., Neville, P., Jackson, C., and Neville, T. 2006. A vegetation map of Valles Caldera National Preserve, New Mexico. Agreement No. 01CRAG0014. University of New Mexico, Albuquerque, NM.

Muldavin, E., and Tonne, P. 2003. A vegetation survey and preliminary ecological assessment of Valles Caldera National Preserve, New Mexico. Cooperative Agreement No. 01CRAG0014. University of New Mexico, Albuquerque, NM.

Murphy, J., Johnson, D., Miller, W., Walker, R., Carroll, E., and Blank, R. 2006. Wildfire effects on soil nutrients and leaching in a Tahoe Basin watershed. Journal of Environmental Quality 35:479-489.

Neary, D., Gottfried, G., and Viegas, D. 2002. Fires and floods: post-fire watershed responses. Forest fire research and wildland fire safety: Proceedings of IV International Conference on Forest Fire Research 2002 Wildland Fire Safety Summit, Luso, Coimbra, Portugal, 18-23 November 2002. Millpress Science Publishers.

New Mexico Environmental Department 2005. Water quality survey summary for the Jemez River watershed. Surface Water Quality Bureau, Santa fe, New Mexico.

New Mexico Water Quality Control Commission 2000. State of New Mexico standards for interstate and intrastate streams. New Mexico Environment Department. Santa Fe, New Mexico.

Nyman, P., Sheridan, G. J., Smith, H. G., and Lane, P. N. 2011. Evidence of debris flow occurrence after wildfire in upland catchments of south-east Australia. Geomorphology 125:383-401.

Oliver, A. A., Reuter, J. E., Heyvaert, A. C., and Dahlgren, R. A. 2012. Water quality response to the Angora Fire, Lake Tahoe, California. Biogeochemistry 111:361-376.

Ortiz, D., and Lange, K. M. 1996. New Mexico water resources data water year 1995. Pages 644. U.S. Geological Survey, Albuquerque, New Mexico.

Ortiz, R. M. 2004. A river in transition: geomorphic and bed sediment response to Cochiti Dam on the Middle Rio Grande, Bernalillo to Albuquerque, New Mexico. Unpublished MS thesis, Department of Earth and Planetary Science. The University of New Mexico, Albuquerque, NM.

Parsons, A. 2002. A. 2002. Mapping post-fire wildfire burn severity using remote sensing and GIS. Pages 9. Proceedings ESRI user conference. San Diego, CA.

Parsons, A., Robichaud, P. R., Lewis, S. A., Napper, C., and Clark, J. T. 2010. Field guide for mapping post-fire soil burn severity. U.S. Department of Agriculture, U.S. Forest Service, Rocky Mountain Research Station.

Passell, H. D., Dahm, C. N., and Bedrick, E. J. 2005. Nutrient and organic carbon trends and patterns in the upper Rio Grande. Science of the Total Environment 345:239-260.

Pausas, J. G., Llovet, J., Rodrigo, A., and Vallejo, R. 2009. Are wildfires a disaster in the Mediterranean basin?–A review. International Journal of Wildland Fire 17:713-723.

Pelletier, J. D., and Orem, C. A. 2014. How do sediment yields from post-wildfire debris-laden flows depend on terrain slope, soil burn severity class, and drainage basin area? Insights from airborne LiDAR change detection. Earth Surface Processes and Landforms 39:1822-1832.

Rhoades, C. C., Entwistle, D., and Butler, D. 2011. The influence of wildfire extent and severity on streamwater chemistry, sediment and temperature following the Hayman Fire, Colorado. International Journal of Wildland Fire 20:430-442.

Romme, W. H., Boyce, M. S., Gresswell, R., Merrill, E. H., Minshall, G. W., Whitlock, C., and Turner, M. G. 2011. Twenty years after the 1988 Yellowstone Fires: lessons about disturbance and ecosystems. Ecosystems 14:1196-1215.

Seager, R., Ting, M. F., Held, I., Kushnir, Y., Lu, J., Vecchi, G., Huang, H. P., Harnik, N., Leetmaa, A., Lau, N. C., Li, C. H., Velez, J., and Naik, N. 2007. Model projections of an imminent transition to a more arid climate in southwestern North America. Science 316:1181-1184.

Shafer, B. M. 2013. Multi-year measurement of wholestream metabolism in a snowmelt-dominated montane ecosystem. Water Resources Program, Professional Project. University of New Mexico, Albuquerque, New Mexico.

Shakesby, R. A., and Doerr, S. H. 2006. Wildfire as a hydrological and geomorphological agent. Earth-Science Reviews 74:269-307.

Sherson, L. R., Van Horn, D. J., Gomez, J. D., Shafer, B. M., Crossey, L. J., and Dahm, C. N. 2015. Nutrient dynamics in a headwater stream: use of continuous water quality sensors to examine responses to wildfire and precipitation events. Hydrologic Processes.

Smith, H. G., Sheridan, G. J., Lane, P. N., Nyman, P., and Haydon, S. 2011. Wildfire effects on water quality in forest catchments: a review with implications for water supply. Journal of Hydrology 396:170-192.

Spencer, C. N., and Hauer, F. R. 1991. Phosphorus and nitrogen dynamics in streams during a wildfire. Journal of the North American Benthological Society 10:24-30.

Stewart, I. T., Cayan, D. R., and Dettinger, M. D. 2004. Changes in snowmelt runoff timing in western North America under abusiness as usual'climate change scenario. Climatic Change 62:217-232.

Strahler, A. N. 1952. Hypsometric (area-altitude) analysis of erosional topology. Geological Society of America Bulletin 63:1117-1142.

Townsend, S. A., and Douglas, M. M. 2000. The effect of three fire regimes on stream water quality, water yield and export coefficients in a tropical savanna (northern Australia). Journal of Hydrology 229:118-137.

Trainer, F. W., Rogers, R. J., and Sorey, M. L. 2000. Geothermal hydrology of Valles Caldera and the southwestern Jemez Mountains, New Mexico. U.S. Department of the Interior U.S. Geological Survey

U.S. Army Corps of Engineers 2009. Final environmental assessment for a temporary deviation in the operation of Cochiti Lake and Jemez Canyon Dam, Sandoval County, New Mexico. Albuquerque District.

U.S. Geological Survey 2015. Current Conditions for New Mexico: streamflow.

Van Horn, D. J., and Reale, J. K. Unpublished. Stream metabolism of the Middle Rio Grande.

Van Horn, D. J., White, C. S., Martinez, E. A., Hernandez, C., Merrill, J. P., Parmenter, R. R., and Dahm, C. N. 2012. Linkages between riparian characteristics, ungulate grazing, and geomorphology and nutrient cycling in montane grassland streams. Rangeland Ecology and Management 65:475-485.

Vannote, R. L., Minshall, G. W., Cummins, K. W., Sedell, J. R., and Cushing, C. E. 1980. The river continuum concept. Canadian Journal of Fisheries and Aquatic Sciences 37:130-137.

Verkaik, I., Rieradevall, M., Cooper, S. D., Melack, J. M., Dudley, T. L., and Prat, N. 2013. Fire as a disturbance in mediterranean climate streams. Hydrobiologia 719:353-382.

Wagner, R. J., Mattraw, H. C., Ritz, G. F., and Smith, B. A. 2006. Guidelines and standard procedures for continuous water-quality monitors: Site selection, field operation, calibration, record computation, and reporting. Pages 51 + attachments. US Department of the Interior, US Geological Survey

Webster, J. R. 2007. Spiraling down the river continuum: stream ecology and the U-shaped curve. Journal of the North American Benthological Society 26:375-389.

Westerling, A. L., Hidalgo, H. G., Cayan, D. R., and Swetnam, T. W. 2006. Warming and earlier spring increase western US forest wildfire activity. Science 313:940-943.

Western Regional Climate Center 2014. Weather station daily summary VCNP Headquarters, New Mexico.

Williams, A. P., Allen, C. D., Macalady, A. K., Griffin, D., Woodhouse, C. A., Meko, D. M., Swetnam, T. W., Rauscher, S. A., Seager, R., Grissino-Mayer, H. D., Dean, J. S., Cook, E. R., Gangodagamage, C., Cai, M., and McDowell, N. G. 2012. Temperature as a potent driver of regional forest drought stress and tree mortality. Nature Climate Change 3:292-297.

Writer, J. W., and Murphy, S. F. 2012. Wildfire Effects on Source-Water Quality—Lessons from Fourmile Canyon Fire, Colorado, and Implications for Drinking-Water Treatment. Fact Sheet 2012-3095. U.S. Geological Survey.

Young, I. T. 1977. Proof without prejudice: use of the Kolmogorov-Smirnov test for the analysis of histograms from flow systems and other sources. Journal of Histochemistry & Cytochemistry 25:935-941.

Young, R. G., and Huryn, A. D. 1996. Interannual variation in discharge controls ecosystem metabolism along a grassland river continuum. Canadian Journal of Fisheries and Aquatic Sciences 53:2199-2211.

DIFFERENTIAL RESPONSES OF PAIRED CATCHMENTS TO CATASTROPHIC WILDFIRE: A MULTI-YEAR STUDY OF WATER QUALITY AND WHOLE-STREAM METABOLISM THROUGHOUT THE GROWING SEASON

Authors: Justin K. Reale[1,3], David J. Van Horn[1,4], Ricardo González-Pinzón[2,5], Matthew Segura[1,6], Mark C. Stone[2,7], Robert R. Parmenter[1,3,8], T. Scott Compton[3,9] Clifford N. Dahm[1,10]

[1] Department of Biology, University of New Mexico, Albuquerque, NM, U.S.A.

[2] Department of Civil Engineering, University of New Mexico, Albuquerque, NM, U.S.A.

[3] Valles Caldera National Preserve, National Park Service, Jemez Springs, NM, U.S.A.

Email Addresses: [3] jreale@unm.edu ; [4] vanhorn@unm.edu; [5] gonzaric@unm.edu; [6] msegur01@unm.edu; [7] stone@unm.edu; [8] robert_parmenter@nps.gov; [9] scott_compton@nps.gov; [10] cdahm@unm.edu

Abstract

Post-fire effects on hydrologic and geomorphic processes are known to alter the sediment loads and water quality of burned catchments and downstream riverine ecosystems. However, the lack of high-frequency and long-term data prior to and following a wildfire limits our understanding of how ecosystem processes respond and recover over time. Using nine years of high-frequency water quality parameters collected during the growing season, combined with streamflow and meteorological records, we analyzed the variability of water quality parameters and their effect on gross primary productivity (GPP) and ecosystem respiration (ER) in two, nearly identical and paired headwater streams, before (3 years of data) and after (6 years of data) a catastrophic wildfire. Pre-fire, we observed a positive correlation between GPP and ER (r^2 >0.4) in the low-turbidity (< 10 NTU) streams. Immediately following the wildfire, both streams had elevated turbidity (3 to 25x pre-fire) and specific conductance (2x pre-fire), > 20% reduction in GPP, < 10% reduction in ER, and positive correlations between GPP and ER (r^2 >0.6). We found that the shorter-term (1 to 3 years post-fire) turbidity, GPP and ER estimates, and mechanisms influencing GPP and ER

were different between the two streams, while the longer-term (4 to 5 years post-fire) responses suggest that both systems returned to near pre-fire conditions. To link our results with catchment hydrology, we analyzed watershed, stream, and wildfire characteristics. Paradoxically, we found that the water quality and ecosystem responses (via metabolism) to the wildfire of these nearly identical streams were different and likely controlled by watershed-specific hydrologic connections with their landscapes. Thus, accounting for such degree of specificity still remains a relevant, open challenge for predicting watershed-scale effects of wildfire disturbances on aquatic ecosystems.

Keywords: whole-stream metabolism, ecosystem respiration, primary production, wildfire, continuous monitoring, headwater streams, water quality.

Introduction

Forested watersheds in the western United States are currently experiencing climate-change-mediated increases in aridity, variability in precipitation patterns, and air temperatures (Cayan and others, 2001; Stewart and others, 2004; Seager and others, 2007). These conditions have resulted in drought-stressed trees with greater susceptibility to disease (Raffa and others, 2008; Weed and others, 2013), increased forest mortality (Breshears and others, 2005; Allen and others, 2010; Williams and others, 2010), and subsequent elevated risk of forest fires. For example, reduced winter precipitation, earlier and faster spring snowmelt, and elevated spring and summer temperatures resulted in extended fire seasons and increased wildfire activity during each decade since the 1970's in western US forests (Westerling and others, 2006; Westerling, 2016). The trend of increased wildfire activity, which is influenced by climatic conditions (Westerling and others, 2003; Flannigan and others, 2009), has significant implications for aquatic ecosystems impacted by wildfire (Gresswell, 1999; Bisson and others, 2003).

Following catastrophic wildfires, substantial portions of the landscape are denuded of vegetation, resulting in hydrological and stream geomorphological instability (Shakesby and Doerr, 2006) including increased overland and debris flows (Moody and Martin, 2001a; Cannon and others, 2008), and elevated mobilization and transport of ash, charcoal, soil and nutrients (Mast and Clow, 2008; Sherson and others, 2015). The magnitude,

frequency, and duration of these events depend on complex relationships between antecedent aridity, burn severity, soil type, land use and land cover, topography, post-fire precipitation patterns, and climate (Moody and Martin, 2001a; Shakesby and Doerr, 2006). Rehabilitation treatments may also influence post-fire sediment yields and flooding (Robichaud and others, 2000; Wagenbrenner and others, 2006). The post-fire hydrologic and geomorphic alterations have the potential to severely impact water quality as recently summarized (Smith and others, 2011b; Bixby and others, 2015; Martin, 2016). For example, post-fire ash and sediment transport results in elevated levels of suspended sediment (Reneau and others, 2007; Goode and others, 2012), turbidity (Murphy and others, 2012; Mast and others, 2016), major ions and specific conductance (Dahm and others, 2015; Reale and others, 2015), nutrients (Betts and Jones, 2009; Sherson and others, 2015), and dissolved and particulate organic matter (Mast and Clow, 2008; Betts and Jones, 2009). Additionally, the loss of riparian canopy cover from the initial burns and from subsequent debris flows (Cannon and others, 2001; Cannon and others, 2008) increases solar radiation and water temperatures (Isaak and others, 2010; Mahlum and others, 2011). Although all of these alterations are known to affect key aquatic ecosystem variables, there is limited information about the long-term effects of wildfires on stream ecosystem processes and on the spatial and temporal recovery of these processes in burned watersheds.

Estimates of stream metabolic state (i.e., gross primary production (GPP) and ecosystem respiration (ER)) are integrative metrics of stream function and embed numerous key factors affected by wildfires across a range of spatial and temporal scales. These factors include channel hydraulics (Mulholland and others, 2001) and geomorphology (Bott and others, 2006), groundwater-surface water interactions (González-Pinzón and others, 2014), photosynthetically active radiation (Bott and others, 2006; Hall and others, 2015), turbidity (Izagirre and others, 2008; Hall and others, 2015), water temperature (Demars and others, 2011; Dodds and others, 2013), nutrient concentrations (McTammany and others, 2007; Bernot and others, 2010) and organic matter supply (Young and Huryn, 1999; Roberts and others, 2007). While many of these factors are likely to be affected by wildfire impacts to stream ecosystems, very few studies have assessed the effects of wildfire on whole-stream metabolism, and the reported

impacts are variable and appear to be contextual (Betts and Jones, 2009; Davis, 2015; Tuckett and Koetsier, 2016).

We use long-term, high-frequency water quality data with supporting physical data to determine pre- and post-fire variations in water quality and whole-stream metabolism in two adjacent second-order streams that were similarly impacted by a large catastrophic wildfire in 2011. Data for river stage, meteorological parameters, and water quality are used to estimate daily rates of GPP and ER to compare the response of these two streams throughout the growing season (typically May through October) over nine years. The goals of this study are to 1) assess water quality and whole-stream metabolism during the growing season for multiple years prior to a severe wildfire, 2) determine the immediate (year one), shorter-term (years two to four) and longer-term (years five and six) impacts of the wildfire on water quality and whole-stream metabolism, and 3) identify mechanisms that influence in-stream metabolic processes during pre- and post-fire conditions.

Materials and methods

Watershed and site descriptions

The 1.25 million year-old (Goff and others, 2006), 21 km wide Valles Caldera (VALL) is located in the volcanic Jemez Mountains of north-central New Mexico, USA (Fig. 1; see https://www.nps.gov/vall/index.htm) . The elevation within the VALL ranges from 2300 m at Redondo Meadow to 3432 m at Redondo Peak, a resurgent volcanic dome (Heiken and others, 1990). The elevational gradient results in high variability in the vegetation communities that include spruce and fir forests above 2740 m; Ponderosa pine (*Pinus ponderosa*) and oak forests below 2740 m, and montane grasslands, wet meadows and wetlands on valley floors (Muldavin and others, 2006). The soils in the VALL are generally classified as forest (andisols, alfisols, and inceptisols) and grassland (mollisols) soils (Muldavin and Tonne, 2003).

After the collapse of the volcano about 1.25 million years ago, resurgent domes (Smith and others, 1970; Phillips and others, 2007) bisected the VALL into two, nearly identical, paired watersheds (Liu and others, 2008): the East Fork Jemez River (EFJR) and the Rio San Antonio (RSA)(Fig. 1). The geomorphology of the EFJR and RSA is highly sinuous (sinuosity index of 1.5 and 2.8, respectively), with low width to depth ratios (11.8

and 10.5, respectively), and low gradients (0.12 and 0.22%, respectively) and readily access their floodplain. Riparian vegetation on both streams within the VALL is dominated by sedges and grasses, and lacks a canopy (Simino, 2002; NMED, 2005; Joseph and Henderson, 2006; Van Horn and others, 2012). Subsurface flow and groundwater contribute the majority of the discharge to both streams, except during the snowmelt pulse and intense monsoonal thunderstorm events when overland flows occur (Liu and others, 2008).

Both the EFJ and RSA have similar mean concentrations of total nitrogen, ammonium and total phosphorus (Liu and others, 2008; Van Horn and others, 2012) and nitrogen is the limiting nutrient for primary production (Van Horn and others, 2012). Submerged Aquatic Macrophyte (SAM) taxa (i.e., *Elodea canadensis*, *Ranunculus aquatilis*, *Potamogeton richardsonii and Stuckenia pectinata*) dominate the primary producer community and are prevalent throughout the growing season, along with periodic algal blooms dominated by green algae (*Cladophora* sp.) and epiphytic algae on the SAM taxa (Thompson et al., unpublished data).

In June through July of 2011, the Las Conchas (LC) fire burned approximately 63,370 hectares of forest, high elevation montane grassland, and meadows in the Jemez Mountains. The burn severity of the LC fire was approximately 20% high, 26% moderate, 39% low, and 15% unburned (Fig. 1c). Following the LC fire, elevated overland flow resulted in rill formation, extensive erosion and deposition, channel incision and avulsion, and debris flows in watersheds within the VALL (Pelletier and Orem, 2014; Orem and Pelletier, 2015).

Continuous measurements

Water quality parameters (i.e., dissolved oxygen (DO), turbidity, specific conductance (SC), pH, and temperature) were collected at 15-minute intervals using YSI 6920 sondes (Yellow Springs Instruments Inc. /Xylem Inc., Yellow Springs, OH, U.S.A.). The sondes were deployed from mid-April to mid-November, with year-to-year variability depending on hydroclimatic conditions (e.g., ice cover, snowpack and snowmelt). Site visits were made every two to four weeks to clean and calibrate the sondes following USGS standard operating procedures (Wagner and others, 2006). Water quality data were

compiled, validated, and corrected for fouling and drift using Aquarius Time-Series 3.3 (Aquatic Informatics, Vancouver, British Columbia, Canada).

Barometric pressure was obtained from the VALL Headquarters climate station (WRCC, 2016), and corrected using the hydrostatic equation (Barry and Chorley, 2003) to estimate site-specific values. Total solar irradiance (SI) data were obtained from the Rio San Antonio and Headquarters climate stations (WRCC, 2016). Photosynthetically active radiation (PAR) was calculated following (Meek and others, 1984).

Stream depth and discharge

Stage measurements and associated discharge estimates were collected on for the EFJR and RSA at flumes within 1.5 km of the sonde deployment sites (Fig. 1). Rating curves near the flumes were also developed to estimate discharge when flows exceeded the capacity of the flume (Condon & Compton, unpublished data). Due to data gaps in the discharge records at the flumes, and high flows, we estimated daily mean discharge for the EFJR and RSA using data from the Jemez River (JR) USGS gage (no. 08324000) located near Jemez Springs, New Mexico (Fig. 1b), using Equation 1 (Gupta, 2014):

$$Q_{EFJR\ or\ RSA} = \frac{Q_{JR}}{A_{JR}} \times A_{EFJR\ or\ RSA} \qquad\qquad \text{Equation 1}$$

where Q_{JR} is daily average discharge measured for JR ($m^3\,s^{-1}$); A_{JR} is the drainage area (1217 km^2) for the JR gage; A_{EFJR} and A_{RSA} are the drainage areas calculated from the location of the sondes (100 and 146 km^2, respectively); Q_{EFJR} and Q_{RSA} are the average discharges estimated for the EFJR and RSA. The rating curves allowed us to relate our daily estimates of Q_{EFJR} and Q_{RSA} with stage values (r^2=0.97 and 0.90, respectively), and estimate daily mean stream depth.

Stream metabolism model

15-minute interval diel DO profiles and environmental variables (water temperature, water salinity, atmospheric pressure, and PAR) were used in the BAyesian Single-station Estimation (BASE V2) modeling package (Grace and others, 2015) to estimate daily mean GPP and ER values at the location of the sondes (Fig. 1). The model estimates metabolic parameters by using the day-time regression method (Kosinski, 1984),

applies temperature, barometric pressure and salinity corrections for 100% DO saturation (Grace and Imberger, 2006), and accounts for the temperature dependency of the respiration and reaeration constants by using mean daily temperature during the model fitting (see Grace et al. 2015). BASE V2 incorporates changes to the model structure following findings of Song and others (2016).

BASE V2 models changes in DO directly using:

$$[DO]_{t+1} = [DO]_t + AI_t^p \text{-} R(\theta^{(T_t - \overline{T})} + K_{DO} * (1.0241^{(T_t - \overline{T})}) * ([DO]_{sat,t} \text{-} [DO]_{mod,t})$$

Equation 2

where t indicates the time interval in the diel profile (15-min). The GPP term is AI_t^p (mg O_2 L^{-1} d^{-1}) where A (-) is a constant that represents GPP per quantum of light, I (μ mol $m^{-2}s^{-1}$) is the incident light intensity, p (-) is an exponent describing the ability of the primary producers to use the incident light and accounts for saturating photosynthesis. R (mg O_2 L^{-1} d^{-1}) is the instantaneous respiration rate, θ (-) describes temperature dependence of respiration, T (°C) is water temperature, $\overline{T}$ (°C) is the mean water temperature over the 24-hour period (°C), K_{DO} (day^{-1}) is the estimated reaeration coefficient, and $[DO]_{sat,t}$ and $[DO]_{mod,t}$ (% saturation) indicate 100% saturation measured concentration and modeled concentration for time t.

We ran 100,000 model iterations and used 50,000 burn-in ('settling') iterations to improve model convergence. We multiplied volumetric GPP and ER (mg O_2 L^{-1} d^{-1}) by estimated daily mean stream depth to convert them to areal (g O_2 m^{-2} d^{-1}) or flux estimates. We followed the developer's guide for model validation (see Supplementary Material in Grace et al. (2015) for details). In addition, we used the measured versus predicted diel DO curves along with measured water temperature and PAR data to confirm curve fits and identify discrepancies in the data or model.

Periods of analysis and statistical methods

We evaluated water quality and whole-stream metabolism throughout the growing season (i.e., longer time scale) to determine the immediate (2011), shorter-term (2012-2014) and longer-term (2015-2016) within-stream effects of wildfire to pre-fire (2008-2011) conditions. We included all days during the growing season from each year that produced reliable metabolism estimates, resulting in an annual range of 76 to 137 days

over a nine-year period with a mean of 104 days on the EFJR, and a range of 72 to 143 days and a mean of 112 days on the RSA (SI Table 1). We filtered the results to include only overlapping days to compare the immediate, shorter- and longer-term responses between the EFJR and RSA. This resulted in an annual range of 60 to 137 days and a mean of 100 days (SI Table 1).

All statistics were implemented in RStudio (RStudio Team, 2015). We calculated the average pre-fire mean value and equi-tailed 90th percentile, two-sided, non-parametric confidence intervals for each stream to define pre-fire conditions. We selected the 90th, rather than the 95th percentile, based on the precautionary principle (Fairweather, 1991; Greystone, 1996). The confidence intervals were calculated using the Package *boot* (Canty and Ripley, 2016), from which we could compare the average pre-fire conditions to the post-fire response each year through 2016. Linear models were used to identify mechanisms that influenced in-stream metabolic processes pre- and post-fire.

Geospatial analyses

ArcGIS (ESRI 2011. ArcGIS Desktop: Release 10. Redlands, CA: Environmental Systems Research Institute) was used to evaluate and compare the watershed characteristics of the EFJR, RSA and their tributaries in relation to the LC fire. We used Hydrologic Unit Codes (HUCs) to delineate each watershed and sub-watershed (USGS, 2014). The HUCs, in combination with the fire maps, allowed us to quantify the total area burned and the area within each burn severity category within each watershed. We used streamlines (USGS, 2016), along with the HUCs and fire maps, to quantify the number of stream kilometers within the burned areas. This value represents the length of stream within a watershed that can directly contribute material to the stream if overland flows were to occur. We estimated stream gradients using a 1-m digital elevation model (USGS, 2017). These results were used to classify streams into low (0.00-0.07), medium (0.07-0.14) and high (0.14 to 0.22) gradient (m km^{-1}) reaches within the burned area, which influences sediment entrainment, transport, and deposition (Bull, 1979). Finally, we measured the distance in river-km from moderate or high burn severity areas to the confluence with the main stem for each impacted watershed (i.e., EFJR or RSA) to quantify the proximity of the disturbance to the main stem. These distances, in combination with the corresponding stream gradient

for these reaches, were used to evaluate the potential transport of burn scar material from the impacted tributaries to the main stem.

Results

Pre-fire water quality and stream metabolism

Pre-fire, daily mean water temperature for the EFJR and RSA (light gray in Fig. 2a & 2e, respectively) varied between and within years, and lacked an apparent trend (Table 1). Additionally, the means, standard deviations and confidence intervals were similar between streams within a given year (Fig. 2 & Table 1), and the observed temperatures from both streams were highly correlated with each other (r^2=0.91) and tightly centered on the 1:1 line (Fig. 4a). For SC, we observed a general trend of increasing mean values and minimal within-year variance for both streams (Fig. 2b & 2f,). While SC data from the two streams were correlated (r^2=0.42; Table 1), the pre-fire values for the RSA were consistently higher than those observed in the EFJR (270 days or 99.6% above the 1:1 line shown in Fig. 4b). The pre-fire turbidity values had very low means and standard deviations for both streams (Table 1, Fig. 2c & 2g). However, values for the EFJR were consistently higher (161 days or 60% below 1:1 line) than those observed in the RSA (Table 1, Fig. 4c). Pre-fire pH values varied between and within years on both streams (Fig. 2d & Fig. 2h) with values from the RSA being slightly elevated (231 days or 85% above the 1:1 line) as compared to those measured in the EFJR (Table 1, Fig. 4d).

Pre-fire GPP and ER on the EFJR (Fig. 3a & 3b, respectively) and RSA (Fig. 3c & 3d, respectively) exhibited variability within and between years and lacked clear inter-annual trends (Table 1 & Fig. 3). ER and GPP values were positively and significantly correlated for both the EFJR (r^2=0.78) and the RSA (r^2=0.47) (Fig. 6). We observed a positive correlation between GPP and ER versus water temperature (SI Fig. 1 & 2, respectively) on the EFJR (r^2=0.36 & 0.41, respectively) and no correlation on the RSA (r^2=0.08 & 0.16, respectively). Metabolism values on both rivers were not strongly correlated with turbidity (Fig. 7) or SC (SI Figure 3 & 4). GPP and ER values between the streams were not strongly correlated (r^2= 0.03 and 0.16, respectively) with each other. While there was a similar distribution of GPP values around the 1:1 line, with 158 days (58%) above and 113 days (32%) below, ER

52

values were consistently higher in the EFJR than in the RSA (235 days or 87% below the 1:1 line) (Fig. 4e & f).

Post-fire water quality and stream metabolism responses

Post-fire, daily mean water temperature on the EFJR and RSA were similar to pre-fire conditions. The strong between-stream correlation persisted (Fig. 4a), and no immediate, shorter-term or longer-term post-fire effects were observed with regards to temperature (Table 1, Fig. 2a & 2e). In contrast, SC concentrations (an indicator of total dissolved solids) increased from pre-fire averages on the EFJR and RSA (Table 1, Fig. 2b & 2f). While values remained elevated through 2016, the greatest increase (nearly double the pre-fire mean) was observed in 2011, the year of the fire. Immediately following the fire, the SC values in the RSA increased above those observed in the EFJR. However, the values for the two streams in subsequent years were well correlated (Table 1, Fig. 4b). Post-fire turbidity on the EFJR (Fig. 2c) was greater than pre-fire conditions (i.e., 20-52 NTU greater than the pre-fire mean) through 2014 and converged to pre-fire averages in 2015 and 2016 (Table 1). The greatest increase in turbidity on the EFJR occurred in 2012, the year after the fire. Turbidity on the RSA (Fig. 2g) was greater than during pre-fire conditions through 2016 (Table 1). The greatest increase in turbidity on the RSA occurred in 2013, two years after the fire. Post-fire turbidity values were higher for the RSA than for the EFJR, a trend that persisted through 2016 (Table 1, Fig. 4c). Similarly, episodic turbidity spikes following monsoon precipitation events on the RSA continued through 2016, with a maximum value of 175 NTU in 2016 (Reale et al., unpublished data). The post-fire pH values on the EFJR and RSA (Fig. 2d & 2h, respectively) both decreased as compared to pre-fire values. However, the decline in the EFJR did not begin until 2013 and values had returned to baseline by 2016, while for the RSA, pH values remained lower from 2012 through 2016.

Mean GPP post-fire on the EFJR remained within the pre-fire confidence interval, with the exception of values for 2012 and 2013, which were elevated (Fig. 3a). In contrast, GPP post-fire on the RSA was below the pre-fire confidence limit for all years except 2015 (Fig. 3c). On the EFJR, the correlation between turbidity and GPP remained weak ($r^2 < 0.14$) and flat in 2011, 2012 and 2015 (Fig. 7) but varied along with the magnitude of the slope in 2013 (negative slope), 2014 (negative slope) and 2016 (positive slope) (Fig. 7). On the RSA,

we observed a negative correlation between turbidity and GPP ($r^2 > 0.3$) post-fire through 2014, no correlation in 2015, and a positive correlation in 2016 (Fig. 7). On the EFJR, we observed a positive correlation between GPP and temperature (SI Fig. 1) in 2011, 2012 and 2016 ($r^2 \geq 0.40$). GPP on the RSA continued to not be correlated with SC (SI Figure 1). We also found no correlation between GPP and SC on the EFJR or RSA post-fire (SI Fig. 3), with the exception of negative correlations during 2013 on the EFJR ($r^2 = 0.53$) and 2011 through 2013 on the RSA ($r^2 \geq 0.39$). While for pre-fire conditions paired GPP values from the two streams had been approximately equally distributed above and below the 1:1 line, for post-fire conditions the majority of the values for the EFJR were higher than those for the RSA (559 days or 90% below the 1:1 line) (Table 1, Fig. 4e & 5a). Additionally, the pre-fire seasonal pattern of a peak in GPP occurring during summer months was not observed on the RSA post-fire during 2011 – 2013. Instead, GPP values remained low and consistent throughout the growing season (Fig. 5a).

Daily mean post-fire ER on the EFJR (Fig. 3b) was within the pre-fire confidence interval in 2011 and 2016, and elevated in 2012 through 2015, while post-fire ER on the RSA (Fig. 3d) remained below the pre-fire confidence interval until 2014, was higher in 2015 and went back to near pre-fire conditions in 2016. Daily values of post-fire ER and GPP on the EFJR were positively correlated through 2016. However, this relationship weakened in 2013 through 2015 with numerous high ER values on days with low GPP estimates (Fig. 4). In 2016, the post-fire ER vs. GPP relationship strengthened with fewer days when ER was high and GPP was low (Fig. 4). In the RSA, post-fire ER and GPP were positively correlated, but the range of the relationship was greatly constrained in 2012 and 2013 as a majority of daily GPP and ER values remained below the pre-fire mean (Fig. 4). In 2015, and to a lesser extent in 2014 and 2016, higher ER values for the RSA were observed and corresponded to an increase in daily GPP values (Fig. 4). Daily mean ER was generally not correlated with water temperature on the EFJR or RSA (SI Fig. 2), with the exception of 2011, 2012 and 2016 on the EFJR when they were positively correlated ($r^2 \geq 0.40$). ER for both ecosystems did not correlate with SC (SI Figure 4). As with the pre-fire data, ER values for the EFJR were higher than those for the RSA. However, the discrepancy increased from 2011-2015 post-fire (Table 1, Fig. 4e & 5b). Additionally, as with GPP, the pre-fire seasonal pattern of a peak in ER occurring during summer months was not observed on the RSA

post-fire during 2011 – 2013, i.e., ER values remained low and consistent throughout the growing season (Fig. 5b).

Geospatial analyses

The LC fire burned approximately 31% (31 km^2) of the EFJR watershed upstream of the sonde (100 km^2) with approximately 28% (28 km^2) of the burn area classified as moderate or high severity (Table 2). Within the EFJR watershed, 25% of the total stream length was contained within the burn perimeter, with 0, 9 and 16% within high, moderate, and low severity burned areas, respectively. This watershed is divided into two sub-watersheds, the Upper East Fork of the Jemez River and the Jaramillo watersheds.

The Upper East Fork of the Jemez River watershed (i.e., upstream of the confluence with Jaramillo Creek) is a low-gradient, highly sinuous system encompassing the Valle Grande, with an average longitudinal slope of 0.01 m km^{-1} (Fig. 1c). Within this sub-watershed, approximately 27% of the area was burned with 24% moderate or high burn severity (Table 2). Also, the LC fire did not impact any medium or high gradient stream reaches in this sub-watershed and only 3.2 river-km of low gradient stream (Fig. 1c,d & Table 3). A total of 57% (22.6 km^2) of the second sub-watershed, the Jaramillo watershed, was burned, with 51% (20 km^2) classified as moderate or high severity (Table 2). The western and southern portions of the Jaramillo watershed are predominantly low gradient, and were not impacted by the LC fire (Fig. 1d & Table 3). The eastern portion of the sub-watershed was impacted, including 4.9 river-km of medium gradient stream (Fig. 1d & Table 3). Downstream of these fire-impacted tributaries, the Jaramillo Creek is a low gradient and highly sinuous stream that travels 3.5 km before the confluence (Fig 1d) with the EFJR. New Mexico highway 4 (NM4) bisects the southern portion of the EFJR watershed and served as a firebreak during the LC fire and continues as a likely ash/debris break during the post-fire years. The road's shoulder and drainage system intercept downslope movement of ash and debris, disconnecting the hillslope burned areas and the EFJR (Fig. 1c).

The LC fire burned approximately 33% (49 km^2) of the RSA watershed upstream of the sonde (146 km^2) with approximately 26% (38 km^2) classified as moderate or high severity (Table 2). Upstream of the sonde, 61% of the total stream length was contained

within the burn perimeter, with 8, 26, and 27% within high, moderate, and low severity burned areas, respectively. Within the RSA watershed, approximately 28% (5.2 km^2) of Rito de Indios (Indios) and 64% (31.7 km^2) of the upper RSA (i.e., upstream of the confluence with Indios) sub-watersheds were burned (Fig. 1d and Table 2). Approximately 21% (4 km^2) and 51% (25 km^2) of the Indios and upper RSA sub-watersheds were classified as moderate or high severity burn, respectively (Table 2). The mainstem of Indios is predominantly a low gradient system, highly sinuous system, with a longitudinal slope of 0.05 (Fig. 1d & Table 3). However, the LC fire impacted several tributaries of Indios that are medium (8.6 river-km) and high (1.8 river-km) gradient. We estimated that the distance from the burn scar within the Indios to the confluence of the RSA was 0.37 river-km and classified this segment as low stream-gradient (Fig. 1d and Table 3). Similarly, the mainstem of the upper RSA is a low-gradient, highly sinuous system, with a longitudinal watershed slope of 0.09 (Fig. 1d, Table 2 & 3). However, the LC fire impacted several tributaries of the upper RSA (Fig. 1d) that are medium (5.3 river-km) and high (2.2 river-km) gradient.

Discussion

This study compares 3 years of pre-fire data with immediate (same year), shorter-term (1-3 years after) and longer-term (4-5 years after) water quality and whole-stream metabolism responses to wildfire in two open-canopy, low-nutrient, low-gradient streams within a large volcanic caldera. The catchments for these streams had very similar burn extent and severity during a large-scale, catastrophic wildfire that occurred in the summer of 2011. We estimated large between-stream variation in ecosystem metabolism within the two catchments in response to differential hydrologic, physical, chemical and biological drivers and their interactions over time. This study adds to the growing list of long-term ecosystem metabolism studies for streams based on dissolved oxygen sensor technology and advances in stream metabolism modeling (Grace and others, 2015; Appling and others, 2016).

Annual to multi-year stream metabolism studies have been reported for intermittent Mediterranean streams (Acuna and others, 2004), deciduous forested headwater streams (Roberts and others, 2007), montane streams (Birkel and others,

2013), urban streams (Smith and Kaushal, 2015; Larsen and Harvey, 2017), and agricultural streams (Griffiths and others, 2013; Roley and others, 2014). This study expands the range of multi-year stream metabolism to two open-canopy, high-light, high-elevation, montane streams, where metabolism studies are few, and overlays the impacts of a catastrophic wildfire on the recovery of these stream ecosystems over a five-year period.

To our knowledge, this study is the first multi-year water quality and whole-stream metabolism study linked to one major wildfire. Previous stream metabolism studies after wildfire have been carried out for one summer period at different times post-fire (Betts and Jones, 2009; Davis, 2015; Tuckett and Koetsier, 2016). These previous studies on the effects of wildfires on stream metabolism provide interesting insights on the responses of various catchments to wildfire at different points in time after disturbance. For example, Betts and Jones (2009) showed that a large wildfire affecting a stream in a boreal forest in Alaska doubled the rates of stream gross primary production and elevated stream respiration rates the summer after the fire, compared to unburned reference sites. Davis (2015) surveyed 18 streams in Idaho wilderness areas with varying fire histories during one summer and found that the extent of post-fire riparian canopy recovery strongly influenced stream metabolic state. Tuckett and Koetsier (2016) studied stream ecosystem metabolism in 31 streams with varying fire histories within the Boise River watershed (Idaho, USA) between July 14 and August 21 of 2005 and found that streams that experienced debris flows after wildfire had higher rates of gross primary production and lower rates of ecosystem respiration. Contrary to the existent literature, our study, based on continuous growing season data that started before a major catastrophic fire in 2011 and extends for five years after the fire, allows a more continuous look at stream ecosystem metabolism and recovery, and facilitates a comparison of recovery trajectories in streams in adjacent catchments.

Immediate responses to hydrologic and geomorphic alterations (2011)

The EFJR and RSA watersheds experienced extensive and rapid hydrologic and geomorphic changes during the first few months following the LC fire. Elevated post-fire peak stream discharges were documented following short-duration, high-intensity monsoon rainfall events, resulting in elevated turbidity and solute concentrations (Reale

and others, 2015; Sherson and others, 2015). During these post-fire storms, several studies documented the removal of ash, charcoal and litter from hillslopes, rill and gully formation, channel incision and scour, all of which resulted in debris-laden flood events that transported and deposited material from the upland watershed onto the low-gradient valley streams (Pelletier and Orem, 2014; Orem and Pelletier, 2015). The combination of the LC fire and the subsequent storm disturbances operating at the hillslope to watershed-scales resulted in elevated erosion rates, additional sources of sediment and ash (Orem and Pelletier, 2016), and subsequently elevated SC (Fig. 2b & c) and turbidity concentrations (Fig. 2f & g). These hydrological and geomorphological impacts and subsequent water quality responses are not unique to the LC fire, as similar post-fire and post-storm elevated peak discharges (Moody and Martin, 2001b; Veenhuis, 2002), accelerated geomorphic processes and debris flows (Cannon and others, 2001; Moody and Martin, 2001a), elevated levels of suspended sediment (Reneau and others, 2007; Goode and others, 2012), and elevated turbidity (Rhoades and others, 2011; Murphy and others, 2012; Mast and others, 2016) and solutes (Mast and Clow, 2008; Mast and others, 2016) have been well documented in other catchments. However, no studies have continuously evaluated the immediate, shorter- and longer-term post-fire impacts to stream metabolism after a major forest fire.

The immediate documented decline in post-fire GPP in both streams can be attributed to numerous factors shown to decrease GPP in other stream studies. These include the alteration of geomorphic characteristics such as changes in stream width and depth (Sweeney and others, 2004; Bott and others, 2006), bed movement with associated dislodgment of biofilms and aquatic macrophytes (Atkinson and others, 2008; Gerull and others, 2012), the occurrence of destructive debris flows (Tuckett and Koetsier, 2016), and reduced light availability (Izagirre and others, 2008; Hall and others, 2015). The observed reductions in GPP due to these physical impacts also were likely linked to the reduced ER in both streams. Ecosystem production and respiration were closely coupled in our study systems pre-fire (Fig. 4), and these parameters are closely connected in other open-canopy, low gradient mountain streams (Hotchkiss and Hall, 2015). In contrast to our results, Betts and Jones (2009) documented an increase in GPP due to elevated concentrations of limiting nutrients and elevated ER due to additional DOC or extent of the hyporheic and transient

58

storage zone immediately following a wildfire. It appears that elevated discharge and turbidity (reducing light availability) observed in the EFJR and RSA outweighed the priming effects of elevated dissolved nutrients on primary producers in headwaters streams that are sometimes detected during the first few weeks following wildfire (Hauer and Spencer, 1998).

Differential shorter-term responses to fire impacts (2012-2014)

We observed several differential responses between the two streams for both water quality and stream metabolism parameters during the shorter-term period (2012-2014) following the fire. In the EFJR, the observed decline in turbidity as compared to immediate post-fire conditions (Fig. 2c) and the associated increase in GPP (Fig. 3a) and ER (Fig. 3b) above pre-fire mean values suggest that several previously documented responses are occurring. These include 1) a rapid decline in the transport of sediments from the landscape into streams during the second year after the fire (Lavine and others, 2006; Smith and others, 2011a), 2) a reduced potential for debris flows and floods as vegetation stabilizes hillslopes and material previously transported from initial debris flow events (Cannon and others, 2011; Kean and others, 2013), and 3) a likely fertilization effect of in-stream primary producers (Silins and others, 2014; Cooper and others, 2015) from the nutrient rich ash and sediment deposited post-fire (Bodi and others, 2014; Emelko and others, 2016).

Our geospatial analyses suggest that low terrain and stream gradient, large percentage of the watershed that was classified as low to moderate burn severity, and considerable portions of the watershed that were unburned (Fig. 1, Table 2 & 3) likely contributed to the rapid water quality recovery of the EFJR (Fig. 2 & Table 1). In addition, rapid regrowth of herbaceous vegetation (grasses and forbs) in the valleys and low gradient slopes of burned forest (Parmenter and others, 2012; Suazo, 2016) likely further accelerated the rate of recovery. Tributaries to the Jaramillo Creek, the other major upstream contributor to the EFJR, were more severely burned, had higher stream gradients, and have been identified as having high (>80%) probability of debris flows (Tillery and Haas, 2016). However, the ~4 km of Jaramillo Creek upstream of the confluence with the EFJR are low gradient, likely buffering and dissipating post-fire pulses

and promoting sediment deposition prior to reaching the EFJR (Figure 1d, Tables 2 & 3). Additionally, the highway present along the southern edge of the fire may also have redirected overland flow, further minimizing the impacts of the post-fire activity on the EFJR.

In contrast, the multi-year suppression of ER and GPP in the RSA suggests that different mechanisms were at play in this watershed for the first few years after the wildfire. The observed elevated turbidity, which is significantly and negatively correlated with GPP post-fire (Fig. 7), likely suppressed both GPP and ER (Fig. 3 & 5). GPP and ER are tightly linked in this system, suggesting that 1) there is continued transport of sediment from the hillslope into the stream (Reneau and others, 2007; Orem and Pelletier, 2016), and/or 2) there is continued re-suspension of ash, charcoal and fine sediments deposited into the stream even during low flow conditions (Ryan and others, 2011). Either of these possibilities could outweigh the positive influence of elevated nutrients on post-fire primary production (Hauer and Spencer, 1998). Our geospatial analyses identified high gradient tributaries (Fig. 1d), including the upper RSA and Rito de Indios, that were substantially impacted by the fire (Table 2 & 3) and likely contributed to the sustained transport and re-suspension of sediment altering water quality (Fig. 2) and ecosystem processes (Fig. 3-5). In addition, Tillery and Haas (2016) identified sub-basins within the RSA watershed that had high probability of debris flows that likely contributed sediments that influenced water quality downstream. These results suggest that hydrologic connections between the upland and adjacent aquatic ecosystems are primary controls on water quality and ecosystem scale processes following high-severity wildfire disturbance that can continue from immediate to shorter-term timescales.

Longer-term recovery post fire (2015-2016)

Four to five years post-fire, both aquatic ecosystems had approached near pre-fire conditions with respect to water quality parameters and measures of ecosystem metabolism. On the EFJR, turbidity, GPP, and ER decreased to near pre-fire mean values, suggesting that similar recovery trajectories observed in other watersheds were occurring in our study systems. This includes 1) a return to pre-fire flow regime and sediment loads (Romme and others, 2011) and 2) a decline in dissolved nutrient content and thus

60

fertilization effect in previously deposited ash and sediment due to uptake by macrophytes (Chambers and others, 1989), microbial uptake and transformation (Jones and Holmes, 1996; Bernot and Dodds, 2005), groundwater and surface water interactions (Dahm and others, 1998) and downstream transport.

The more gradual return to pre-fire values on the RSA indicates that in streams that are strongly linked to ongoing disturbance in the surrounding watershed, sediment loading from the erosion of destabilized hillslopes remains elevated. However, by the fifth year following the fire, we observed an overall reduction in turbidity (Table 1 & Fig. 2) and reduced suppression of GPP and ER (Fig. 3 & 5). These responses suggest recovery and a return to pre-fire conditions including; minimal additional transport of sediments into the stream, a reduction in the resuspension of fine sediments during base flow conditions (Ryan and others, 2011), and greater light availability stimulating GPP (Mulholland and others, 2001; Bernot and others, 2010).

Conclusions

1) Immediately following a catastrophic wildfire, turbidity and specific conductance values increased substantially and measures of whole stream metabolism declined in each of two streams in nearly identical, paired watersheds.

2) From one to three years following the fire, streams in these two paired watersheds responded differently: one stream with tight hydrologic connections to the landscape experienced persistently high turbidity and suppressed GPP and ER, likely due to light limitation, while the other stream had much lower turbidity levels and elevated GPP and ER, likely due to fertilization of nutrient-rich fire debris.

3) Both ecosystems returned to near pre-fire water quality and metabolism values by six years after the fire.

4) Long-term, high-frequency data, both pre- and post-fire are necessary to accurately assess the impacts of wildfire on ecosystem processes in aquatic environments.

Acknowledgements

Figures

Figure 1: (a) Maps showing the Rio Grande and the burn perimeter of the Las Conchas (LC) wildfire in north-central New Mexico, USA, (b) water-quality stations, streams of interest, perimeter of the LC fire, and key landmarks, (c) the U.S. Forest Service burn severity map for the LC fire, water quality, discharge and meteorological (MET) monitoring locations and streams of interest and, (d) average stream gradient (m km^{-1}) and sub-watershed boundaries in relation to the burn perimeter of the LC fire.
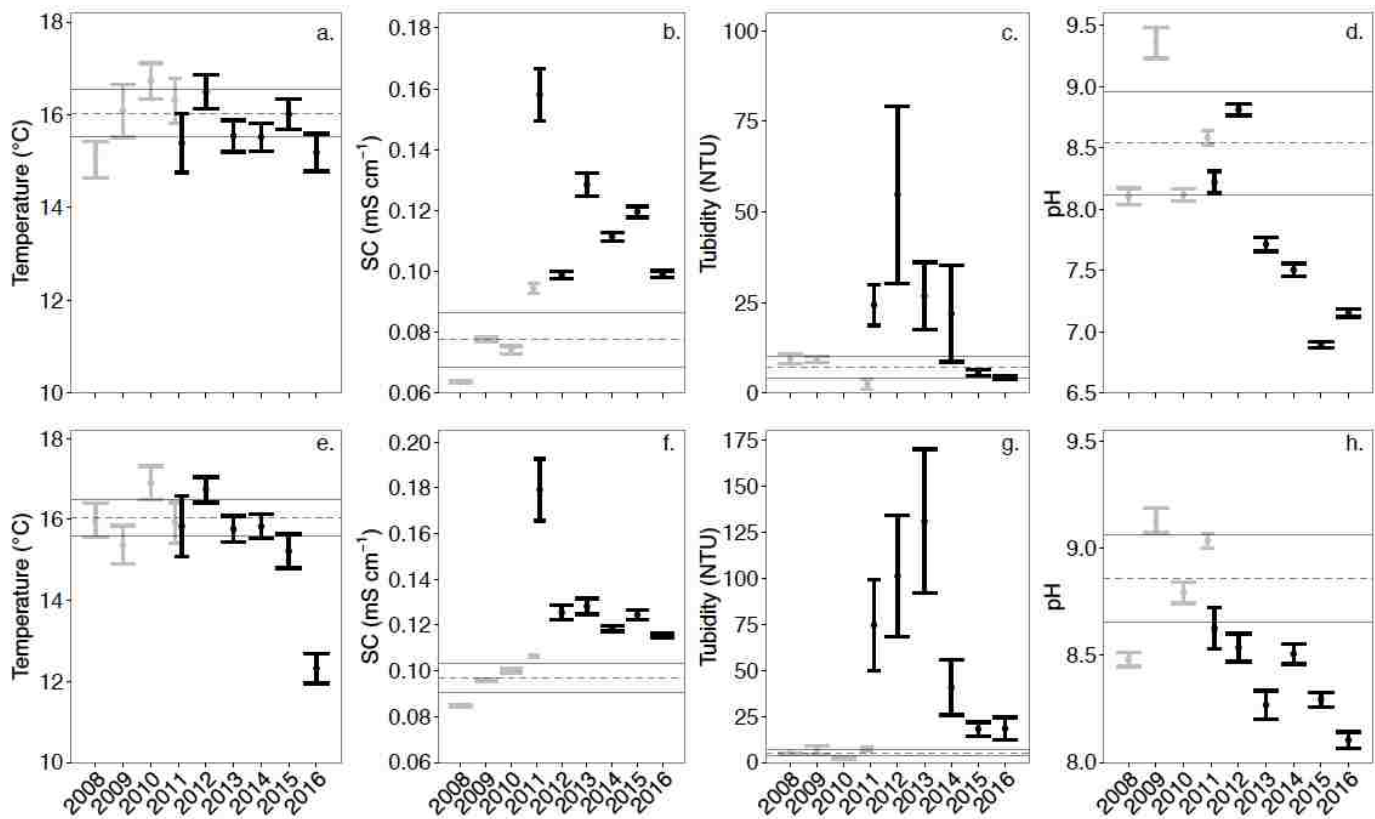
Figure 2: Daily mean water temperature (°C), specific conductivity, SC (mS cm^{-1}), log10 turbidity (NTU), and pH (pH units) during the growing season (Mid-May through September), pre-(2008-2011) and post-Las Conchas fire (2011-2016) for East Fork Jemez River (a-d) and Rio San Antonio (e-h). Grey lines represent the compiled growing season mean values and 90% confidence intervals for pre-fire for each stream.
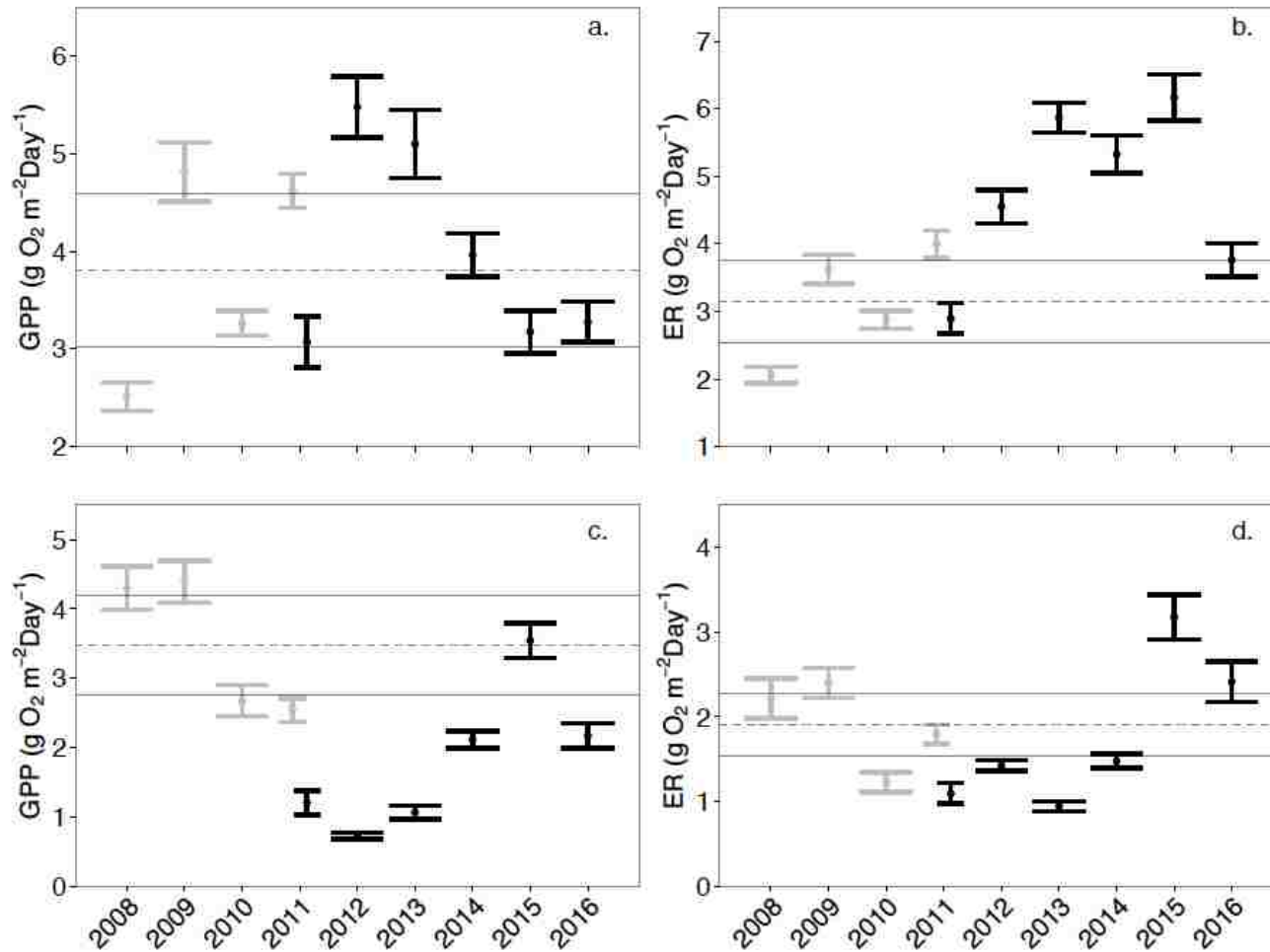
Figure 3: Daily mean Gross Primary Productivity (GPP) and Ecosystem Respiration (ER) on the East Fork Jemez River (a, b) and the Rio San Antonio (c, d) during the growing season (Mid-May through September). Grey lines represent the compiled pre-fire growing season mean values and 90% confidence intervals for each stream.
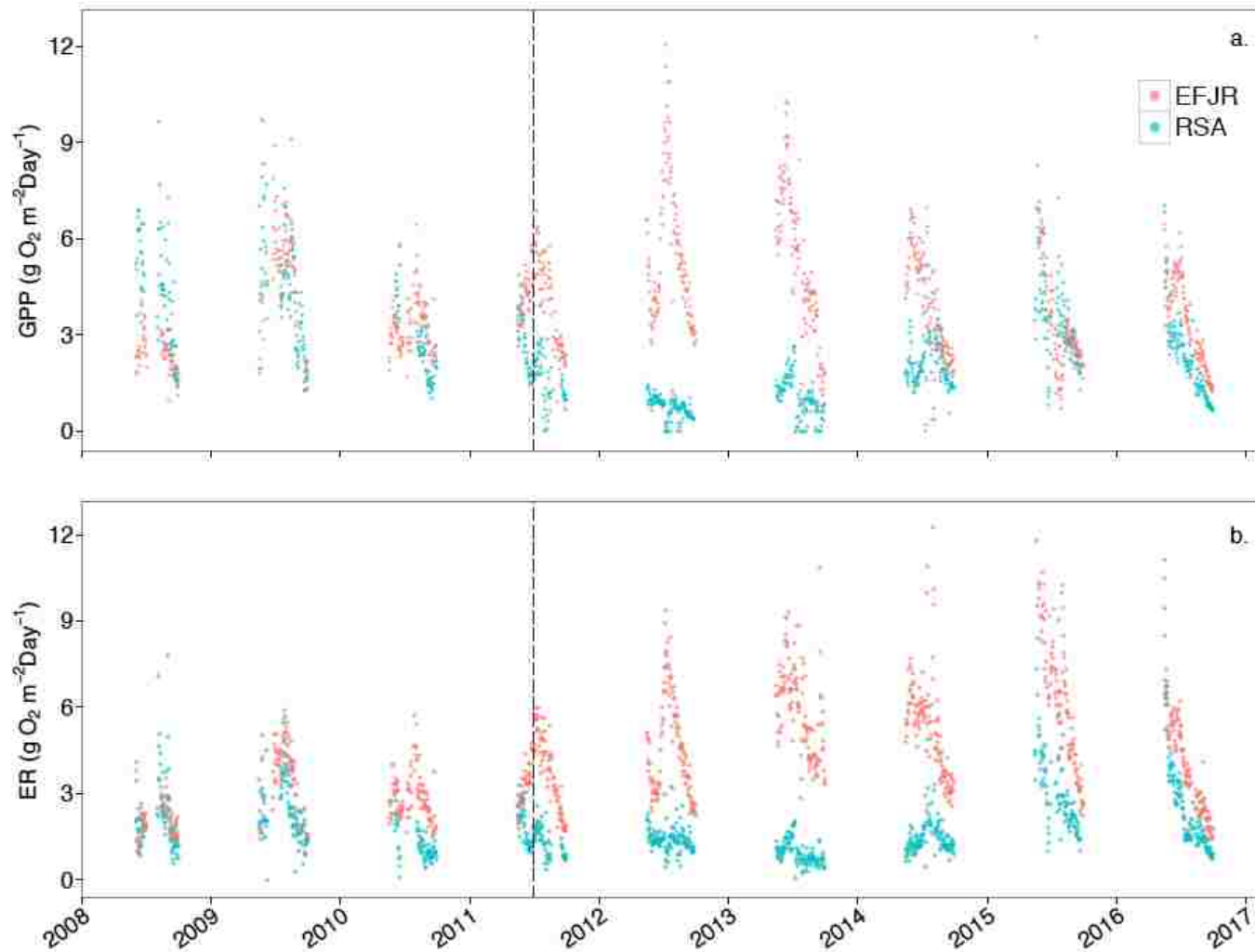
Figure 5: (a) Daily mean Gross Primary Productivity (GPP) and (b) Ecosystem Respiration (ER) on the East Fork Jemez River (red) and the Rio San Antonio (blue) during the growing season (Mid-May through September) by year (2008-2016). Black vertical dashed line represents the Las Conchas fire.
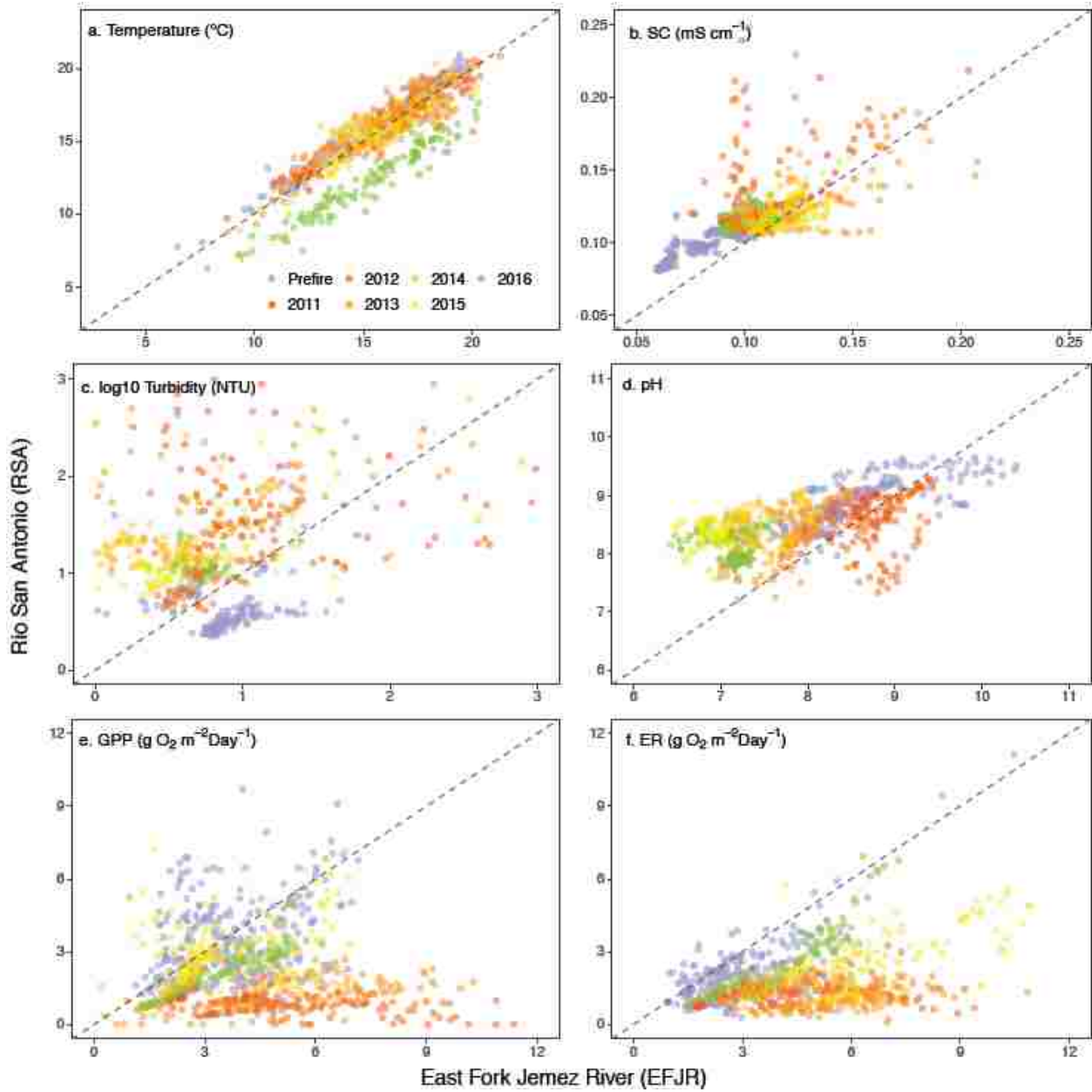
Figure 4: Comparison of daily mean water temperature (°C), specific conductivity, SC (mS cm^{-1}), log10 turbidity (NTU), pH (pH units), Gross Primary Productivity (GPP, g O$_2$ m^{-2} d^{-1}) and Ecosystem Respiration (ER, g O$_2$ m^{-2} d^{-1}) on the East Fork Jemez River (EFJR, x axis) and the Rio San Antonio (RSA, y axis) during the growing season (Mid-May through September), pre-(2008-2011) and post-Las Conchas fire (2011-2016).
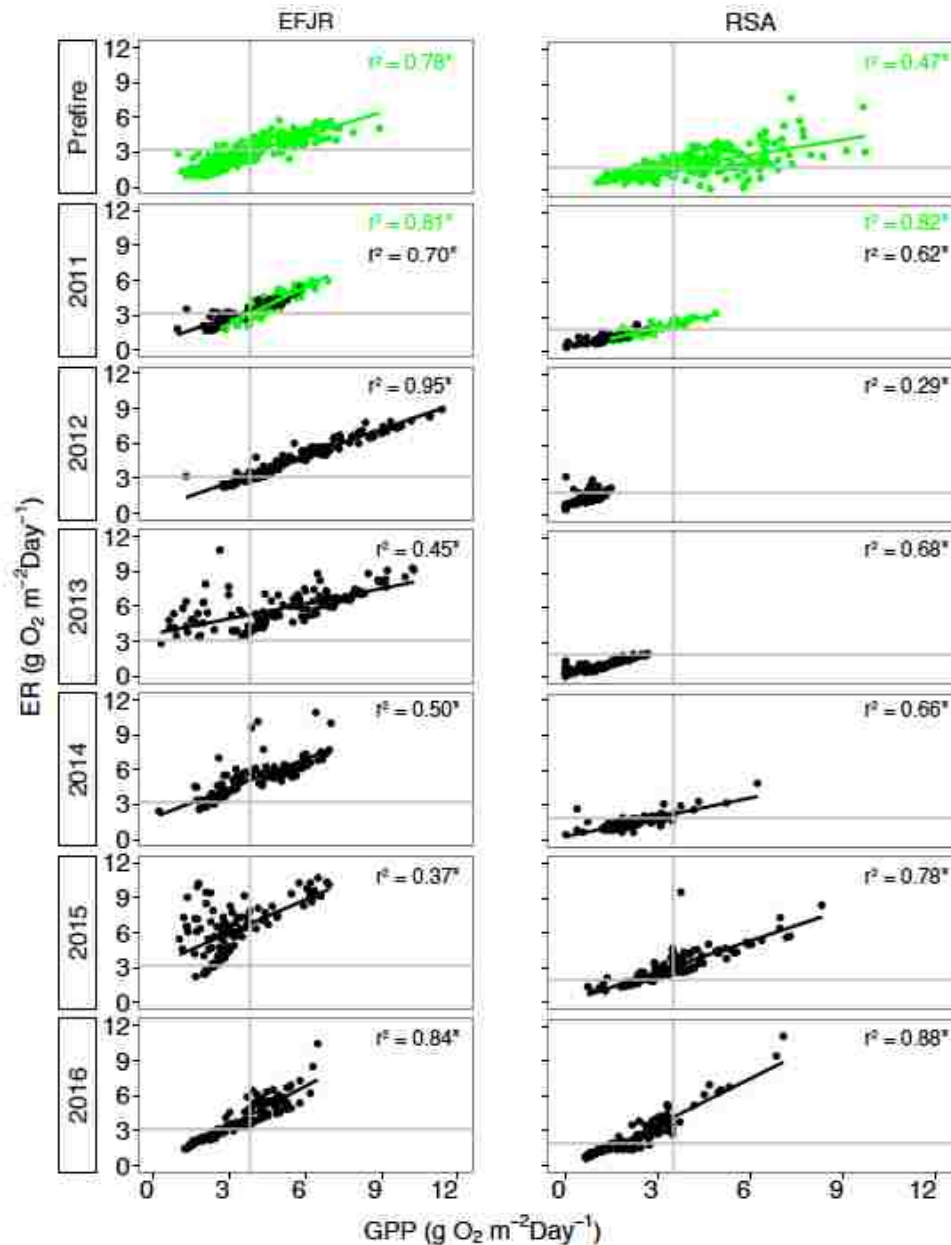
Figure 6: Daily mean Gross Primary Productivity (GPP, g O_2 m^{-2} d^{-1}) versus daily mean Ecosystem Respiration (ER, g O_2 m^{-2} d^{-1}) versus estimates for the growing season (Mid-May through September), pre-fire (green) and each year following the Las Conchas fire (black) on the East Fork Jemez River (EFJR; left column) and Rio San Antonio (RSA; right column). Grey lines represent the compiled growing season mean values pre-fire for each stream. * p value ≤ 0.05.
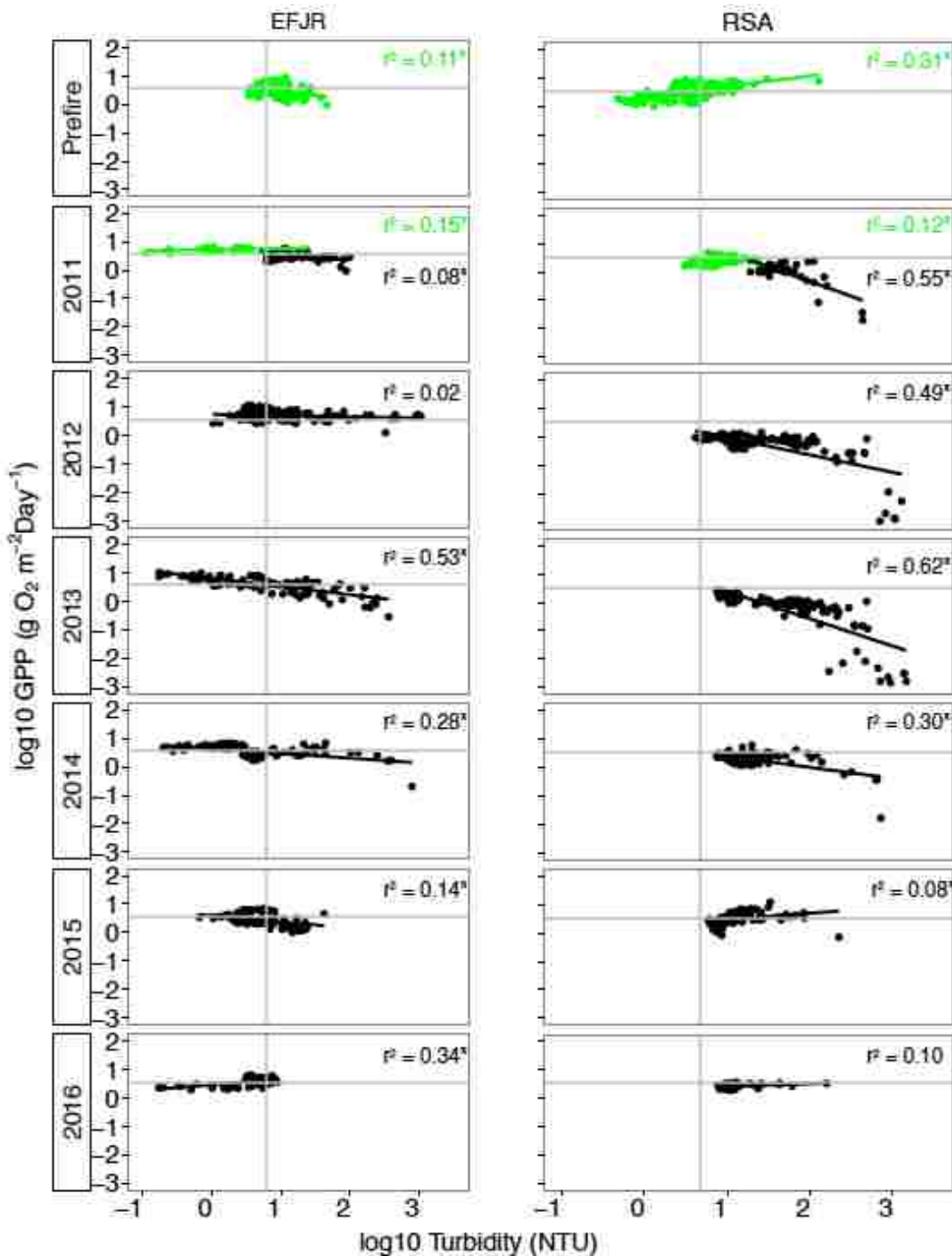
Figure 7: Log10 transformed daily mean turbidity (NTU) versus Log10 transformed Gross Primary Productivity (GPP, g O_2 m^{-2} d^{-1}) estimates for the growing season (Mid-May through September), pre-fire (green) and each year following the Las Conchas fire (black) on the East Fork Jemez River (EFJR; left column) and Rio San Antonio (RSA; right column). Grey lines represent the compiled growing season mean values pre-fire for each stream. * p value ≤ 0.05.

Tables

	Temperature		SC		Turbidity		GPP		ER	
	EFJR	RSA	EFJR	RSA	EFJR	RSA	EFJR	RSA	EFJR	RSA
2008	15.0 (2.1)	16.0 (2.3)	0.064 (0.002)	0.085 (0.003)	9.5 (7.2)	4.8 (2.5)	2.5 (0.8)	4.3 (1.3)	2.1 (0.6)	2.2 (1.3)
2009	16.1 (3.2)	15.4 (2.8)	0.078 (0.004)	0.096 (0.002)	9.4 (4.8)	6.6 (13.1)	4.8 (1.7)	4.4 (1.1)	3.6 (1.2)	2.4 (1.1)
2010	16.7 (2.4)	16.9 (2.1)	0.074 (0.007)	0.100 (0.004)	NA	2.2 (2.0)	3.3 (0.8)	2.7 (0.6)	2.9 (0.8)	1.2 (0.6)
2011	16.3 (2.6)	15.9 (2.5)	0.095 (0.009)	0.106 (0.002)	2.5 (5.2)	7.4 (4.0)	4.6 (0.9)	2.5 (0.6)	4.0 (1.1)	1.8 (0.6)
Pre-fire	**16.1 (2.6)**	**16.0 (2.5)**	**0.077 (0.012)**	**0.096 (0.008)**	**8.1 (6.4)**	**5.3 (7.8)**	**3.8 (1.5)**	**3.6 (1.7)**	**3.1 (1.2)**	**2.0 (1.1)**
2011	15.4 (2.6)	16.0 (2.6)	0.158 (0.035)	0.194 (0.072)	24.3 (23.3)	132.4 (212.5)	3.1 (1.8)	1.1 (0.7)	2.9 (0.9)	2.2 (4.9)
2012	16.5 (2.5)	16.7 (2.2)	0.099 (0.009)	0.126 (0.226)	54.8 (167.5)	101.1 (229.5)	5.5 (2.2)	0.7 (0.3)	4.6 (1.7)	1.4 (0.4)
2013	15.5 (2.3)	15.7 (2.2)	0.128 (0.026)	0.130 (0.024)	26.8 (58.9)	206.5 (355.4)	5.1 (2.4)	1.1 (0.7)	5.9 (1.5)	2.4 (6.6)
2014	15.5 (2.1)	15.9 (2.1)	0.112 (0.009)	0.119 (0.009)	22.0 (88.3)	59.9 (172.0)	4.0 (1.5)	2.1 (1.0)	5.3 (1.9)	1.9 (4.5)
2015	16.0 (2.1)	15.4 (2.7)	0.120 (0.012)	0.124 (0.013)	5.7 (5.9)	34.3 (90.4)	3.2 (1.4)	3.8 (2.5)	6.2 (2.2)	5.8 (10.9)
2016	15.2 (2.8)	12.3 (2.6)	0.099 (0.007)	0.115 (0.006)	5.5 (5.8)	18.3 (24.2)	3.3 (1.5)	2.3 (1.2)	3.8 (1.8)	2.5 (1.7)
Post-fire	**15.7 (2.4)**	**15.2 (2.8)**	**0.115 (0.020)**	**0.126 (0.023)**	**24.2 (88.1)**	**69.7 (177.1)**	**4.1 (2.0)**	**1.9 (1.4)**	**4.9 (2.0)**	**1.8 (1.3)**

Table 1: Compiled year averages (standard deviation) from daily mean water temperature (°C), specific conductance, SC (mS cm^{-1}), turbidity (NTU), Gross Primary Productivity (GPP, g O_2 m^{-2} d^{-1}), and Ecosystem Respiration (ER, g O_2 m^{-2} d^{-1}) for the growing season (Mid-May through September), pre-fire (2008-2011) and each year following the Las Conchas fire (2011-2016), and the compiled pre- and post-fire mean on the East Fork Jemez River (EFJR) and Rio San Antonio (RSA). Bold rows are the combined pre- and post-fire mean. NA= no data available.

Watershed	Sub-watershed	Total area (km²)	Burn severity	Area (km²)	Area (%)
RSA	Rito de Indios	19	High	1.7	9.1
			Moderate	2.2	12
			Low	1.3	7
			Unchanged	13.8	73.8
	Upper RSA	49.4	High	13.1	26.6
			Moderate	12.2	24.6
			Low	6.4	12.9
			Unchanged	17.7	35.9
	Sonde	146	High	18.8	12.9
			Moderate	19.1	13.1
			Low	11.4	7.8
			Unchanged	96.7	66.2
EFJR	Upper EFJR	32.9	High	1.5	4.6
			Moderate	6.3	19.1
			Low	0.9	2.9
			Unchanged	24.2	73.5
	Jaramillo	39.4	High	9.7	24.7
			Moderate	10.2	25.9
			Low	2.7	6.7
			Unchanged	16.8	42.7
	Sonde	100	High	11.2	11.2
			Moderate	16.5	16.5
			Low	3.6	3.6
			Unchanged	68.7	68.7

Table 2: Total watershed area (km²) and cumulative area (km² and percentage) within each of the burn severity classes (i.e., unchanged, low, moderate, and high) for the EFJR and RSA watersheds calculated from the location of the water quality sonde and contributing sub-watersheds that were impacted by the Las Conchas fire.

Watershed	Sub-watershed	Mean watershed slope	River-km to fire	Stream gradient	% burned of total river-km	% unburned of total river-km	River-km burned	River-km unburned
RSA	Upper RSA	0.09	1.4	High	13.6	8.0	2.2	1.3
				Medium	32.7	15.4	5.3	2.5
				Low	14.8	16.0	2.4	2.6
				Total	60.5	39.5	9.8	6.4
	Rito de Indios	0.05	0.4	High	4.8	0.0	1.8	0
				Medium	23.0	5.6	8.6	2.1
				Low	32.9	33.2	12.3	12.4
				Total	61.0	39.0	22.8	14.6
	Sonde	0.06	11.8	High	7.5	2.4	4	1.3
				Medium	25.9	8.6	13.9	4.6
				Low	27.4	28.0	14.7	15
				Total	60.8	39.2	32.6	21
EFJR	Upper EFJR	0.01	NA	High	0.0	0.0	0	0
				Medium	0.0	18.3	0	5.1
				Low	11.5	70.1	3.2	19.5
				Total	11.5	88.5	3.2	24.6
	Jaramillo Creek	0.04	3.1	High	0.0	0.0	0	0
				Medium	19.5	0.0	4.7	0
				Low	20.3	60.2	4.9	14.5
				Total	39.8	60.2	9.6	14.5
	Sonde	0.05	5.6	High	0.0	0.0	0	0
				Medium	9.1	9.8	4.7	5.1
				Low	15.6	65.5	8.1	34
				Total	24.7	75.3	12.8	39.1

Table 3: Mean sub-watershed slope, distance (river-km) to the fire burn scar classified as moderate or high burn severity, and percentage of river-km classified as low (0.00-0.07), moderate (0.07-0.14) or high (0.15-0.22) gradient (m km-1) unburned and burned by the Las Conchas fire within each sub-watershed within the greater EFJR and RSA watersheds. NA= distance could not be calculated due to the lack of a moderate or high burn severity parcel within the watershed.

Supplemental figures and tables
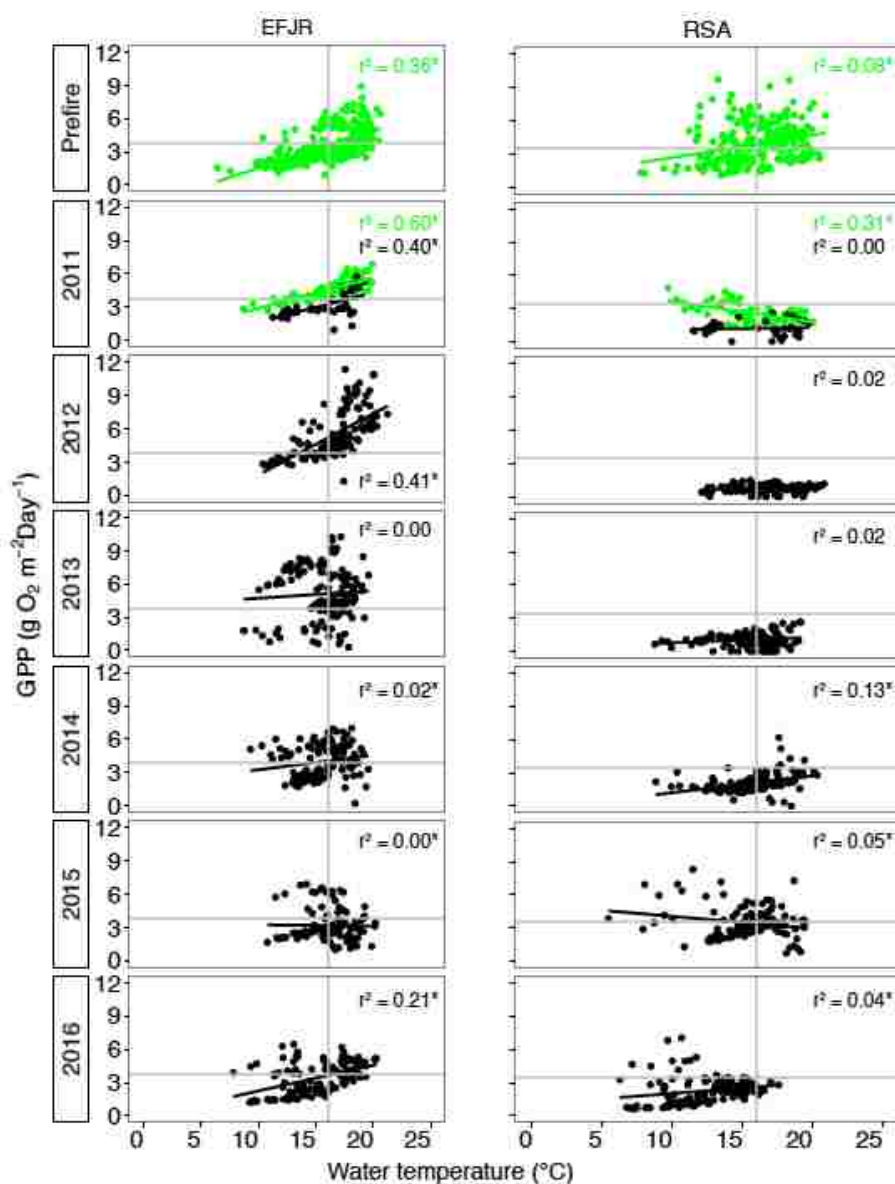
Supplemental Information Figure 1: Log10 transformed Gross Primary Productivity (
O_2 m^{-2} d^{-1}) estimates for the growing season (Mid-May through September) versus da
mean water temperature (°C), pre-fire (green) and each year following the Las Conch
(black) on the East Fork Jemez River (EFJR; left column) and Rio San Antonio (RSA; r
column). Grey lines represent the compiled growing season mean values pre-fire for
stream. * p value ≤ 0.05.
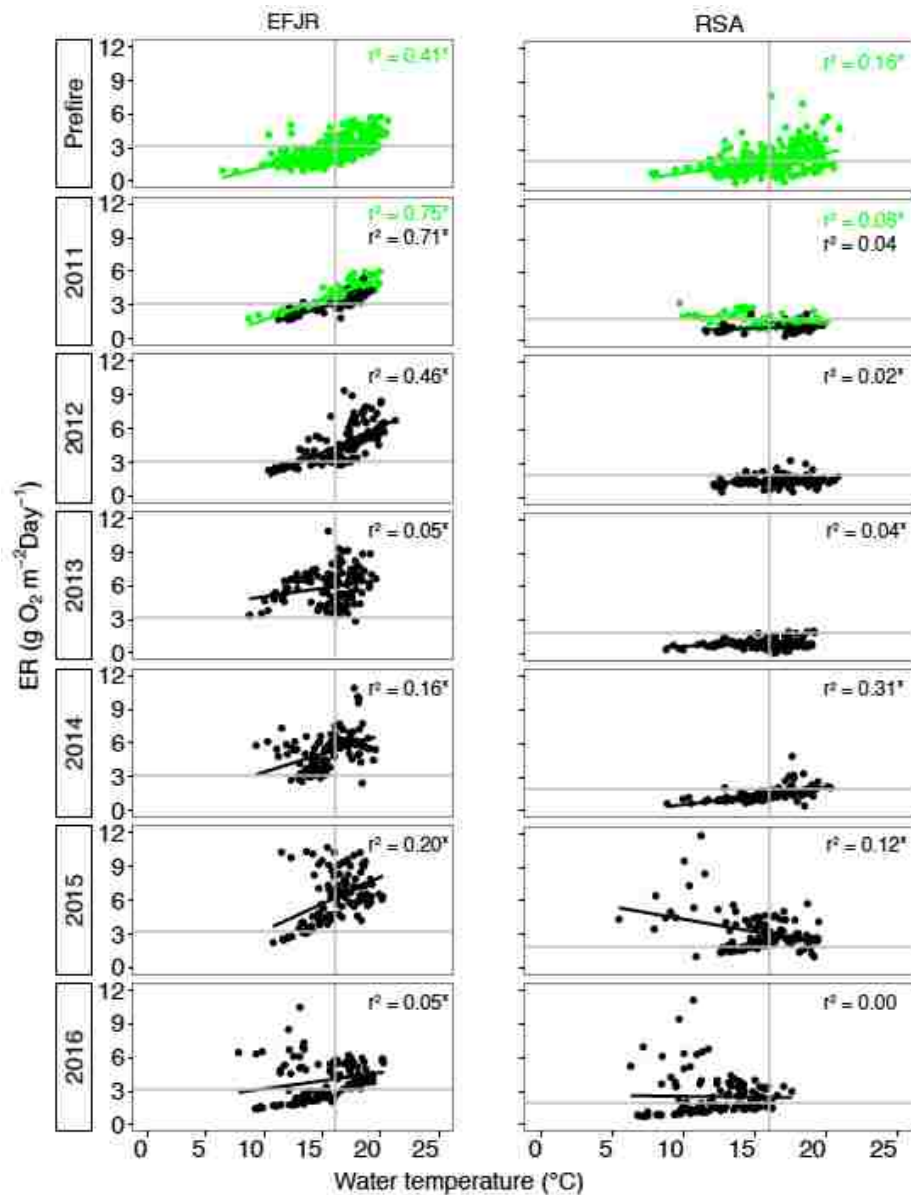
Supplemental Information Figure 2: Log10 transformed Ecosystem Respiration (ER, g O_2 m^{-2} d^{-1}) estimates for the growing season (Mid-May through September) versus daily mean water temperature (°C), pre-fire (green) and each year following the Las Conchas fire (black) on the East Fork Jemez River (EFJR; left column) and Rio San Antonio (RSA; right column). Grey lines represent the compiled growing season mean values pre-fire for each stream. * p value ≤ 0.05.
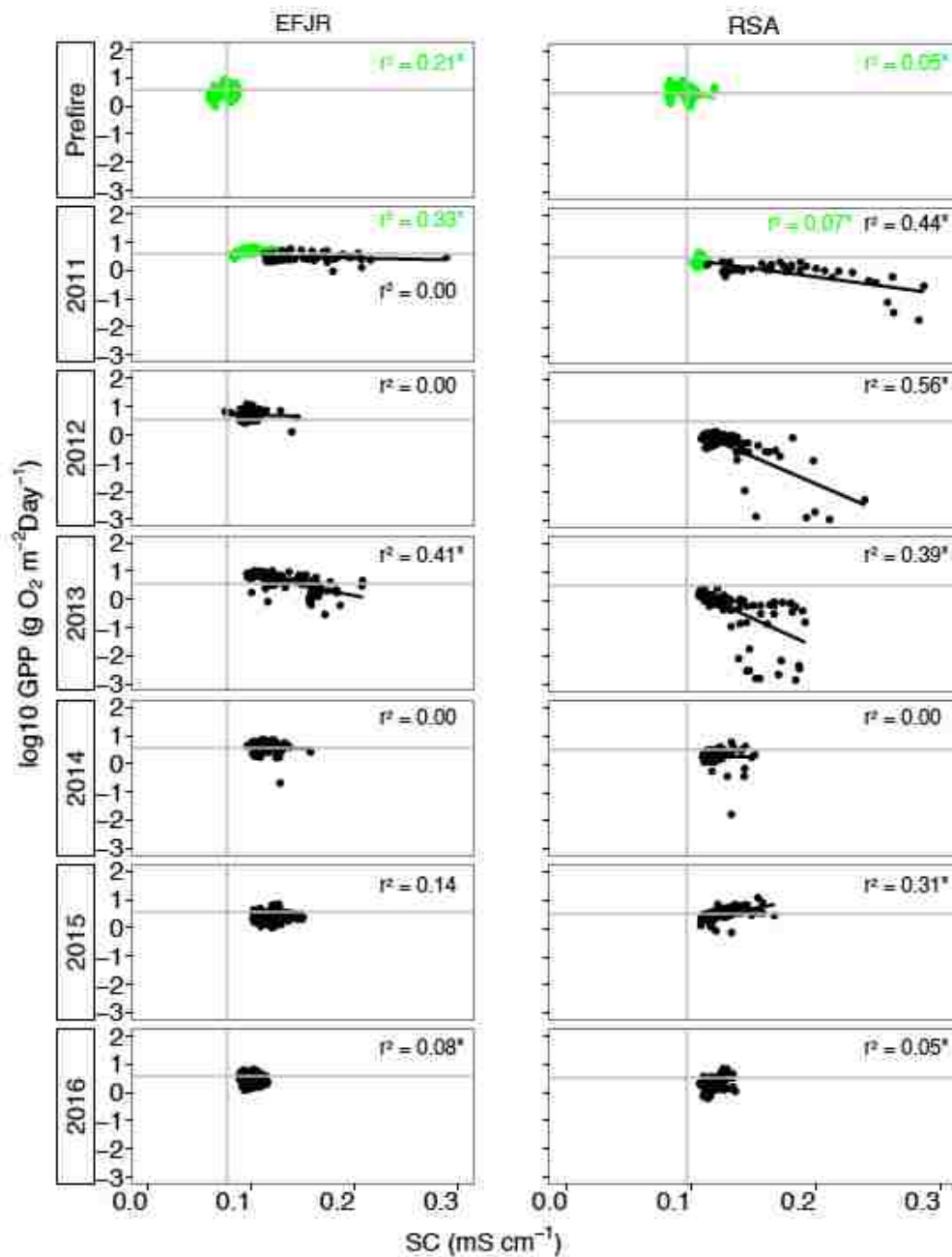
Supplemental Information Figure 3: Log10 transformed Gross Primary Productivity (GPP, g O_2 m^{-2} d^{-1}) estimates for the growing season (Mid-May through September) versus daily mean specific conductance (SC, mS cm-1), pre-fire (green) and each year following the Las Conchas fire (black) on the East Fork Jemez River (EFJR; left column) and Rio San Antonio (RSA; right column). Grey lines represent the compiled growing season mean values pre-fire for each stream. * p value ≤ 0.05.
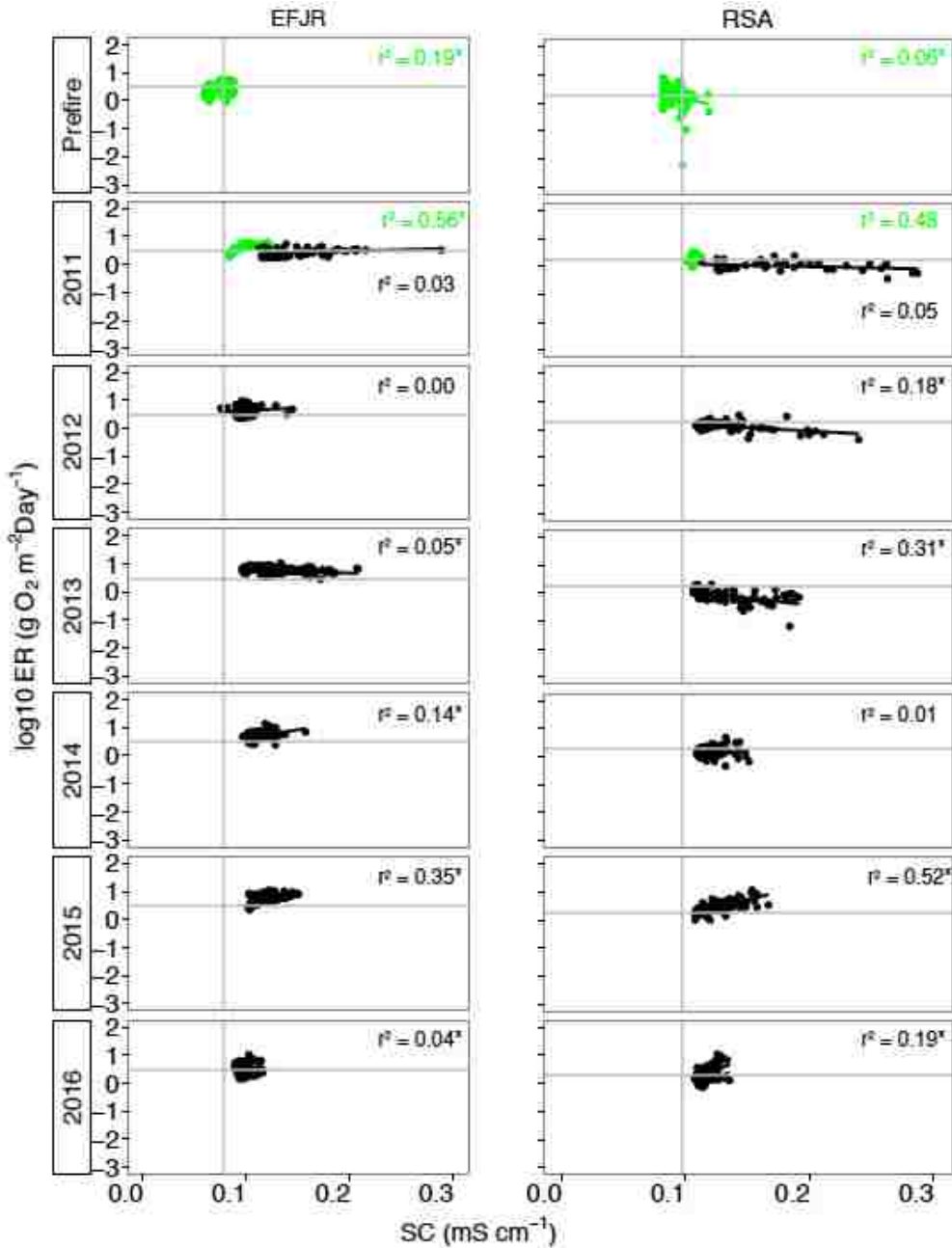
Supplemental Information Figure 4: Log10 transformed Ecosystem Respiration (ER, g O_2 m^{-2} d^{-1}) estimates for the growing season (Mid-May through September) versus daily mean Specific Conductance (SC, mS cm^{-1}) pre-fire (green) and each year following the Las Conchas fire (black) on the East Fork Jemez River (EFJR; left column) and Rio San Antonio (RSA; right column). Grey lines represent the compiled growing season mean values pre-fire for each stream. * p value ≤ 0.05.

Year	EFJR	RSA	Overlapping
2008	76	84	67
2009	88	99	66
2010	105	72	60
2011 (pre-fire)	77	69	75
2011 (post-fire)	48	39	27
2012	131	134	127
2013	132	123	118
2014	127	131	120
2015	117	113	95
2016	127	133	127

Supplemental Information Table 1: Count of days during from each year that produced reliable metabolism estimates on the East Fork Jemez River (EFJR), Rio San Antonio (RSA), and overlapping days (i.e., days when the data were available and reliable from both streams) during the growing season (Mid-May through September) pre- and post-Las Conchas fire.

References

Acuna V, Giorgi A, Munoz I, Uehlinger U, Sabater S. 2004. Flow extremes and benthic organic matter shape the metabolism of a headwater Mediterranean stream. Freshwater Biology 49: 960-971.

Allen CD, Macalady AK, Chenchouni H, Bachelet D, McDowell N, Vennetier M, Kitzberger T, Rigling A, Breshears DD, Hogg EH, Gonzalez P, Fensham R, Zhang Z, Castro J, Demidova N, Lim JH, Allard G, Running SW, Semerci A, Cobb N. 2010. A global overview of drought and heat-induced tree mortality reveals emerging climate change risks for forests. Forest Ecology and Management 259: 660-684.

Appling A, Hall Jr R, Arroita M, Yackulic C. 2016. streamMetabolizer: models for estimating aquatic photosynthesis and respiration. R package version 0.9. 32.

Atkinson BL, Grace MR, Hart BT, Vanderkruk KE. 2008. Sediment instability affects the rate and location of primary production and respiration in a sand-bed stream. Journal of the North American Benthological Society 27: 581-592.

Barry RG, Chorley RJ. 2003. Atmosphere, weather and climate. New York, New York: Routledge.

Bernot MJ, Dodds WK. 2005. Nitrogen retention, removal, and saturation in lotic ecosystems. Ecosystems 8: 442-453.

Bernot MJ, Sobota DJ, Hall RO, Mulholland PJ, Dodds WK, Webster JR, Tank JL, Ashkenas LR, Cooper LW, Dahm CN. 2010. Inter-regional comparison of land-use effects on stream metabolism. Freshwater Biology 55: 1874-1890.

Betts EF, Jones JB. 2009. Impact of wildfire on stream nutrient chemistry and ecosystem metabolism in boreal forest catchments of interior Alaska. Arctic, Antarctic, and Alpine Research 41: 407-417.

Birkel C, Soulsby C, Malcolm I, Tetzlaff D. 2013. Modeling the dynamics of metabolism in montane streams using continuous dissolved oxygen measurements. Water Resources Research 49: 5260-5275.

Bisson PA, Rieman BE, Luce C, Hessburg PF, Lee DC, Kershner JL, Reeves GH, Gresswell RE. 2003. Fire and aquatic ecosystems of the western USA: current knowledge and key questions. Forest Ecology and Management 178: 213-229.

Bixby RJ, Cooper SD, Gresswell RE, Brown LE, Dahm CN, Dwire KA. 2015. Fire effects on aquatic ecosystems: an assessment of the current state of the science. Freshwater Science 34: 1340-1350.

Bodi MB, Martin DA, Balfour VN, Santin C, Doerr SH, Pereira P, Cerda A, Mataix-Solera J. 2014. Wild land fire ash: production, composition and eco-hydro-geomorphic effects. Earth-Science Reviews 130: 103-127.

Bott TL, Newbold JD, Arscott DB. 2006. Ecosystem metabolism in piedmont streams: reach geomorphology modulates the influence of riparian vegetation. Ecosystems 9: 398-421.

Breshears DD, Cobb NS, Rich PM, Price KP, Allen CD, Balice RG, Romme WH, Kastens JH, Floyd ML, Belnap J, Anderson JJ, Myers OB, Meyer CW. 2005. Regional vegetation die-off in response to global-change-type drought. Proceedings of the National Academy of Sciences of the United States of America 102: 15144-15148.

Bull WB. 1979. Threshold of critical power in streams. GSA Bulletin 90: 453-464.

Cannon SH, Bigio ER, Mine E. 2001. A process for fire-related debris flow initiation, Cerro Grande fire, New Mexico. Hydrological Processes 15: 3011-3023.

Cannon SH, Boldt EM, Laber JL, Kean JW, Staley DM. 2011. Rainfall intensity–duration thresholds for postfire debris-flow emergency-response planning. Natural Hazards 59: 209-236.

Cannon SH, Gartner JE, Wilson RC, Bowers JC, Laber JL. 2008. Storm rainfall conditions for floods and debris flows from recently burned areas in southwestern Colorado and southern California. Geomorphology 96: 250-269.

Canty A, Ripley B. 2016. boot: Bootstrap R (S-Plus) functions. R package version.

Cayan DR, Dettinger MD, Kammerdiener SA, Caprio JM, Peterson DH. 2001. Changes in the onset of spring in the western United States. Bulletin of the American Meteorological Society 82: 399-415.

Chambers P, Prepas E, Bothwell M, Hamilton H. 1989. Roots versus shoots in nutrient uptake by aquatic macrophytes in flowing waters. Canadian Journal of Fisheries and Aquatic Sciences 46: 435-439.

Cooper SD, Page HM, Wiseman SW, Klose K, Bennett D, Even T, Sadro S, Nelson CE, Dudley TL. 2015. Physicochemical and biological responses of streams to wildfire severity in riparian zones. Freshwater Biology 60: 2600-2619.

Dahm CN, Candelaria-Ley R, Reale CS, Reale JK, Van Horn DJ. 2015. Extreme water quality degradation following a catastrophic forest fire. Freshwater Biology 34: 14261442.

Dahm CN, Grimm NB, Marmonier P, Valett HM, Vervier P. 1998. Nutrient dynamics at the interface between surface waters and groundwaters. Freshwater Biology 40: 427-451.

Davis EA. 2015. Wildfire effects on stream metabolism: Aquatic succession is mediated by local riparian succession and stream geomorphology [MSc thesis]. School of Aquatic and Fishery Science. Seattle, Washington: University of Washington, p74.

Demars B, Manson J, Ólafsson J, Gíslason G, Friberg N. 2011. Stream hydraulics and temperature determine the metabolism of geothermal Icelandic streams. Knowledge and Management of Aquatic Ecosystems 402: 17.

Dodds WK, Veach AM, Ruffing CM, Larson DM, Fischer JL, Costigan KH. 2013. Abiotic controls and temporal variability of river metabolism: multiyear analyses of Mississippi and Chattahoochee River data. Freshwater Science 32: 1073-1087.

Emelko MB, Stone M, Silins U, Allin D, Collins AL, Williams CH, Martens AM, Bladon KD. 2016. Sediment-phosphorus dynamics can shift aquatic ecology and cause downstream legacy effects after wildfire in large river systems. Global change biology 22: 1168-1184.

Fairweather PG. 1991. Statistical power and design requirements for environmental monitoring. Marine and freshwater research 42: 555-567.

Flannigan MD, Krawchuk MA, de Groot WJ, Wotton BM, Gowman LM. 2009. Implications of changing climate for global wildland fire. International journal of wildland fire 18: 483-507.

Gerull L, Frossard A, Gessner MO, Mutz M. 2012. Effects of shallow and deep sediment disturbance on whole-stream metabolism in experimental sand-bed flumes. Hydrobiologia 683: 297-310.

Goff F, Gardner JN, Reneau SL, Goff CJ. 2006. Preliminary geologic map of the Redondo Peak quadrangle, Sandoval County, New Mexico. New Mexico Bureau of Geology and Mineral Resources: Socorro, NM

González-Pinzón R, Haggerty R, Argerich A. 2014. Quantifying spatial differences in metabolism in headwater streams. Freshwater Science 33: 798-811.

Goode JR, Luce CH, Buffington JM. 2012. Enhanced sediment delivery in a changing climate in semi-arid mountain basins: implications for water resource management and aquatic habitat in the northern Rocky Mountains. Geomorphology 139: 1-15.

Grace M, Imberger S. 2006. Stream metabolism: performing & interpreting measurements. Water Studies Centre Monash University, Murray Darling Basin Commission and New South Wales Department of Environment and Climate Change, p204.

Grace MR, Giling DP, Hladyz S, Caron V, Thompson RM, Mac Nally R. 2015. Fast processing of diel oxygen curves: Estimating stream metabolism with BASE (BAyesian Single-station Estimation). Limnology and Oceanography-Methods 13: 103-114.

Gresswell RE. 1999. Fire and aquatic ecosystems in forested biomes of North America. Transactions of the American Fisheries Society 128: 193-221.

Greystone. 1996. Environmental Study and Analysis of Concentrations of Mercury in the Pecos River, New Mexico. Prepared for the US Army Corps of Engineers. Albuquerque, New Mexico. Greystone, Englewood, CO. February 1996.

Griffiths NA, Tank JL, Royer TV, Roley SS, Rosi-Marshall EJ, Whiles MR, Beaulieu JJ, Johnson LT. 2013. Agricultural land use alters the seasonality and magnitude of stream metabolism. Limnology and Oceanography 58: 1513-1529.

Gupta R. 2014. Hydrology and hydraulic systems. Long Grove, Illinois: Waveland Press Inc.

Hall RO, Yackulic CB, Kennedy TA, Yard MD, Rosi-Marshall EJ, Voichick N, Behn KE. 2015. Turbidity, light, temperature, and hydropeaking control primary productivity in the Colorado River, Grand Canyon. Limnology and Oceanography 60: 512-526.

Hauer FR, Spencer CN. 1998. Phosphorus and nitrogen dynamics in streams associated with wildfire: a study of immediate and longterm effects. International Journal of Wildland Fire 8: 183-198.

Heiken G, Goff F, Gardner JN, Baldridge W, Hulen J, Nielson DL, Vaniman D. 1990. The Valles/Toledo Caldera Complex, Jemez Volcanic Field, New Mexico. Annual Review of Earth and Planetary Sciences 18: 27.

Hotchkiss ER, Hall RO. 2015. Whole-stream 13C tracer addition reveals distinct fates of newly fixed carbon. Ecology 96: 403-416.

Isaak DJ, Luce CH, Rieman BE, Nagel DE, Peterson EE, Horan DL, Parkes S, Chandler GL. 2010. Effects of climate change and wildfire on stream temperatures and salmonid thermal habitat in a mountain river network. Ecological Applications 20: 1350-1371.

Izagirre O, Agirre U, Bermejo M, Pozo J, Elosegi A. 2008. Environmental controls of whole-stream metabolism identified from continuous monitoring of Basque streams. Journal of the North American Benthological Society 27: 252-268.

Jones JB, Holmes RM. 1996. Surface-subsurface interactions in stream ecosystems. Trends in Ecology & Evolution 11: 239-242.

Joseph S, Henderson H. 2006. Water quality survey summary for the Valles Caldera National Preserve watershed (from VCNP boundary to headwaters) 2001. Surface Water Quality Bureau, New Mexico Environment Department, Santa fe, NM, p23.

Kean JW, McCoy SW, Tucker GE, Staley DM, Coe JA. 2013. Runoff-generated debris flows: Observations and modeling of surge initiation, magnitude, and frequency. Journal of Geophysical Research: Earth Surface 118: 2190-2207.

Kosinski RJ. 1984. A comparison of the accuracy and precision of several open-water oxygen productivity techniques. Hydrobiologia 119: 139-148.

Larsen L, Harvey J. 2017. Disrupted carbon cycling in restored and unrestored urban streams: Critical timescales and controls. Limnology and Oceanography 62.

Lavine A, Kuyumjian GA, Reneau SL, Katzman D, Malmon DV. 2006. A five-year record of sedimentation in the Los Alamos reservoir, New Mexico, following the Cerro Grande Fire. Bernard JM editor. Joint 8th Federal Interagency Sedimentation Conference and 3rd Federal Interagency Hydrologic Modeling Conference, April 2-6, 2006, Reno, Nevada, USA: U.S. Geological Survey, Reston, Virginia, p951-959.

Liu F, Parmenter R, Brooks PD, Conklin MH, Bales RC. 2008. Seasonal and interannual variation of streamflow pathways and biogeochemical implications in semi-arid, forested catchments in Valles Caldera, New Mexico. Ecohydrology 1: 239-252.

Mahlum SK, Eby LA, Young MK, Clancy CG, Jakober M. 2011. Effects of wildfire on stream temperatures in the Bitterroot River Basin, Montana. International Journal of Wildland Fire 20: 240-247.

Martin DA. 2016. At the nexus of fire, water and society. Philosophical Transactions of the Royal Society B 371: 20150172.

Mast MA, Clow DW. 2008. Effects of 2003 wildfires on stream chemistry in Glacier National Park, Montana. Hydrological Processes 22: 5013-5023.

Mast MA, Murphy SF, Clow DW, Penn CA, Sexstone GA. 2016. Water-quality response to a high-elevation wildfire in the Colorado Front Range. Hydrological Processes 30: 1811-1823.

McTammany M, Benfield E, Webster J. 2007. Recovery of stream ecosystem metabolism from historical agriculture. Journal of the North American Benthological Society 26: 532-545.

Meek D, Hatfield J, Howell T, Idso S, Reginato R. 1984. A generalized relationship between photosynthetically active radiation and solar radiation. Agronomy Journal 76: 939-945.

Moody JA, Martin DA. 2001a. Initial hydrologic and geomorphic response following a wildfire in the Colorado Front Range. Earth Surface Processes and Landforms 26: 1049-1070.

Moody JA, Martin DA. 2001b. Post-fire, rainfall intensity–peak discharge relations for three mountainous watersheds in the western USA. Hydrological processes 15: 2981-2993.

Muldavin E, Neville P, Jackson C, Neville T. 2006. A vegetation map of Valles Caldera National Preserve, New Mexico. Agreement No. 01CRAG0014. Albuquerque, NM: University of New Mexico.

Muldavin E, Tonne P. 2003. A vegetation survey and preliminary ecological assessment of Valles Caldera National Preserve, New Mexico. Cooperative Agreement No. 01CRAG0014. University of New Mexico, Albuquerque, NM.

Mulholland P, Fellows CS, Tank J, Grimm N, Webster J, Hamilton S, Martí E, Ashkenas L, Bowden W, Dodds W. 2001. Inter-biome comparison of factors controlling stream metabolism. Freshwater Biology 46: 1503-1517.

Murphy SF, McCleskey R. B., Writer JH. 2012. Effects of flow regime on stream turbidity and suspended solids after wildfire, Colorado Front Range. IAHS-AISH publication: 51-58.

NMED. 2005. Water quality survey summary for the Jemez River watershed. Santa fe, New Mexico: Surface Water Quality Bureau.

Orem CA, Pelletier JD. 2015. Quantifying the time scale of elevated geomorphic response following wildfires using multi-temporal LiDAR data: An example from the Las Conchas fire, Jemez Mountains, New Mexico. Geomorphology 232: 224-238.

Orem CA, Pelletier JD. 2016. The predominance of post-wildfire erosion in the long-term denudation of the Valles Caldera, New Mexico. Journal of Geophysical Research: Earth Surface 121: 843-864.

Parmenter RR, Oertel RW, Compton TS, Kindschuh S, Peyton M, Meyer W, Caldwell C, Jacobi GZ, Myers O, Zeigler M. 2012. Fire and floods in the Valles Caldera National Preserve, New Mexico: The 2011 Las Conchas Fire impacts on montane species diversity and food webs. 97th Ecological Society of America Annual Convention. Portland, OR: Ecological Society of America.

Pelletier JD, Orem CA. 2014. How do sediment yields from post-wildfire debris-laden flows depend on terrain slope, soil burn severity class, and drainage basin area? Insights from airborne LiDAR change detection. Earth Surface Processes and Landforms 39: 1822-1832.

Phillips EH, Goff F, Kyle PR, McIntosh WC, Dunbar NW, Gardner JN. 2007. The 40Ar/39Ar age constraints on the duration of resurgence at the Valles caldera, New Mexico. Journal of Geophysical Research: Solid Earth 112.

Raffa KF, Aukema BH, Bentz BJ, Carroll AL, Hicke JA, Turner MG, Romme WH. 2008. Cross-scale drivers of natural disturbances prone to anthropogenic amplification: the dynamics of bark beetle eruptions. Bioscience 58: 501-517.

Reale JK, Van Horn DJ, Condon KE, Dahm CN. 2015. The effects of catastrophic wildfire on water quality along a river continuum Freshwater Science 34: 1426-1442.

Reneau SL, Katzman D, Kuyumjian GA, Lavine A, Malmon DV. 2007. Sediment delivery after a wildfire. Geology 35: 151-154.

Rhoades CC, Entwistle D, Butler D. 2011. The influence of wildfire extent and severity on streamwater chemistry, sediment and temperature following the Hayman Fire, Colorado. International Journal of Wildland Fire 20: 430-442.

Roberts BJ, Mulholland PJ, Hill WR. 2007. Multiple scales of temporal variability in ecosystem metabolism rates: results from 2 years of continuous monitoring in a forested headwater stream. Ecosystems 10: 588-606.

Robichaud PR, Beyers JL, Neary DG. 2000. Evaluating the effectiveness of postfire rehabilitation treatments: US Department of Agriculture, Forest Service, Rocky Mountain Research Station Fort Collins, Colorado.

Roley SS, Tank JL, Griffiths NA, Hall Jr RO, Davis RT. 2014. The influence of floodplain restoration on whole-stream metabolism in an agricultural stream: insights from a 5-year continuous data set. Freshwater Science 33: 1043-1059.

Romme WH, Boyce MS, Gresswell R, Merrill EH, Minshall GW, Whitlock C, Turner MG. 2011. Twenty years after the 1988 Yellowstone Fires: lessons about disturbance and ecosystems. Ecosystems 14: 1196-1215.

RStudio Team. 2015. RStudio: integrated development environment for R. Boston, Massachusetts: RStudio Inc, .

Ryan SE, Dwire KA, Dixon MK. 2011. Impacts of wildfire on runoff and sediment loads at Little Granite Creek, western Wyoming. Geomorphology 129: 113-130.

Seager R, Ting MF, Held I, Kushnir Y, Lu J, Vecchi G, Huang HP, Harnik N, Leetmaa A, Lau NC, Li CH, Velez J, Naik N. 2007. Model projections of an imminent transition to a more arid climate in southwestern North America. Science 316: 1181-1184.

Shakesby RA, Doerr SH. 2006. Wildfire as a hydrological and geomorphological agent. Earth-Science Reviews 74: 269-307.

Sherson LR, Van Horn DJ, Gomez JD, Shafer BM, Crossey LJ, Dahm CN. 2015. Nutrient dynamics in a headwater stream: use of continuous water quality sensors to examine responses to wildfire and precipitation events. Hydrological Processes 29: 3193-3207.

Silins U, Bladon KD, Kelly EN, Esch E, Spence JR, Stone M, Emelko MB, Boon S, Wagner MJ, Williams CHS, Tichkowsky I. 2014. Five-year legacy of wildfire and salvage logging impacts on nutrient runoff and aquatic plant, invertebrate, and fish productivity. Ecohydrology 7: 1508-1523.

Simino J. 2002. East Fork of the Jemez River stream inventory report. U.S. Forest Service, Santa Fe National Forest, Jemez Ranger District.

Smith HG, Sheridan GJ, Lane PN, Noske PJ, Heijnis H. 2011a. Changes to sediment sources following wildfire in a forested upland catchment, southeastern Australia. Hydrological Processes 25: 2878-2889.

Smith HG, Sheridan GJ, Lane PNJ, Nyman P, Haydon S. 2011b. Wildfire effects on water quality in forest catchments: A review with implications for water supply. Journal of Hydrology 396: 170-192.

Smith RL, Bailey RA, Ross C. 1970. Geologic map of the Jemez mountains, New Mexico.

Smith RM, Kaushal SS. 2015. Carbon cycle of an urban watershed: exports, sources, and metabolism. Biogeochemistry 126: 173-195.

Song C, Dodds WK, Trentman MT, Rüegg J, Ballantyne F. 2016. Methods of approximation influence aquatic ecosystem metabolism estimates. Limnology and Oceanography: Methods 14: 557-569.

Stewart IT, Cayan DR, Dettinger MD. 2004. Changes in snowmelt runoff timing in western North America under a 'business as usual' climate change scenario. Climatic Change 62: 217-232.

Suazo MM. 2016. Montane valley grassland plant communities are highly resistant to wildfire [MSc thesis]. Department of Biology. Albuquerque, New Mexico: University of New Mexico.

Sweeney BW, Bott TL, Jackson JK, Kaplan LA, Newbold JD, Standley LJ, Hession WC, Horwitz RJ. 2004. Riparian deforestation, stream narrowing, and loss of stream ecosystem services. Proceedings of the National Academy of Sciences of the United States of America 101: 14132-14137.

Tillery AC, Haas JR. 2016. Potential postwildfire debris-flow hazards—A prewildfire evaluation for the Jemez Mountains, north-central New Mexico. U.S. Geological Survey Scientific Investigations Report p23.

Tuckett QM, Koetsier P. 2016. Mid-and long-term effects of wildfire and debris flows on stream ecosystem metabolism. Freshwater Science 35: 445-456.

USGS. 2014. National Watershed Boundary Dataset. National Geospatial Technical Operations Center.

USGS. 2016. National Hydrography Dataset. USGS National Geospatial Technical Operations Center (NGTOC): Rolla, MO and Denver, CO.

USGS. 2017. 1-meter Digital Elevation Models. USGS National Map 3DEP Downloadable Data Collection: U.S. Geological Survey.

Van Horn DJ, White CS, Martinez EA, Hernandez C, Merrill JP, Parmenter RR, Dahm CN. 2012. Linkages between riparian characteristics, ungulate grazing, and geomorphology and nutrient cycling in montane grassland streams. Rangeland Ecology and Management 65: 475-485.

Veenhuis JE. 2002. Effects of wildfire on the hydrology of Capulin and Rito de los Frijoles Canyons, Bandelier National Monument, New Mexico. U.S. Geological Survey, Water-Resources Investigations Report.

Wagenbrenner J, MacDonald L, Rough D. 2006. Effectiveness of three post-fire rehabilitation treatments in the Colorado Front Range. Hydrological Processes 20: 2989-3006.

Wagner RJ, Mattraw HC, Ritz GF, Smith BA. 2006. Guidelines and standard procedures for continuous water-quality monitors: Site selection, field operation, calibration, record computation, and reporting. U.S. Department of the Interior, U.S. Geological Survey, Reston Virginia, p 51 + attachments.

Weed AS, Ayres MP, Hicke JA. 2013. Consequences of climate change for biotic disturbances in North American forests. Ecological Monographs 83: 441-470.

Westerling AL. 2016. Increasing western US forest wildfire activity: sensitivity to changes in the timing of spring. Philosophical Transactions of the Royal Society B 371: 10.

Westerling AL, Gershunov A, Brown TJ, Cayan DR, Dettinger MD. 2003. Climate and wildfire in the western United States. Bulletin of the American Meteorological Society 84: 595.

Westerling AL, Hidalgo HG, Cayan DR, Swetnam TW. 2006. Warming and earlier spring increase western US forest wildfire activity. Science 313: 940-943.

Williams AP, Allen CD, Millar CI, Swetnam TW, Michaelsen J, Still CJ, Leavitt SW. 2010. Forest responses to increasing aridity and warmth in the southwestern United States. Proceedings of the National Academy of Sciences of the United States of America 107: 21289-21294.

WRCC. 2016. Valles Caldera National Preserve, Headquarters Climate Station. Reno, Nevada: Western Regional Climate Center, Desert Research Institute, https://wrcc.dri.edu/vallescaldera/

Young RG, Huryn AD. 1999. Effects of land use on stream metabolism and organic matter turnover. Ecological Applications 9: 1359-1376.

EFFECTS OF A CATASTROPHIC WILDFIRE ON DOWNSTREAM FISH ASSEMBLAGES IN AN ARIDLAND RIVER

Authors: Justin K. Reale [1,2,8], Thomas P. Archdeacon [3,9], David J. Van Horn [2,10], Eric J. Gonzales [4,5,11], Robert K. Dudley [6,7,12], Thomas F. Turner [2,6,13], Clifford N. Dahm [2,14]

[1] U.S. Army Corps of Engineers, Albuquerque, NM, U.S.A.

[2] Department of Biology, University of New Mexico, Albuquerque, NM, U.S.A.

[3] U.S. Fish and Wildlife Service, New Mexico Fish and Wildlife Conservation Office, Albuquerque, NM, U.S.A.

[4] SWCA Environmental Consultants, Albuquerque, NM, U.S.A. (formerly)

[5] U.S. Bureau of Reclamation, Albuquerque, NM, U.S.A. (current)

[6] Division of Fishes, Museum of Southwestern Biology, University of New Mexico, Albuquerque, NM, U.S.A.

[7] American Southwest Ichthyological Researchers, Albuquerque, NM, U.S.A.

Email Addresses: [8]justin.k.reale@usace.army.mil; [9]thomas_archdeacon@fws.gov; [10]vanhorn@unm.edu; [11]egonzales@usbr.gov; [12]dudleyrk@unm.edu; [13] turnert@unm.edu; [14]cdahm@unm.edu

Abstract

Post-wildfire effects on coldwater fish assemblages in headwater streams within, or close to, the burned areas are fairly well known; however, few studies have evaluated the effects of catastrophic high intensity and large areal wildfires on downstream non-salmonid assemblages. Using data from long-term fish community surveys and high-frequency water quantity and quality monitoring, we analyzed pre- and post-fire differences in the cypriniform dominated community at two sites on a large river (i.e., Rio Grande [7th order])

> 20 km downstream of a major wildfire in the Jemez Mountains, NM. We also evaluated the effects of a >1000-year flood (three years post-fire) on the fish assemblage in a post-fire environment. Pre-fire, we observed moderate between-site overlap in commonly detected and abundant species, along with seasonal and interannual variability in fish assemblage composition. Episodic small dissolved oxygen (DO) sags were observed pre-fire, but concentrations remained greater than 5.5 mg L^{-1} throughout the year. During the first three years post-fire, we observed multiple severe DO sags (< 3 mg L^{-1}) at both sites. We observed a differential response in total abundance and fish assemblage variables between sites. While declines in total abundance, diversity, and evenness were observed post-fire in the upstream assemblage, the downstream assemblage appeared to be generally unimpacted by effects of the fire. Following a major flood in 2013, species-specific and fish assemblage response variables remained unchanged at downstream site. A further reduction in total and species-specific fish abundance was observed at the upstream site after the flood. We attribute the differential post-fire and post-flood response at the two sites, with similar assemblage composition and flow regimes, to the proximity and extent of fire-impacted watersheds upstream. Our results highlight the need to evaluate watershed-specific hydrologic, water quality, and biotic responses at different spatial scales to fully assess the impacts of wildfire on downstream aquatic ecosystems.

Keywords: wildfire, desert fish assemblages, disturbance, Rio Grande, water quality.

Introduction

Pronounced climatic changes have been documented in the western United States (US), including below-average winter precipitation and earlier spring snowmelt (Stewart et al., 2004; Westerling et al., 2006), and elevated spring and summer temperatures (Mote et al., 2018; Westerling, 2016; Westerling et al., 2006), and increased aridity (Abatzoglou and Williams, 2016; Littell et al., 2009). These changes, in combination with other climate-mediated processes such as insect outbreaks (Bentz et al., 2010; Raffa et al., 2008), have resulted in widespread forest stress and mortality (Adams et al., 2012; Breshears et al., 2005). Synergistically, the increase in climate-mediated wildfire activity (Westerling et al.,

2003), including an expansion of the wildfire season (Westerling, 2016; Westerling et al., 2006), increased burned area (Littell et al., 2009; Williams and Abatzoglou, 2016) and increased fire severity (Miller et al., 2009; van Mantgem et al., 2013), has resulted in further forest mortality throughout the western US (Williams et al., 2010).

Severe wildfires create large-scale disturbances that induce hydrologic and geomorphologic change in burned watersheds (Shakesby and Doerr, 2006). Impacts include enhanced and accelerated flooding, surface erosion, mass wasting, and debris flows (Cannon et al., 2008; Moody et al., 2013). Water quality impacts include elevated sediment loads (Kunze and Stednick, 2006; Ryan et al., 2011), turbidity (Mast et al., 2016; Murphy et al., 2012; Reale et al., 2015), solutes (Sherson et al., 2015; Silins et al., 2014) and organic matter (Betts and Jones, 2009; Earl and Blinn, 2003; Mast and Clow, 2008; Murphy et al., 2015). Low dissolved oxygen and hypoxia (< 2 mg L^{-1}) events also have been documented post-fire (Dahm et al., 2015; Lyon and O'Connor, 2008; Sherson et al., 2015) and attributed to intensified chemical and/or biological oxygen demand from burn-scar derived inputs to streams and rivers (Dahm et al., 2015).

Negative impacts to water quality have significant implications for downstream river ecosystems and biota (Bisson et al., 2003; Bixby et al., 2015; Minshall et al., 1989). While information on fish assemblage responses is limited, it is suggested that despite harsh post-fire hydrologic, geomorphic and water quality conditions, native fish populations can be resistant or resilient to fire disturbance (Dunham et al., 2003). Re-colonization of the fish assemblage post-fire is often rapid (Bisson et al., 2003; Gresswell, 1999; Rieman and Clayton, 1997a), However, knowledge of fish community responses to fire-associated stream conditions relies heavily on research focusing on cold (i.e., streams with maximum daily mean water temperatures < 22^{0}C; Lyons et al. 1996) headwater streams (i.e., 1st and 2nd order) within or near the burn scar (Gresswell, 1999). Very few studies (e.g., Lyon and O'Connor 2008; Whitney et al. 2015a; Whitney et al. 2015b) have assessed the effects of wildfire on non-salmonid (i.e., warm water) fish assemblages in larger rivers (≥ 4th order) downstream (i.e., ≥ 10 river-km) from the burn scar.

We use long-term fish assemblage data, with supporting high-frequency water quantity and quality data, to evaluate drivers of pre- and post-fire variations in a

cypriniform dominated assemblage at two sites in a large river (i.e., Rio Grande [7th order]) downstream (i.e., > 20 km) of a catastrophic wildfire that burned the Jemez Mountains, NM in 2011. The goals of our study were to 1) assess the immediate (year one) and short-term (years two to five) fish assemblage and water quality responses post-fire in comparison to pre-fire conditions, and 2) evaluate the effects of an extreme flood event (occurring in year three after the fire) on the fish assemblage and water quality in a post-fire environment.

Methods

Study site

The Middle Rio Grande (MRG) is defined as the section of the Rio Grande from the U.S. Geological Survey (USGS) stream gage at Otowi (USGS 08313000) near Santa Fe, NM in the north to Elephant Butte Reservoir in the south (Fig. 1). The MRG is a highly regulated system with discharge controlled predominantly by reservoir releases and agricultural water demand (Bestgen and Platania, 1991). Cochiti Dam is the primary flood and sediment control structure in the MRG and has caused a reduction in overbank flooding (Crawford et al., 1996; Molles et al., 1998), and channel armoring and substrate coarsening (Lagasse, 1980; Richard, 2001). Downstream of the Otowi gage, the river receives limited surface water inflow (Ortiz and Lange, 1996) and lacks perennial tributaries (Richard and Julien, 2003). However, numerous ephemeral and intermittent streams, both upstream and downstream of Cochiti Dam, contribute surface water and sediment during periods of intense monsoonal rainfall or rapid snowmelt (Moore and Anderholm, 2002) (Fig 1). The river usually remains perennial through the city of Albuquerque (Bestgen and Platania, 1990), while downstream reaches are frequently dried due to agricultural water demand during summer and autumn (Archdeacon, 2016).

Wildfire characteristics

The Las Conchas (LC) fire burned ~633 km² in the Jemez Mountains, NM during the summer of 2011 (Fig. 1). The burn severity was ~20% high, 26% moderate, and 54% low or unburned (USDA Forest Service, 2011). The LC fire burned the headwaters of the Jemez

River along with the headwaters of numerous smaller catchments containing intermittent rivers that discharge into the Rio Grande upstream and downstream of Cochiti Dam (Dahm et al., 2015; USACE, 2012). Following the LC fire, elevated overland flow resulted in rill formation, extensive erosion and deposition, channel incision and avulsion, debris flows and flooding within and downstream of the burn scar (Dahm et al., 2015; Orem and Pelletier, 2015; Pelletier and Orem, 2014; USACE, 2012). These runoff events also resulted in episodic pulses of degraded water quality that periodically drove dissolved oxygen to 0.0 mg L^{-1} and propagated over ~50 river-km on the Rio Grande downstream of Cochiti Dam (Dahm et al., 2015). These episodic sags continued through 2013 with associated concentrations of dissolved oxygen of less than 3 mg L^{-1} (Reale et al., 2015).

Monitoring locations and methodology

We focused on two locations within the mainstem of the Rio Grande, NM that are downstream of intermittent tributaries affected by the LC fire. These sites have multi-year fish assemblage data along with nearby representative streamflow and high-frequency water quality data (Fig. 1). The first location is upstream of Cochiti Dam within the White Rock Canyon River Reach (White Rock). Fish assemblage data were collected during sixteen surveys conducted over 5 years of monitoring between 2010 and 2014 (SWCA 2014) at the Buckman diversion (29.6 river-km upstream of Cochiti Dam, Fig 1). Fish were sampled with a backpack electrofishing unit (LR-24, Smith Root, Inc., Vancouver, Washington) along seven established transects, sampling all habitats that were accessible with chest waders. The Las Conchas fire burned 155 km^2 upstream of Cochiti Dam, and the distance from the fish-monitoring site to the burn was 24 river-km (Table 1). The USGS streamflow gage at Otowi is 5.2 river-km upstream of the fish monitoring location. The second fish-monitoring location is the bridge crossing at US 550 (US 550), which is 45.6 km downstream of Cochiti Dam (Fig. 1). Fish were sampled from 2006 to 2015 at US 550 (Dudley et al., 2016 and references therein) by rapidly drawing a 3.1 m x 1.8 m small mesh (ca. 5 mm) seine through 18 discrete habitat types less than 15 m long. Mesohabitats with similar conditions that did not exceed depths/velocities for efficient seining were sampled, regardless of streamflow conditions. Eighty-three surveys were conducted over the 10

years of continuous monitoring (2006–2015), but there was a gap in the record from January to August 2009. The Las Conchas fire burned 228 km^2 that discharges into the Rio Grande downstream of Cochiti, and the distance from the fish-monitoring site to the burn was 50 river-km (Table 1). Streamflow data were obtained from the USGS stream gage at San Felipe (08319000), which is 20.1 river-km upstream of US 550 (Fig. 1). At both sites, all non-larval fish (> ~15 mm Standard Length) were identified to species in the field using taxonomic keys provided in Sublette et al. (1990), while phylogenetic classification followed Nelson et al. (2004).

To evaluate water quality conditions, we obtained 15-minute resolution data from a network of continuously deployed multi-parameter (dissolved oxygen [DO], turbidity, specific conductance (SC), pH, and temperature) YSI 6920 or EXO sondes (Yellow Springs Instruments Inc. /Xylem Inc., Yellow Springs, OH, U.S.A.) (Dahm et al., 2013). A sonde 26.6 river-km downstream of Buckman was used to assess post-fire conditions within the White Rock Reach (period of record 2012 - present). The Las Conchas fire burned 255 km^2 upstream of the sonde, and the distance from the site to the burn was 7 river-km (Table 1). To evaluate pre- and post-fire water quality at US 550, data was used from a sonde deployed within 300 m of the fish sampling location (period or record 2006 - present). Site visits were made every two to four weeks to clean and calibrate the sondes following USGS standard operating procedures (Wagner et al., 2006). Water quality data were compiled, validated, and corrected for fouling and drift using Aquarius Workstation 3.3 (Aquatic Informatics, Vancouver, British Columbia, Canada).

We focused on DO only for this study, as previous studies identified that DO had frequently deteriorated to levels < 3 mg L^{-1} upstream and downstream of Cochiti on the Rio Grande through 2013 (Reale et al., 2015; Van Horn et al., 2014). Such major and frequent sags may be detrimental to the fish assemblage. SC and pH also were impacted at the two sites by the fire (Reale et al., 2015; Van Horn et al., 2014), but not to levels that were exceeded MRG water quality standards for aquatic life (NMWQCC, 2000). Turbidity was not evaluated, due to a high pre-fire background (i.e., regularly >200 NTU) and many values greater than the maximum detection limit of the probes deployed at US 550 (Reale et al., 2015). The Las Conchas fire and 2013 flood event did not change the canopy structure of

the open-canopy Rio Grande. Thus, fire- or flood-induced impacts to water temperature (via loss of riparian canopy cover and increased solar radiation) are unlikely, and were not evaluated further.

The fish assemblage

The MRG fish assemblage is dominated by native cyprinids (minnows) and non-native catostomids (suckers) (Dudley et al., 2016; Platania, 1991) in terms of richness and abundance. Native cyprinids are predominantly short-lived (< 5 years) and capable of completing their life cycle in 1 or 2 years (Turner et al., 2010). Representative non-native species in the MRG are White Sucker (*Catostomus commersonii* (CATCOM)) and Common Carp (*Cyprinus carpio*) (Platania, 1991). These species are some of the largest and long-lived species in the MRG (Turner et al., 2010).

Data analysis and statistical methods

Non-larval fish count data were expressed as the total number collected by species at each site during each survey. Total and species-specific abundance data (i.e., total catch) were analyzed. To quantify assemblage structure for each survey, we calculated diversity and evenness using abundance data. We calculated Shannon's diversity index (H') values using Equation 1 (Shannon and Weaver, 1949),

$$H' = -\sum_{i=1}^{S} p_i \ln(p_i) \qquad \text{(Equation 1)}$$

where $\sum$ is the sum of all species (S) and p_i is the proportional abundance of species i (i.e., n_i/N) relative to all individuals (N). H' combines information on species richness and the distribution of individuals among species (Magurran, 2013). A greater number of species and a more even distribution of species both result in an increase in Shannon's diversity index. The maximum value for Shannon's diversity is achieved when all species in a sample are equally abundant.

Shannon's evenness (*J'*) values were calculated for each survey using Equation 2 (Pielou, 1966):

$$J' = H'/\ln(S) \qquad \text{(Equation 2)}$$

where S is the total number of species encountered. J' expresses how evenly the individuals within the assemblage are distributed among different species (Heip et al., 1998). When there are similar proportions of all species, Shannon's evenness approaches its maximum value of one. When the abundances are dissimilar (a mixture of rare and common species), Shannon'sevenness approaches zero. H' and J' were calculated in R Studio (RStudio Team, 2015) using the package *vegan* (Oksanen et al., 2007).

To define pre-fire conditions, we calculated the pre-fire mean value and 90% non-parametric confidence intervals (CI, i.e., upper (UCL) and lower confidence limit (LCL)) for H', J', and total and species-specific abundance for both sampling sites. We selected the 90th, rather than the 95th percentile, based on the precautionary principle (e.g., Gray 1990; Fairweather 1991). Confidence intervals were calculated using the package *boot* (Canty and Ripley, 2016), from which we could assess pre-fire, post-fire, and post-flood changes in species and assemblage metrics.

Results

Analyses of fish assemblage data at the Buckman and US 550 sites are dominated by cypriniform fishes, and show moderate overlap in commonly detected and abundant species prior to the Las Conchas fire (Table 2). The Buckman assemblage appears to be a subset of the 550 assemblage (Table 2). These analyses are consistent with previous comparisons upstream and downstream of Cochiti Dam (Platania, 1991). Native cyprinids commonly observed at both sites include Fathead Minnow *Pimephales promelas* (PIMPRO), Flathead Chub *Platygobio gracilis* (PLAGRA), and Longnose Dace *Rhinichthys cataractae (RHICAT)*. Red Shiner *Cyprinella lutrensis* (CYPLUT) was also abundant at US 550, but not at Buckman. Mean annual discharge for the period of analysis at Buckman and US 550 were similar at 29.2 and 30.4 $m^3 s^{-1}$, respectively (Table 1). Based on the definition by Lyons et al. (1996), Buckman and US 550 are classified as coldwater sites for the period of analysis with an annual average maximum daily temperature of 15.2 and 15.8 °C, respectively (Table 2).

Buckman

Prior to the fire, a clear snowmelt pulse was observed in 2010 but largely absent in 2011 (Fig. 2a). DO at this site during this time period was not assessed, as a sonde was not deployed within the reach until 2012 (Fig. 2b). Pre-fire total fish abundances ranged from 49 to 122 with a mean of 80 (Fig. 2c). Mean H' (Fig. 2d) and J' (Fig. 2e), prior to the fire were 2.7 and 0.77, respectively. The species CATCOM, PLAGRA, and RHICAT, were collected in each of the four pre-fire surveys with pre-fire mean values of 14, 17, and 37 individuals, respectively (Fig. 3a, c & d). The pre-fire mean for PIMPRO was 10, and this species was detected in 3 of 4 surveys. CATCOM abundance peaked in the July survey (Fig. 3a). In contrast, PIMPRO, PLAGRA and RHICAT did not exhibit a clear seasonal trend (Fig. 3b-3d).

In the fish survey at the end of the monsoon season immediately following the wildfire (2011), total catch (Fig 2c), H' (Fig. 2d), and J' (Fig. 2e) were below the pre-fire lower confidence limit. Total abundance was minimally influenced, with a drop from 49 to 38 between the survey prior to the onset of water quality events and survey at the end of the 2011 monsoon season. H' and J' were also minimally reduced (i.e., from 2.4 to 1.9, and 0.8 to 0.5, respectively) prior to the onset of water quality events and survey at the end of the 2011 monsoon season. Similar declines in total catch, H, and J', were observed between the July and September surveys the previous year prior to the fire (Fig. 2c-2e). The species-specific response (Fig. 3) immediately following the fire was muted, as CATCOM, PIMRO and PLAGRA abundances remained constant or increased in comparison to the previous survey (Fig. 3a-3c). The lone fish species at the Buckman site that responded strongly immediately after the wildfire was RHICAT abundance (Fig. 3d).

In the first two years following the fire (2012 and 2013), spring snowmelt pulses were largely absent from the hydrograph (Fig. 2a). During this time period, episodic DO sags were observed throughout the monsoon seasons of 2012 and 2013 with minimum DO concentrations often below 2 mg L^{-1} (Fig. 2b). Outside of the monsoon season, DO concentrations remained above 5 mg L^{-1} (Fig. 2b). Post-fire, mean total catch (Fig. 2c), H' (Fig. 2d), and J' (Fig. 2e), were 36, 1.9 and 0.5 respectively, below their respective pre-fire lower confidence limits. CATCOM and PLAGRA were detected in each of the 8 post-fire

samples with mean values of 9 and 15 individuals, respectively (Fig. 3a & 3c). The post-fire mean for PIMPRO was 1.4, and this species was detected in 5 of 8 surveys (Fig. 3b). Mean post-fire abundance for RHICAT was 8 fish per survey, and it was observed in 6 of 8 samples (Fig. 3d). The post-fire mean abundance for CATCOM (Fig. 3a) and PLAGRA (Fig. 3c) remained within the pre-fire CI. In contrast, the post-fire mean abundance for PIMPRO and RHICAT was below the pre-fire LCI (Fig. 3b & 3d, respectively). The annual peak in CATCOM abundance in July persisted post-fire (Fig. 3a). Post-fire, PIMPRO, PLAGRA, and RHICAT abundance continued to exhibit no clear seasonal trend (Fig. 3b-3d).

The day prior to the major flood event of September 2013 the mean daily discharge estimate was 14 m^3 s^{-1} at the Otowi gage (Fig. 2a). The peak instantaneous and daily mean discharge estimates during the flood event were 226 and 97 m^3 s^{-1}, respectively. Unfortunately, the sonde measuring water quality was lost during the event, and the stilling well was buried under several feet of sediment (Dahm et al., 2013). In the three fish assemblage samples following the large flood event, total catch, H' and J' were the lowest observed during the period of analysis (Fig 2c-2d). As a result, the post-flood mean total abundance, H', and J' (9, 0.8, and 0.06, respectively), were well below the corresponding pre-fire lower confidence limits and the post-fire mean values (Fig. 2c-2e). CATCOM was detected in each of the four post-flood surveys, and a seasonal peak in July persisted (Fig. 3a). PLAGRA (Fig. 3c) and RHICAT (Fig. 3d) were not detected in the first thee sampling events following the flood of September 2013.

In February 2014, the sonde was redeployed and DO sags were observed beginning in July 2014, with concentrations dropping below 3 mg L^{-1} (Fig. 2c). Total catch, H', and J' increased during the July 2014 survey, but remained below the pre-fire lower confidence limit (Fig. 2c-2d). PIMPRO remained absent from the site (Fig. 3b), and a single PLAGRA (Fig. 3c) and RHICAT (Fig. 3d) were collected during the July 2014 survey. In contrast, CATCOM abundance was within the pre-fire CI (Fig. 3a).

US 550

Hydrologic, continuous water quality, and fish assemblage data at the US 550 were assessed prior to the Las Conchas fire. Hydrologic conditions were comparable to those

observed at White Rock with clear snowmelt pulses occurring in 2007-2010 (Fig. 4a). Spring snowmelt pulses were largely absent from the hydrograph in 2006 and 2011 (Fig. 4a). Episodic spikes in discharge from monsoonal thunderstorms were observed during the summer months, with a varying degree of frequency and severity depending on the strength of the monsoon (Fig. 4a). Dissolved oxygen concentrations were predominantly greater than 6 mg L^{-1} with a seasonal peak occurring during the winter months (Fig. 4b) and slight (concentrations did not drop below 5.5 mg L^{-1}) episodic sags in July through September (Fig. 4b).

Total fish abundance at the US 550 site varied seasonally (Fig. 4c) with values frequently above (during the summer months) and below (during the winter months) the pre-fire mean (126 fish per survey) and confidence interval. Mean H' (Fig. 4d) and J' at the US 550 site during the pre-fire period were 0.99 and 0.67, respectively (Fig. 4e). Considerable interannual variability in both H' and J' was observed in comparison to the pre-fire mean and CI (Fig. 4c & d). We were unable to calculate J' for three surveys pre-fire at the US 550 site due to H' values of zero (when total fish catch was zero). An annual peak in CATCOM was observed in July each year pre-fire in those years where July data were available (Fig. 5a). The exception to this pattern was in 2009 when a gap in the record shifted the apparent annual peak to September (Fig. 5a). Outside of this short-lived summer spike, CATCOM abundance (mean of 23.4 ± 61) was low or was absent (20 of 44 surveys) from the site during most months (Fig. 5a). PIMPRO was also an uncommon fish species that was documented in only 14 of 44 surveys pre-fire, with a mean abundance of 1.3. PLAGRA was observed in 42 of 44 pre-fire surveys with a mean of 25 individuals per survey (Fig. 5c). RHICAT (Fig. 5d) and CYPLUT (Fig. 5e) also were commonly detected (77% and 88% of surveys, respectively) averaging 16.3 and 17.7 individuals per survey, respectively.

Over the course of the monsoon season in 2011, numerous episodic DO sags were observed at the US 550 site with 10 sags of < 4 mg L^{-1} in July and August (Fig. 4b). Despite these poor water quality conditions in 2011 immediately following the fire, we did not detect a statistically significant impact on the fish assemblage (Fig 3c-3d) or to specific species (Fig. 4).

In the two years that followed the fire (i.e., 2012 and 2013), a strong spring snowmelt pulse was absent from the hydrograph at the US 550 site (Fig. 4a). A single DO sag was documented in 2012 below 3 mg L^{-1} at the US 550 site (Fig. 4b). Multiple sags in 2013 were observed during the monsoon season, with minimum values near 3 mg L^{-1} (Fig. 4b). The post-fire total mean abundance was 187 fish per survey (Fig. 4c) at the site, which was greater than the pre-fire upper confidence limit (157). Post-fire, the mean H' was 1.05, and remained within the pre-fire CI (0.99-1.11, Fig. 4d). The mean J' post-fire was slightly reduced (by 0.06), but this change was below the pre-fire lower confidence limit (0.68, Fig. 4e). The post-fire mean CATCOM abundance was 23 (within the pre-fire CI). CATCOM was detected in 16 of 20 post-fire surveys post-fire, and the annual peak in CATCOM abundance was observed in 2012 and 2013 (Fig. 5a). The post-fire mean abundance for PIMPRO was 5, greater than the pre-fire upper confidence limit, and this species was detected in 3 of 4 surveys (Fig. 5b). PLAGRA (Fig. 5c) and CYPLUT (Fig. 5e) were detected in all 20 post-fire surveys with mean values of 46 and 53 individuals, respectively. These values were both greater than the pre-fire upper confidence limit. The mean post-fire abundance for RHICAT (Fig. 5d) was 19. This was within the pre-fire CI, and the species was detected in 16 of 20 post-fire surveys.

Two days prior to the first of several high-flow events, the daily mean discharge estimate was 9 m^{3}s^{-1} on September 9, 2013 at the US 550 site (Fig. 4a). Between September 11th and 17th, five high flow events with instantaneous discharge estimates greater than 56 m^{3}s^{-1} were measured. The largest event exceeded 268 m^{3}s^{-1}. Four DO sags were observed during this high flow period with minimum DO concentrations between 4.8 and 5.4 mg L^{-1} (Fig. 4b). Total abundance dropped from 337 to 96 fish in the survey immediately following the flood. The abundance drop was large, but remained within the pre-fire CI (Fig. 5c). H' and J' remained relatively unchanged (a 0.05 and 0.11 increase, respectively) in the sample immediately following the flood. A clear species-specific response in the sample immediately following the large flood event was not detected (Fig. 5).

A strong spring snowmelt pulse in 2014 and 2015 was absent from the hydrograph at the US 550 site (Fig. 4a). Continued episodic spikes in discharge and less severe (i.e., minimum concentration >5.4 mg L^{-1}) DO sags were observed during the summer months in

2014 and 2015 (Fig. 5a). The mean post-flood total fish abundance at the US 550 site was 97 fish and remained within the pre-fire CI (Fig. 5c). The mean post-flood H' decreased below the pre-fire CI with values of zero during two surveys (Feb and March 2014) while J' remained within the pre-fire CI (Fig. 5d). An annual summer spike in CATCOM abundance was absent in 2014 and dampened in 2015 (Fig. 5a). The post-flood mean CATCOM abundance was 4, below the pre-fire lower confidence limit of 23. Similarly, mean post-flood CPYLUT abundance also dropped below the pre-fire lower confidence limit (Fig. 5e). In contrast, the mean post-flood abundance for PIMPRO, PLAGRA and RHICAT (8, 29, and 21, per survey) were within or greater than their respective pre-fire confidence intervals (Fig. 5 b-5d).

Discussion

This study used long-term fish assemblage data with supporting high-frequency water quantity and quality data to evaluate pre- and post-fire variations in the Rio Grande fish assemblage at two sites > 20 river-km downstream of the catastrophic Las Conchas wildfire. We assessed the immediate (summer and fall of 2011) and short-term (years two and three post-fire) fish assemblage and water quality responses in comparison to pre-fire conditions. We also evaluated the effects of a major flood event (occurring in September of 2013 in year three after the fire) on the fish assemblage and water quality in a post-fire environment. We determined that both sites are classified as coldwater sites. However, both reaches are dominated by support a combination of cool and warm water fish species (Platania, 1991), likely due to a wide range in habitat characteristics (e.g., water temperature, silt loads, water velocity, and substrate type). This research adds to the short list of studies that have evaluated the response of a non-salmonid fish assemblage in larger rivers (≥ 4th order) downstream (i.e., ≥ 10 river-km) of a wildfire disturbance (Lyon and O'Connor, 2008; Whitney et al., 2015a). Additionally, this is the first study to use long-term, high frequency, water quality data to help understand these impacts.

Post-fire fish assemblage and water quality responses (August 2011-September 2013)

During the monsoon season immediately following the fire in 2011, several

precipitation events within the burn scar of the Las Conchas wildfire resulted in severe flooding and debris flows (Fresquez and Jacobi, 2012; Grimm et al., 2013; Tillery and Haas, 2016; USACE, 2012), and water quality impacts (pH and DO sags and turbidity and SC spikes) within the headwater streams that discharge into the Rio Grande below Cochiti Dam (Reale et al., 2015; Sherson et al., 2015). The magnitude of the flood pulses from these intermittent rivers were largely attenuated once they reached the Rio Grande, resulting in small increases (< 20 $m^3 s^{-1}$) in discharge (Dahm et al., 2015). For example, large DO sags, but no flood events, were documented at both sites for two years following the wildfire. These severe and frequent DO sags propagated at least 90 river-km on the Rio Grande downstream of Cochiti Dam (Dahm et al., 2015). However, at the 550 site we did not detect a notable impact to the total fish assemblage (Fig 4c-4e) or to specific species (Fig. 5) during the monsoon season immediately following the fire, despite observed fish kills at the site and nearby (Dudley, 2011; Radford, 2011). In contrast, fewer fish were collected from White Rock during post-fire surveys than during pre-fire surveys (i.e., 2010), and all the tested fish assemblage response variables were lower than the pre-fire lower confidence interval (Fig. 2c-2e). The differential fish assemblage response between sites could be attributed to the suspended concentrations observed within the two reaches immediately following the fire. Concentrations upstream of Cochiti Dam (> 28000 mg^{-1}) were nearly 2x greater than downstream (< 15000 mg^{-1}) during the initial post-fire pulses in 2011. The controlled hypolimnetic releases from Cochiti Dam likely reduced the suspended sediment load, in addition to removing the water quality fire-effects from events that originated upstream (Dahm et al., 2015). Another attribute that can mitigate the impacts of disturbances on fish assemblages is access to refugia, which can provide source populations for recolonizing streams following fire-induced extirpation (Whitney et al., 2017). However, both the Buckman and US 550 sites lack nearby perennial tributaries (Moore and Anderholm, 2002; Ortiz and Lange, 1996) which serve as refugia (Gresswell, 1999; Rieman and Clayton, 1997b), and thus we can rule out this possible differentiating factor.

A more likely factor that may contribute to this site-specific response is proximity to the burned area. In a study from an aridland river in Australia, Lyon and O'Connor (2008)

observed a 95-100% initial reduction in fish abundance at sites less than 55 river-km from the source of a post-fire sediment slug on the Buckland River (a 4th order river). The reduction in fish abundance at these sites was sustained for up to 12 months, but after 24 months, the fish assemblage showed signs of recovery. In contrast, the authors observed no measurable short- or long-term reduction in total fish abundance following a post-fire sediment slug at sites greater than 55 river-km downstream, despite observing dead or dying fish and measuring a DO sag that remained less than 2 mg L^{-1} for greater than 12 hours at 70 river-km downstream of the source of the sediment slug. Similar results were documented in southern NM on the upper Gila River, in which fire impacts to fish assemblages attenuated with increasing distance from the burned area (Whitney et al., 2015a; Whitney et al., 2015b). Thus, we attribute differences in fish abundance and assemblage structure across sites to the proximity of surveys to the burn, as the US 550 site is nearly twice the distance from the burn in comparison to the Buckman site (Table 1, Fig. 1). In addition, there are notably more fire-impacted intermittent tributaries within close proximity to the Buckman site (Fig. 1), which increased the probability of isolated and intense monsoon storm flow events transporting burn material into the Rio Grande.

In addition to impacting abundance and general assemblage composition, previous studies of post-fire fish assemblages have documented differential responses of native versus non-native species. For example, following two consecutive fires in the upper Gila River in southern NM, researchers observed a reduction in native fish abundance, biomass and occupancy, and an increased probability of extinction (Whitney et al., 2015a; Whitney et al., 2015b). Lack of resiliency was attributed to the extent, severity and occurrence of post-fire events that exceeded the tolerance range of these species, although they evolved in a system with considerable hydrologic variability. Specifically, the colder water native fish assemblage of the Gila River have been found to be severely impacted by wildfires and attributed to physiological intolerance to post-fire water conditions, specifically hypoxic blackwater conditions, elevated sedimentation rates, and elevated turbidity (Brown et al., 2001; Propst et al., 1992; Whitney et al., 2015a). In contrast, non-native warmwater fishes were less affected in terms of occupancy, extinction probability, abundance, and biomass. The authors attributed the differential response to the tolerance of non-natives to harsh

abiotic conditions, and to being classified as habitat generalists.

We attribute the relative lack of species-specific responses at the US 550 site to the composition, physiological tolerances to poor water quality, resilience, and life history strategies of the MRG fish assemblage. The Rio Grande is a flashy ecosystem with ephemeral and intermittent channels contributing surface water and sediment during monsoon events (Moore and Anderholm, 2002), with turbidity often > 4000 NTU during such events (Reale et al., 2015). The mean suspended sediment concentration on the Rio Grande upstream and downstream of Cochiti Dam exceeded 900 mg L^{-1} during the study (Table 1). These harsh abiotic conditions, in combination with flow regulation, habitat fragmentation, and habitat alteration, have led to a resilient and species poor MRG fish assemblage (Bestgen and Platania, 1991; Dudley and Platania, 2007; Hoagstrom et al., 2010; Platania, 1991). While the vulnerability of the Buckman assemblage is likely driven by habitat fragmentation of the Rio Grande (Dudley and Platania, 2007), low species diversity within the reach (Platania, 1991; SWCA, 2014), and relative isolation from potential sources of recolonizing fish (Pringle, 2003; Pringle, 1997)

Interannual and within-year variability in abundance and species diversity of MRG fishes is strongly influenced by factors related to spawning seasonality and hydrologic conditions within a given year (Krabbenhoft et al., 2014; Pease et al., 2006; Turner et al., 2010). For example, PLAGRA and RHICAT are classified as intermediate and opportunistic spawners, as larvae appear after the descending limb of the snowmelt pulse (Turner et al., 2010). Similarly, PIMPRO also is an intermediate spawner, but cues in on periods of flow equilibrium (Turner et al., 2010). While CATCOM is classified as an early spawner as larvae first appear on the ascending limb of the snowmelt pulse (Turner et al., 2010). Lastly, CYPLUT spawning occurs late summer during stable base flow conditions (Turner et al., 2010). This variability in spawning strategy and timing, in addition to hydrologic variability within a given year, could influence the fish assemblage response post-fire.

Post-flood fish assemblage response in a post-fire environment (2013)

During the period of 9-16 September 2013, two dissipating tropical storms, one from the Pacific Ocean and a second from the Gulf of Mexico, converged producing

sustained and heavy rainfall resulting in widespread flooding in Colorado and NM (Gochis et al., 2015; Trenberth et al., 2015). Numerous fire-impacted and proximal watersheds that discharge into the Rio Grande upstream of Cochiti (Fig. 1) received over 6 inches of precipitation within 24 hours (i.e., greater-than-1000-yr return period precipitation events). This resulted in widespread and severe flooding (Pinson et al., 2014; Walterscheid, 2015). Flooded tributaries provided copious amounts of sediment at confluences throughout the reach (Wolf Engineering, 2014), including the fish monitoring sites in this study (SWCA, 2014), which provided a unique opportunity to investigate the impacts of a major post-fire flood disturbance on downstream fish assemblages. The suspended sediment concentrations upstream and downstream of Cochiti Dam were similar during this period (53000 and 45000 mg L^{-1}, respectively), despite several sediment sinks (e.g., Cochiti Dam and Jemez Canyon) that could reduce the suspended load downstream.

The large observed post-flood reduction in total and species-specific fish abundance, diversity, and evenness at the upstream Buckman site suggests that impacts to native fishes in particular, were intensified by this post-fire disturbance. This trend was evident in data for three native minnows (i.e., PIMPRO, PLAGRA and RHICAT), which were commonly collected both pre- and post-fire at Buckman, but were absent from the site during each of the first three surveys after the flood event. In fourth survey 10 mo. following the flood event, only a single individual RHICAT and PLAGRA were collected, and PIMPRO remained absent.

This response is of interest, as native fishes are often considered to be more resilient to flash flooding in flood prone catchments than non-native species that did not evolve under these conditions (Minckley and Meffe, 1987). A variety of species-specific mechanisms may be responsible for this reduction in native fishes. First, RHICAT is an obligate gravel-cobble riffle species that seeks shelter (Sublette et al., 1990) and forages for benthic macroinvertebrates (Thompson et al., 2001) in these habitats. Following the 2013 flood, benthic macroinvertebrate density decreased and the Hilsenhoff Biotic Index increased (a lower abundance of taxa sensitive to water quality degradation) at the Buckman sampling site (SWCA, 2014). Thus, we hypothesize that degraded water quality, disturbed benthic sediments, and sediment deposition all reduced gravel-rock riffle habitat

and food availability and negatively impacted RHICAT abundance. In contrast to RHICAT, PLAGRA is associated with a natural flow regime, strong currents, shifting sand substrate, and turbid-river environments (Bonner and Wilde, 2000; Cross and Moss, 1987; Quist et al., 2004) and feeding efficiencies of this species are reportedly un-impacted by high turbidity levels (Bonner and Wilde, 2002) commonly observed during post-fire water quality events (Dahm et al., 2015; Reale et al., 2015).

These adaptations would appear to buffer this species from the effects of post-fire flood events, however, this species also feeds on benthic macroinvertebrates (Fisher et al., 2002; Olund and Cross, 1961), which were impacted post-fire and post-flood (Fresquez and Jacobi, 2012; SWCA, 2014), may be responsible for the observed post-flood declines. Similarly, PIMPRO has a high tolerance low dissolved oxygen and high turbidity (Ankley and Villeneuve, 2006; Klinger et al., 1982; Robb and Abrahams, 2003) suggesting that it could withstand the poor water quality conditions during the post-fire flood event. However, the elevated sedimentation rates throughout the reach (Wolf Engineering, 2014), including the fish monitoring sites in this study (SWCA, 2014), likely reduced recruitment of this nesting minnow (Sublette et al., 1990). In contrast, to the native species, a non-native sucker (CATCOM) was detected in each of the four surveys immediately after the flood at the Buckman site, and this species exhibited similar seasonal trends comparable to pre- and post-fire years. We attribute the lack of a post-flood response in CATCOM abundance to 1) early spawning (Krabbenhoft et al., 2014; Turner et al., 2010) such that by September young-of-year CATCOM were able to withstand the harsh abiotic conditions (Lobón-Cerviá, 1996; Pearsons et al., 1992), 2) adaptable habitat requirements (Corbett and Powles, 1986; Twomey et al., 1984) and diet (Eder and Carlson, 1977; Sublette et al., 1990), 3) upstream populations repopulated the affected reach, particularly given the downstream drift of larvae (Corbett and Powles, 1986) and widespread distribution within the Rio Grande (Platania, 1991). In addition, large body size and mobility (Bunt et al., 1999), and compensatory reproductive capacity (Rose et al., 2001) are also factors that could contribute to rapid recovery of CATCOM.

As with the immediate post-fire results, the fish assemblage at the downstream 550 site was un-impacted by the 2013 flood event. This lack of response can likely be attributed

to several water quality and quantity factors. First, the Cochiti and Jemez Canyon dams dampened flood pulses and sediment bed load on the mainstem and the largest tributary in this reach, respectively, unlike at the Buckman site where no dampening occurred. Additionally, while Peralta Canyon did deposit large quantities of bed material into the river during this period plugging the Rio Grande (AuBuchon and Bui, 2014), the inputs were ~ 42 river-km upstream of the fish sampling site. However, due to the low stream gradient of the Rio Grande downstream of Cochiti Dam (Ortiz, 2004), the river likely did not have the stream power to propagate the bed load downstream to the fish sampling site. In contrast, the flood pulse and slugs of low DO propagated a much greater distance and were documented far downstream (Fig. 2a & 2b), however, these water quality excursions were less severe than those observed immediately following the fire and do not appear to have exceeded the tolerance range of the fish assemblages at this downstream site.

Conclusions

1) Immediately following a catastrophic wildfire, similar cypriniform dominated assemblages responded differently at two sites on a large (i.e., 7th order) river responded differently depending on their distance from the burn.

2) Following a major flood three years later, the fish community at the downstream fire-resilient site remained largely unchanged, whereas multiple native fish species declined dramatically at the upstream assemblage at the fire-impacted site.

3) To predict the response of a downstream fish assemblage following a wildfire, one must consider proximity to the burn, total area burned upstream of the study area, the proximity of sediment sinks (e.g., upstream lakes or reservoirs), and species-specific life history.
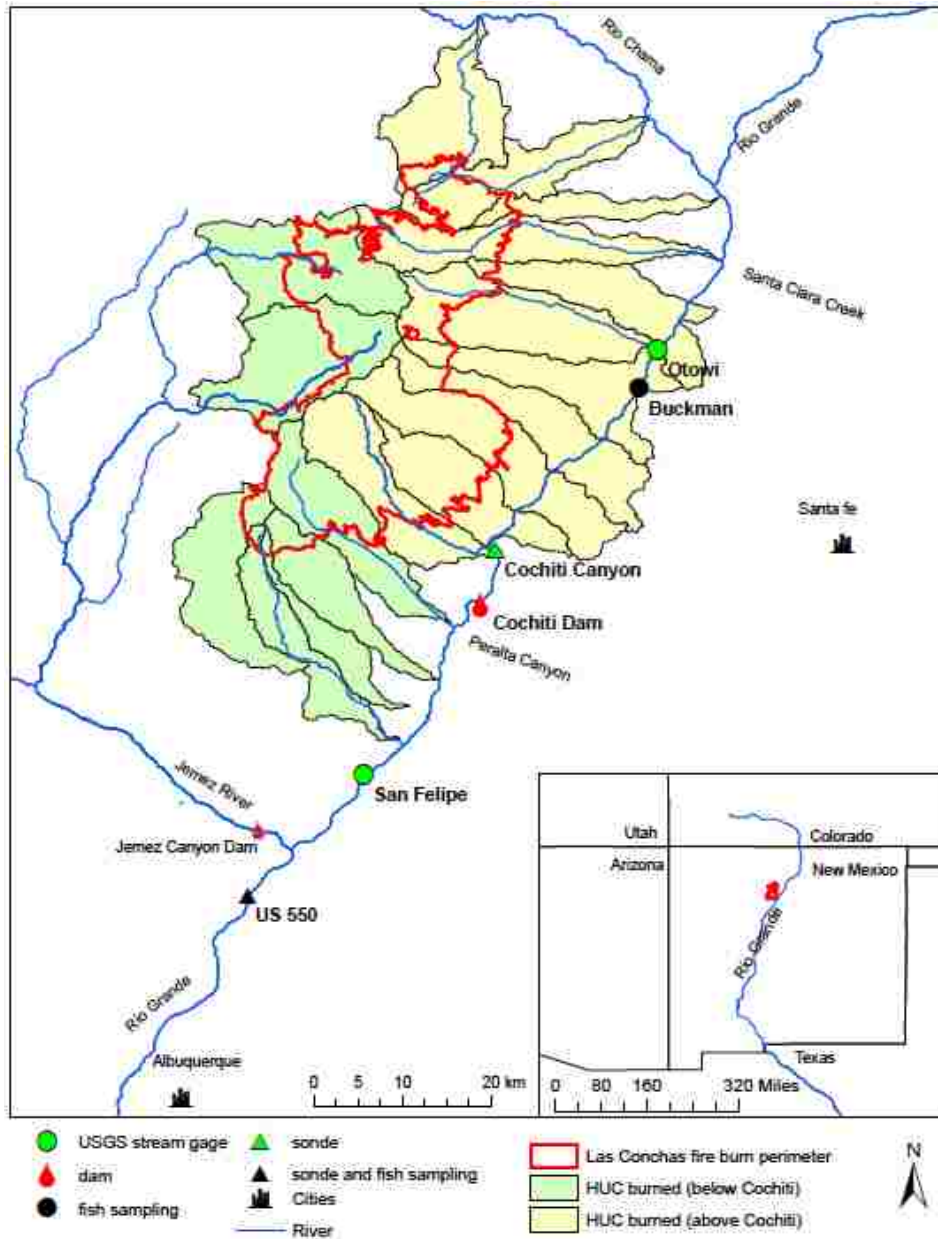
Figures

Figure 1: Maps showing the Rio Grande (lower right) and the burn perimeter of the Las Conchas (LC) wildfire in north-central NM, USA. The main water-quality stations, fish monitoring locations, streams of interest, perimeter of the LC fire, key landmarks, and watershed boundaries (i.e., Hydrologic Unit Codes [HUC]) that were impacted by the LC fire are shown.

Figure 2: (a) Daily mean stream discharge ($m^3 s^{-1}$) measured from the USGS gage at Otowi (USGS gage No. 08313000), (b) dissolved oxygen (DO; $mg L^{-1}$) collected at 15-minute increments downstream of Cochiti Canyon, (c) total number of fish, (d) Shannon's diversity, and (e) Shannon's evenness at the Buckman Diversion within the White Rock reach of the Rio Grande. The red vertical dashed line represents the onset of degraded water quality events following the Las Conchas fire. The red dots represent fish assemblage sampling occasions. The blue vertical dashed line represents the September 2013 flood event. Grey horizontal lines represent the compiled pre-fire mean values and 90% confidence intervals. Red and blue horizontal dashed lines represent the compiled post-fire and post-flood mean values, respectively. The date (x-axis) has been abbreviated to two digits (i.e., MM-YY).
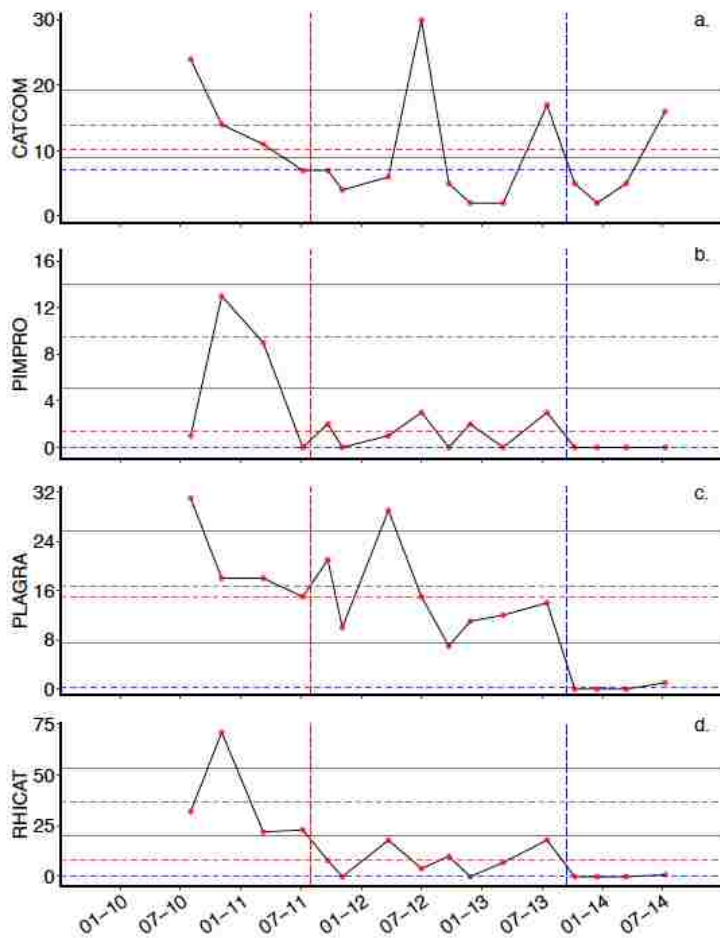
Figure 3: Total abundance of (a) White Sucker *Catostomus commersonii (CATCOM), (b)* Fathead Minnow *Pimephales promelas (PIMPRO), (c)* Flathead Chub *Platygobio gracilis (PLAGRA),* and *(d)* Longnose Dace *Rhinichthys cataractae (RHICAT)* collected at the Buckman Diversion within the White Rock reach of the Rio Grande. The red vertical dashed line represents the onset of water quality events following the Las Conchas fire. The red dots represent fish assemblage sampling occasions. The blue vertical dashed line represents the September 2013 flood event. Grey horizontal lines represent the compiled pre-fire mean values and 90% confidence intervals. Red and blue horizontal dashed lines represent the compiled post-fire and post-flood mean values, respectively. The date (x-axis) has been abbreviated to two digits (i.e., MM-YY).
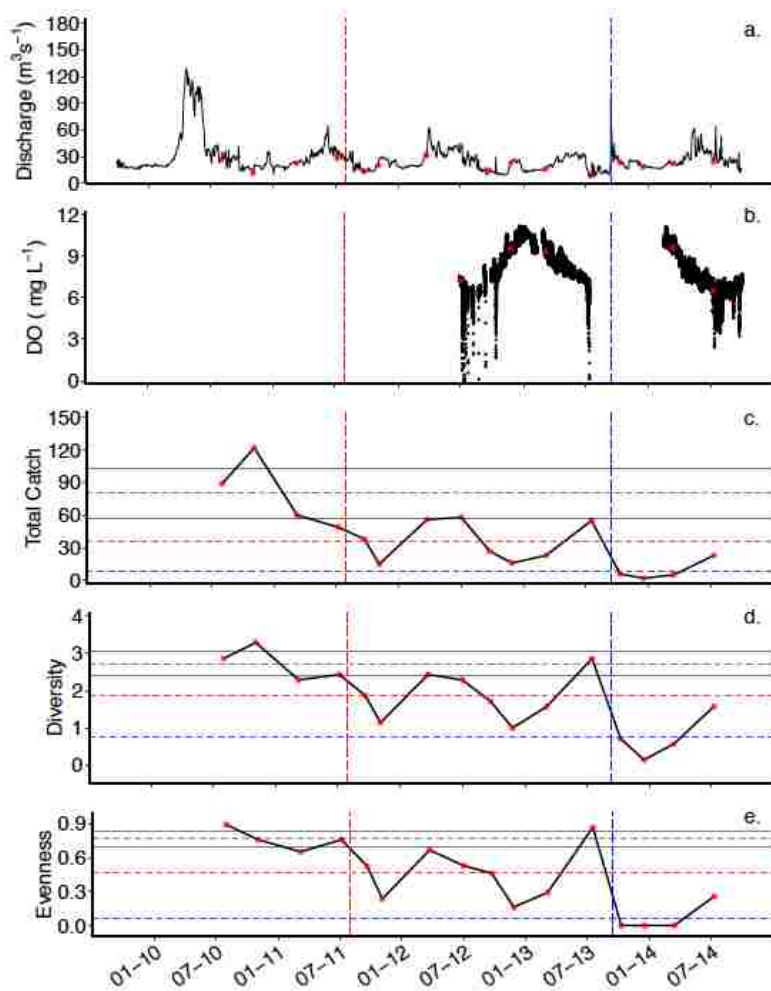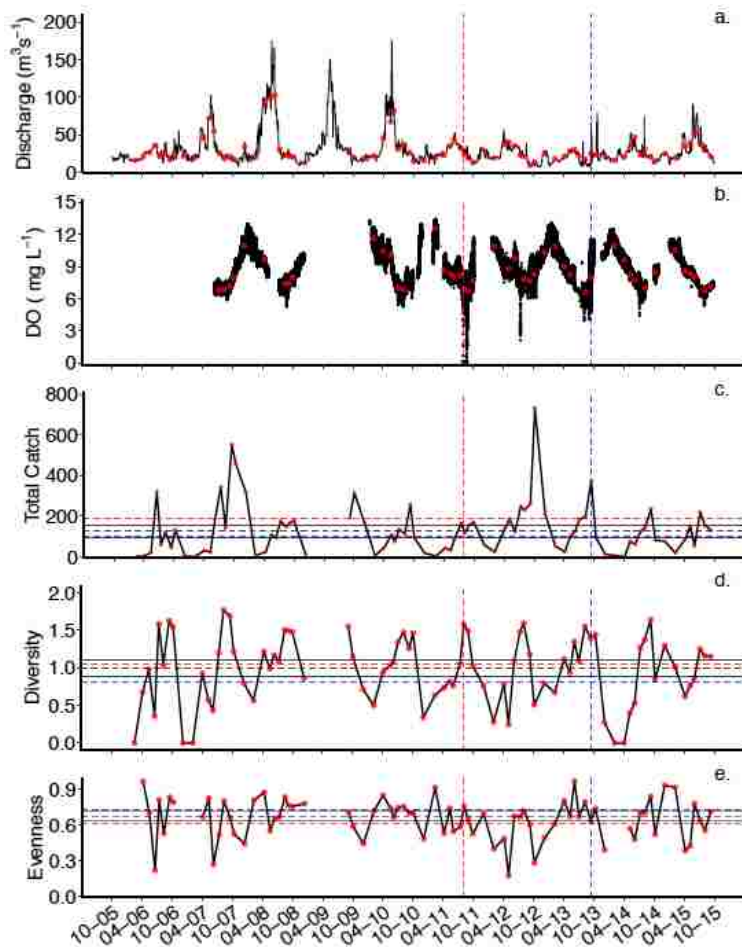
Figure 4: (a) Daily mean stream discharge ($m^3\ s^{-1}$) measured from the USGS gage at San Felipe (USGS gage No. 0831900), (b) dissolved oxygen (DO; mg L^{-1}) collected at 15-minute increments, (c) total number of fish, (d) Shannon's diversity, and (e) Shannon's evenness collected at the U.S. 550 Bridge on the Rio Grande. The red dots represent fish assemblage sampling occasions. The red vertical dashed line represents the onset of water quality events following the Las Conchas fire. The blue vertical dashed line represents the September 2013 flood event. Grey horizontal lines represent the compiled pre-fire mean values and 90% confidence intervals. Red and blue horizontal dashed lines represent the compiled post-fire and post-flood mean values, respectively. Post-fire and post-flood mean values were jittered to reduce overlap. The date (x-axis) has been abbreviated to two digits (i.e., MM-YY).

111
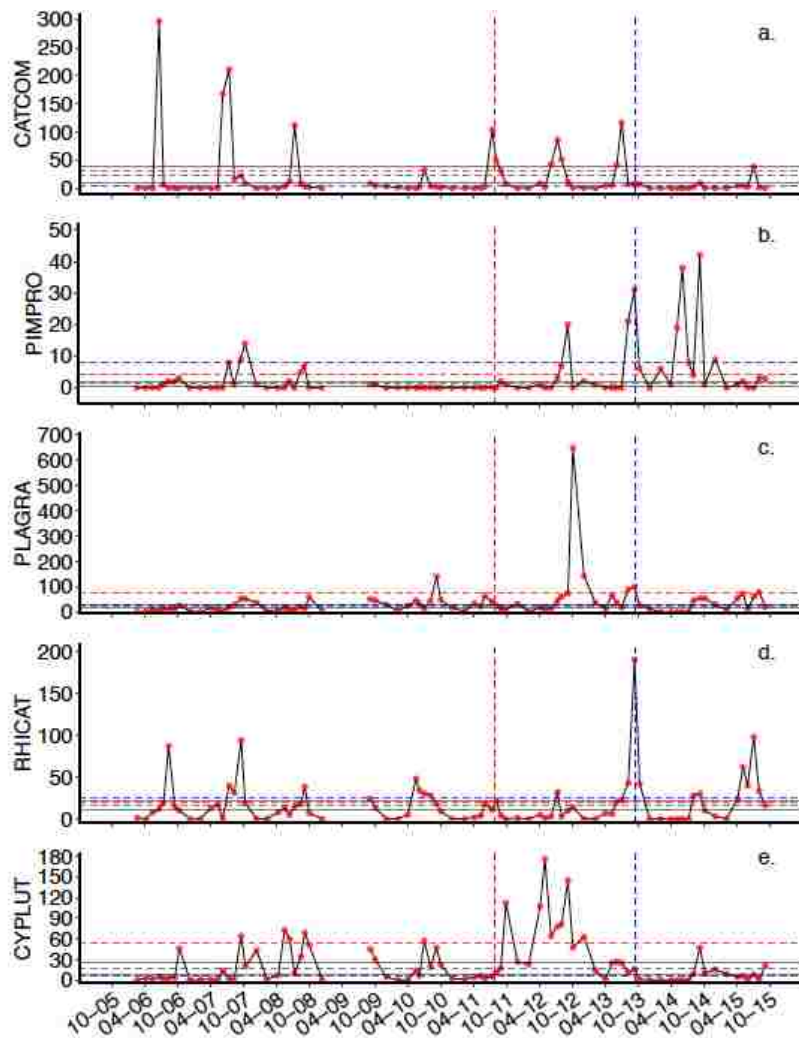
Figure 5: Total abundance of (a) White Sucker *Catostomus commersonii (CATCOM,) (b)* Fathead Minnow *Pimephales promelas (PIMPRO), (c)* Flathead Chub *Platygobio gracilis (PLAGRA), (d)* Longnose Dace *Rhinichthys cataractae (RHICAT), and (e)* Red Shiner *Cyprinella lutrensis (CYPLUT)* collected at the U.S. 550 Bridge of the Rio Grande. The red vertical dashed line represents the onset of water quality events following the Las Conchas fire. The red dots represent fish assemblage sampling occasions. The blue vertical dashed line represents the September 2013 flood event. Grey horizontal lines represent the compiled pre-fire mean values and 90% confidence intervals. Red and blue horizontal dashed lines represent the compiled post-fire and post-flood mean values, respectively. Post-fire and post-flood mean values were jittered to reduce overlap. The date (x-axis) has been abbreviated to MM-YY.

112

Tables

Measurement	Units	Buckman	US 550
Annual mean river discharge	$m^3 s^{-1}$	29.15	30.4
Annual mean suspended sediment	$mg L^{-1}$	925	940
Maximum mean daily temperature	^0C	15.2	15.8
Temperature classification	-	Coldwater	Coldwater
Stream order	-	7	7
Area burned	km^2	155 (255)	228
Las Conchas distance	km	24 (7)	50

Table 1: Study site characteristics of the Rio Grande at White Rock and U.S. 550. Annual mean river discharge was calculated from nearby USGS gages (Otowi and San Felipe, respectively) for water years (i.e., 1OCT-30SEP) that fish data were analyzed. Annual mean suspended sediment was calculated from nearby USGS gages (Otowi and Albuquerque (USGGS No. 08330000)), respectively) for water years (i.e., 1OCT-30SEP) that fish data were analyzed. Maximum mean daily temperature was calculated using all available sonde data during the period of analysis. Temperature classifications (cold water <22°C, warm water >24°C) are from Lyons et al. (1996). Stream order was determined from the USGS National Hydrography Dataset (NHD). Total area burned was calculated using the Las Conchas burn perimeter in ArcGIS. Las Conchas distance is the shortest watercourse distance from the sonde to the perimeter of the wildfire and was measured using the burn perimeter in Google Earth. Total area burned and Las Conchas distance for White Rock was calculated from the fish sampling and sonde location, as these sampling points are not co-located. The values inside parentheses represent the measurements from the sonde. Total area burned and Las Conchas distance for U.S. 550 was calculated from the co-located fish sampling and sonde location.

Scientific Name	Common Name	Abbrev.	Native?	Buckman	US 550
Order Clupeiformes					
Family Clupeidae	**herrings**				
Dorosoma cepedianum	Gizzard Shad	DORCEP	Yes		x
Order Cypriniformes					
Family Cyprinidae	**carps and minnows**				
Carassius auratus	Goldfish	CARAUR	No		x
Cyprinus carpio	Common Carp	CYPCAR	No	x	x
Cyprinella lutrensis	Red Shiner	CYPLUT	Yes	x	x
Gila pandora	Rio Grande Chub	GILPAN	Yes	x	x
Hybognathus amarus	Rio Grande Silvery Minnow	HYBAMA	Yes		x
Pimephales promelas	Fathead Minnow	PIMPRO	Yes	x	x
Platygobio gracilis	Flathead Chub	PLAGRA	Yes	x	x
Rhinichthys cataractae	Longnose Dace	RHICAT	Yes	x	x
Family Catostomidae	**suckers**				
Catostomus commersonii	White Sucker	CATCOM	No	x	x
Catostomus [Pantosteus] plebeius	Rio Grande Sucker	CATPLE	Yes	x	
Carpiodes carpio	River Carpsucker	CARCAR	Yes		x
Order Siluriformes					
Family Ictaluridae	**North American catfishes**				
Ameiurus melas	Black Bullhead	AMEMEL	No		x
Ameiurus natalis	Yellow Bullhead	AMENAT	No		x
Ictalurus punctatus	Channel Catfish	ICTPUN	No	x	x

Order Salmoniformes

Family Salmonidae	**trouts and salmons**				
Salmo trutta	Brown Trout	SALTRU	No	x	x

Order Cyprinodontiformes

Family Poeciliidae	**livebearers**				
Gambusia affinis	Western Mosquitofish	GAMAFF	No	x	x

Order Perciformes

Family Moronidae	**temperate basses**				
Morone chrysops	White Bass	MORCHR	No		x
Family Centrarchidae	**sunfishes**				
Lepomis cyanellus	Green Sunfish	LEPCYA	No		x
Lepomis macrochirus	Bluegill	LEPMAC	Yes	x	x
Micropterus dolomieu	Smallmouth Bass	MICDOL	No	x	
Micropterus salmoides	Largemouth Bass	MICSAL	No	x	x
Pomoxis annularis	White Crappie	POMANN	No	x	x
Family Percidae	**perches and darters**				
Perca flavescens	Yellow Perch	PERFLA	No		x
Sander vitreus	Walleye	SANVIT	No		x

Table 2: Scientific names, common names, and species codes for fish collected in the Middle Rio Grande during the period of analysis at Buckman and U.S. 550. Native status was determined by Propst (1999).

References

Abatzoglou, J.T., Williams, A.P., 2016. Impact of anthropogenic climate change on wildfire across western US forests. Proceedings of the National Academy of Sciences USA 113, 11770-11775.

Adams, H.D., Luce, C.H., Breshears, D.D., Allen, C.D., Weiler, M., Hale, V.C., Smith, A.M.S., Huxman, T.E., 2012. Ecohydrological consequences of drought- and infestation-triggered tree die-off: insights and hypotheses. Ecohydrology 5, 145-159.

Ankley, G.T., Villeneuve, D.L., 2006. The fathead minnow in aquatic toxicology: past, present and future. Aquatic Toxicology 78, 91-102.

Archdeacon, T.P., 2016. Reduction in spring flow threatens Rio Grande Silvery Minnow: trends in abundance during river intermittency. Transactions of the American Fisheries Society 145, 754-765.

AuBuchon, J., Bui, C., 2014. Peralta Arroyo Eastern Terrace Flow Augmentation:Design Report., U.S. Department of the Interior, Bureau of Reclamation, Upper Colorado Region, Albuquerque Area Office, Albuquerque, New Mexico, p. 100.

Bentz, B.J., Regniere, J., Fettig, C.J., Hansen, E.M., Hayes, J.L., Hicke, J.A., Kelsey, R.G., Negron, J.F., Seybold, S.J., 2010. Climate Change and Bark Beetles of the Western United States and Canada: Direct and Indirect Effects. Bioscience 60, 602-613.

Bestgen, K.R., Platania, S.P., 1990. Extirpation of N otropis simus simus (Cope) and N otropis orca Woolman (Pisces: Cyprinidae) from the Rio Grande in New Mexico, with Notes on Their Life History.

Bestgen, K.R., Platania, S.P., 1991. Status and conservation of the Rio Grande silvery minnow, Hybognathus amarus. The Southwestern Naturalist, 225-232.

Betts, E.F., Jones, J.B., 2009. Impact of wildfire on stream nutrient chemistry and ecosystem metabolism in boreal forest catchments of interior Alaska. Arctic, Antarctic, and Alpine Research 41, 407-417.

Bisson, P.A., Rieman, B.E., Luce, C., Hessburg, P.F., Lee, D.C., Kershner, J.L., Reeves, G.H., Gresswell, R.E., 2003. Fire and aquatic ecosystems of the western USA: current knowledge and key questions. Forest Ecology and Management 178, 213-229.

Bixby, R.J., Cooper, S.D., Gresswell, R.E., Brown, L.E., Dahm, C.N., Dwire, K.A., 2015. Fire effects on aquatic ecosystems: an assessment of the current state of the science. Freshwater Science 34, 1340-1350.

Bonner, T.H., Wilde, G.R., 2000. Changes in the Canadian River fish assemblage associated with reservoir construction. Journal of Freshwater Ecology 15, 189-198.

Bonner, T.H., Wilde, G.R., 2002. Effects of turbidity on prey consumption by prairie stream fishes. Transactions of the American Fisheries Society 131, 1203-1208.

Breshears, D.D., Cobb, N.S., Rich, P.M., Price, K.P., Allen, C.D., Balice, R.G., Romme, W.H., Kastens, J.H., Floyd, M.L., Belnap, J., Anderson, J.J., Myers, O.B., Meyer, C.W., 2005. Regional vegetation die-off in response to global-change-type drought. Proceedings of the National Academy of Sciences of the United States of America 102, 15144-15148.

Brown, D.K., Echelle, A.A., Propst, D.L., Brooks, J.E., Fisher, W.L., 2001. Catastrophic wildfire and number of populations as factors influencing risk of extinction for Gila trout (Oncorhynchus gilae). Western North American Naturalist 61, 139–148.

Bunt, C.M., Katopodis, C., McKinley, R., 1999. Attraction and passage efficiency of white suckers and smallmouth bass by two Denil fishways. North American Journal of Fisheries Management 19, 793-803.

Cannon, S.H., Gartner, J.E., Wilson, R.C., Bowers, J.C., Laber, J.L., 2008. Storm rainfall conditions for floods and debris flows from recently burned areas in southwestern Colorado and southern California. Geomorphology 96, 250-269.

Canty, A., Ripley, B., 2016. boot: Bootstrap R (S-Plus) functions, R package version.

Corbett, B., Powles, P., 1986. Spawning and larva drift of sympatric walleyes and white suckers in an Ontario stream. Transactions of the American Fisheries Society 115, 41-46.

Crawford, C., Ellis, L., Molles, M., 1996. The Middle Rio Grande bosque: an endangered ecosystem. New Mexico Journal of Science 36, 276-299.

Cross, F., Moss, R., 1987. Historic changes in fish communities and aquatic habitats in plains streams of Kansas. Community and evolutionary ecology of North American stream fishes. University of Oklahoma Press, Norman, 155-165.

Dahm, C.N., Candelaria-Ley, R., Reale, C.S., Reale, J.K., Van Horn, D.J., 2015. Extreme water quality degradation following a catastrophic forest fire. Freshwater Biology 34, 14261442.

Dahm, C.N., Van Horn, D.J., Reale, J.K., Candelaria-Ley, R., Reale, C.S., 2013. Continuous water quality monitoring of the Rio Grande and Rio Chama. University of New Mexico, Report submitted to the U.S. Army Corps of Engineers, Albuquerque, NM.

Dudley, R.K., 2011. Field notes for Rio Grande Silvery Minnow population monitoring program results from december 2010 to october 2011.

Dudley, R.K., Platania, S.P., 2007. Flow regulation and fragmentation imperil pelagic-spawning riverine fishes. Ecological Applications 17, 2074-2086.

Dudley, R.K., Platania, S.P., White, G.C., 2016. Rio Grande Silvery Minnow population monitoring program results from February to December 2015. , Annual report to the Middle Rio Grande Endangered Species Collaborative Program and the US Bureau of Reclamation, Albuquerque, NM. .

Dunham, J.B., Young, M.K., Gresswell, R.E., Rieman, B.E., 2003. Effects of fire on fish populations: landscape perspectives on persistence of native fishes and nonnative fish invasions. Forest Ecology and Management 178, 183-196.

Earl, S.R., Blinn, D.W., 2003. Effects of wildfire ash on water chemistry and biota in South-Western USA streams. Freshwater Biology 48, 1015-1030.

Eder, S., Carlson, C.A., 1977. Food habits of carp and white suckers in the South Platte and St. Vrain rivers and Goosequill Pond, Weld County, Colorado. Transactions of the American Fisheries Society 106, 339-346.

Fisher, S.J., Willis, D.W., Olson, M.M., Krentz, S.C., 2002. Flathead chubs, Platygobio gracilis, in the upper Missouri River: the biology of a species at risk in an endangered habitat. Canadian Field-Naturalist 116, 26-41.

Fresquez, P.R., Jacobi, G.Z., 2012. Bioassessment of the Rio Grande Upstream and Downstream of Los Alamos National Laboratory, New Mexico, USA. Journal of Environmental Protection 3, 1596.

Gochis, D., Schumacher, R., Friedrich, K., Doesken, N., Kelsch, M., Sun, J., Ikeda, K., Lindsey, D., Wood, A., Dolan, B., Matrosov, S., Newman, A., Mahoney, K., Rutledge, S., Johnson, R., Kucera, P., Kennedy, P., Sempere-Torres, D., Steiner, M., Roberts, R., Wilson, J., Yu, W., Chandrasekar, V., Rasmussen, R., Anderson, A., Brown, B., 2015. The Great Colorado Flood of September 2013. Bulletin of the American Meteorological Society 96, 1461-1487.

Gresswell, R.E., 1999. Fire and aquatic ecosystems in forested biomes of North America. Transactions of the American Fisheries Society 128, 193-221.

Grimm, N.B., Staudinger, M.D., Staudt, A., Carter, S.L., Chapin, F.S., Kareiva, P., Ruckelshaus, M., Stein, B.A., 2013. Climate-change impacts on ecological systems: introduction to a US assessment. Frontiers in Ecology and the Environment 11, 456-464.

Heip, C.H., Herman, P.M., Soetaert, K., 1998. Indices of diversity and evenness. Oceanis 24, 61-88.

Hoagstrom, C.W., Remshardt, W.J., Smith, J.R., Brooks, J.E., 2010. Changing fish faunas in two reaches of the Rio Grande in the Albuquerque basin. Southwestern Naturalist 55, 78-88.

Klinger, S.A., Magnuson, J.J., Gallepp, G.W., 1982. Survival mechanisms of the central mudminnow (Umbra limi), fathead minnow (Pimephales promelas) and brook stickleback (Culaea inconstans) for low oxygen in winter. Environmental Biology of Fishes 7, 113-120.

Krabbenhoft, T.J., Platania, S.P., Turner, T.F., 2014. Interannual variation in reproductive phenology in a riverine fish assemblage: implications for predicting the effects of climate change and altered flow regimes. Freshwater Biology 59, 1744-1754.

Kunze, M.D., Stednick, J.D., 2006. Streamflow and suspended sediment yield following the 2000 Bobcat fire, Colorado. Hydrological Processes 20, 1661-1681.

Lagasse, P.F., 1980. An assessment of the response of the Rio Grande to dam construction-

Cochiti to Isleta, U. S., Army Corps of Engineers, Albuquerque, NM.

Littell, J.S., McKenzie, D., Peterson, D.L., Westerling, A.L., 2009. Climate and wildfire area burned in western US ecoprovinces, 1916–2003. Ecological Applications 19, 1003-1021.

Lobón-Cerviá, J., 1996. Response of a stream fish assemblage to a severe spate in northern Spain. Transactions of the American Fisheries Society 125, 913-919.

Lyon, J.P., O'Connor, J.P., 2008. Smoke on the water: can riverine fish populations recover following a catastrophic fire-related sediment slug? Austral Ecology 33, 794-806.

Lyons, J., Wang, L., Simonson, T.D., 1996. Development and validation of an index of biotic integrity for coldwater streams in Wisconsin. North American Journal of Fisheries Management 16, 241-256.

Magurran, A.E., 2013. Measuring biological diversity. Blackwell Publishing, Malden, MA.

Mast, M.A., Clow, D.W., 2008. Effects of 2003 wildfires on stream chemistry in Glacier National Park, Montana. Hydrological Processes 22, 5013-5023.

Mast, M.A., Murphy, S.F., Clow, D.W., Penn, C.A., Sexstone, G.A., 2016. Water-quality response to a high-elevation wildfire in the Colorado Front Range. Hydrological Processes 30, 1811-1823.

Miller, J.D., Safford, H., Crimmins, M., Thode, A., 2009. Quantitative evidence for increasing forest fire severity in the Sierra Nevada and southern Cascade Mountains, California and Nevada, USA. Ecosystems 12, 16-32.

Minckley, W.L., Meffe, G.K., 1987. Differential selection by flooding in stream-fish communities of the arid American Southwest. Community and evolutionary ecology of North American stream fishes. University of Oklahoma Press, Norman, 93-104.

Minshall, G.W., Brock, J.T., Varley, J.D., 1989. Wildfires and Yellowstone's stream ecosystem. BioScience 39, 707-715.

Molles, M.C., Crawford, C.S., Ellis, L.M., Valett, H.M., Dahm, C.N., 1998. Managed flooding for riparian ecosystem restoration. BioScience, 749-756.

Moody, J.A., Shakesby, R.A., Robichaud, P.R., Cannon, S.H., Martin, D.A., 2013. Current research issues related to post-wildfire runoff and erosion processes. Earth-Science Reviews 122, 10-37.

Moore, S.J., Anderholm, S.K., 2002. Spatial and temporal variations in streamflow, dissolved solids, nutrients, and suspended sediment in the Rio Grande Valley Study Unit, Colorado, New Mexico, and Texas, 1993-95. US Department of the Interior, US Geological Survey Albuquerque, New Mexico.

Mote, P.W., Li, S., Lettenmaier, D.P., Xiao, M., Engel, R., 2018. Dramatic declines in snowpack in the western US. npj Climate and Atmospheric Science 1, 2.

Murphy, S.F., McCleskey R. B., Writer, J.H., 2012. Effects of flow regime on stream turbidity and suspended solids after wildfire, Colorado Front Range. IAHS-AISH publication, 51-58.

Murphy, S.F., McCleskey, R.B., Martin, D.A., 2015. The role of precipitation type, intensity, and spatial distribution in source water quality after wildfire. Environmental Research Letters 10, 084007.

Nelson, J.S., Crossman, E.J., Espinosa-Perez, H., Findley, L.T., Gilbert, C.R., Lea, R.N., Williams, J.D., 2004. Common and scientific names of fishes from the United States, Canada and Mexico., Sixth ed. American Fisheries Society Special Publication, Bethesda, Maryland.

NMWQCC, 2000. Standards for interstate and intrastate surface waters, in: New Mexico Water Quality Control Commission (Ed.), 20.6.4, Santa fe, NM, p. 53.

Oksanen, J., Kindt, R., Legendre, P., O'Hara, B., Stevens, M.H.H., Oksanen, M.J., Suggests, M., 2007. The vegan package. Community ecology package 10, 631-637.

Olund, L.J., Cross, F.B., 1961. Geographic variation in the North American cyprinid fish, Hybopsis gracilis. University of Kansas.

Orem, C.A., Pelletier, J.D., 2015. Quantifying the time scale of elevated geomorphic response following wildfires using multi-temporal LiDAR data: An example from the Las Conchas fire, Jemez Mountains, New Mexico. Geomorphology 232, 224-238.

Ortiz, D., Lange, K.M., 1996. New Mexico water resources data water year 1995. U.S. Geological Survey Albuquerque, New Mexico, p. 644.

Ortiz, R.M., 2004. A river in transition: geomorphic and bed sediment response to Cochiti Dam on the Middle Rio Grande, Bernalillo to Albuquerque, New Mexico, Unpublished MS thesis, Department of Earth and Planetary Science. The University of New Mexico, Albuquerque, NM.

Pearsons, T.N., Li, H.W., Lamberti, G.A., 1992. Influence of habitat complexity on resistance to flooding and resilience of stream fish assemblages. Transactions of the American Fisheries society 121, 427-436.

Pease, A.A., Justine Davis, J., Edwards, M.S., Turner, T.F., 2006. Habitat and resource use by larval and juvenile fishes in an arid-land river (Rio Grande, New Mexico). Freshwater Biology 51, 475-486.

Pelletier, J.D., Orem, C.A., 2014. How do sediment yields from post-wildfire debris-laden flows depend on terrain slope, soil burn severity class, and drainage basin area? Insights from airborne LiDAR change detection. Earth Surface Processes and Landforms 39, 1822-1832.

Pielou, E.C., 1966. The measurement of diversity in different types of biological collections. Journal of theoretical biology 13, 131-144.

Pinson, A.O., Scissons, S.K., Brown, S.W., Walther, D.E., 2014. Post flood report: record rainfall and flooding events during September 2013 in New Mexico, Southeastern Colorado and Far West Texas, U.S. Army Corps of Engineers, Albuquerque District https://nmfma.clubexpress.com/docs.ashx?id=190302.

Platania, S.P., 1991. Fishes of the Rio Chama and Upper Rio Grande, New Mexico, with preliminary comments on their longitudinal distribution. Southwestern Naturalist 36, 186-193.

Pringle, C., 2003. What is hydrologic connectivity and why is it ecologically important? Hydrological Processes 17, 2685-2689.

Pringle, C.M., 1997. Exploring how disturbance is transmitted upstream: going against the flow. Journal of the north american Benthological society 16, 425-438.

Propst, D.L., 1999. Threatened and endangered fishes of New Mexico. New Mexico Department of Game and Fish Santa Fe, NM.

Propst, D.L., Stefferud, J.A., Turner, P.R., 1992. Conservation and status of Gila trout, *Oncorhynchus gilae*. The Southwestern Naturalist, 117-125.

Quist, M.C., Hubert, W.A., Rahel, F.J., 2004. Relations among Habitat Characteristics, Exotic Species, and Turbid-River Cyprinids in the Missouri River Drainage of Wyoming. Transactions of the American Fisheries Society 133, 727-742.

Radford, J., 2011. Fish kills blamed on forest fire soot in river, Corrales Comment, 1-24 ed.

Raffa, K.F., Aukema, B.H., Bentz, B.J., Carroll, A.L., Hicke, J.A., Turner, M.G., Romme, W.H., 2008. Cross-scale drivers of natural disturbances prone to anthropogenic amplification: the dynamics of bark beetle eruptions. Bioscience 58, 501-517.

Reale, J.K., Van Horn, D.J., Condon, K.E., Dahm, C.N., 2015. The effects of catastrophic wildfire on water quality along a river continuum Freshwater Science 34, 1426-1442.

Richard, G., Julien, P., 2003. Dam impacts on and restoration of an alluvial river-Rio Grande, New Mexico. International Journal of Sediment Research 18, 89-96.

Richard, G.A., 2001. Quantification and prediction of lateral channel adjustments downstream from Cochiti Dam, Rio Grande, NM. Colorado State University.

Rieman, B., Clayton, J., 1997a. Wildfire and native fish: issues of forest health and conservation of sensitive species. Fisheries 22, 6-15.

Rieman, B., Clayton, J., 1997b. Wildlife and native fish: Issues of forest health and conservation of sensitive species. Fisheries 22, 6-15.

Robb, T., Abrahams, M., 2003. Variation in tolerance to hypoxia in a predator and prey species: an ecological advantage of being small? Journal of Fish Biology 62, 1067-1081.

Rose, K.A., Cowan, J.H., Winemiller, K.O., Myers, R.A., Hilborn, R., 2001. Compensatory density dependence in fish populations: importance, controversy, understanding and prognosis. Fish and Fisheries 2, 293-327.

RStudio Team, 2015. RStudio: integrated development environment for R. RStudio Inc, , Boston, Massachusetts.

Ryan, S.E., Dwire, K.A., Dixon, M.K., 2011. Impacts of wildfire on runoff and sediment loads at Little Granite Creek, western Wyoming. Geomorphology 129, 113-130.

Shakesby, R.A., Doerr, S.H., 2006. Wildfire as a hydrological and geomorphological agent. Earth-Science Reviews 74, 269-307.

Shannon, C., Weaver, W., 1949. The Mathmatical Theory of Information. University of Illinois Press, Urbana, Illinois.

Sherson, L.R., Van Horn, D.J., Gomez, J.D., Shafer, B.M., Crossey, L.J., Dahm, C.N., 2015. Nutrient dynamics in a headwater stream: use of continuous water quality sensors to examine responses to wildfire and precipitation events. Hydrological Processes 29, 3193-3207.

Silins, U., Bladon, K.D., Kelly, E.N., Esch, E., Spence, J.R., Stone, M., Emelko, M.B., Boon, S., Wagner, M.J., Williams, C.H.S., Tichkowsky, I., 2014. Five-year legacy of wildfire and

salvage logging impacts on nutrient runoff and aquatic plant, invertebrate, and fish productivity. Ecohydrology 7, 1508-1523.

Stewart, I.T., Cayan, D.R., Dettinger, M.D., 2004. Changes in snowmelt runoff timing in western North America under a 'business as usual' climate change scenario. Climatic Change 62, 217-232.

Sublette, J., Hatch, M., Sublette, M., 1990. The fishes of New Mexico. University of New Mexico Press.

SWCA, 2014. Physical and biological assessment of the effects of sediment discharge from the Buckman Direct Diversion Project year 5 report, Prepared for: Buckman Direct Diversion Board, City and County of Santa Fe, New Mexico, Albuquerque, New Mexico.

Thompson, A.R., Petty, J.T., Grossman, G.D., 2001. Multi-scale effects of resource patchiness on foraging behaviour and habitat use by longnose dace, Rhinichthys cataractae. Freshwater Biology 46, 145-160.

Tillery, A.C., Haas, J.R., 2016. Potential postwildfire debris-flow hazards—A prewildfire evaluation for the Jemez Mountains, north-central New Mexico. U.S. Geological Survey Scientific Investigations Report p. 23.

Trenberth, K.E., Fasullo, J.T., Shepherd, T.G., 2015. Attribution of climate extreme events. Nature Climate Change 5, 725-730.

Turner, T.F., Krabbenhoft, T.J., Burdett, A.S., 2010. Reproductive phenology and fish community structure in an arid-land river system, in: Gido, K.B., Jackson, D.A. (Eds.), Community ecology of stream fishes: concepts, approaches, and techniques. American Fisheries Society Symposium, Bethesda, Maryland, pp. 427-446.

Twomey, K.A., Williamson, K.L., Nelson, P.C., 1984. Habitat suitability index models and instream flow suitability curves: white sucker. US Fish and Wildlife Service.

USACE, 2012. Las Conchas fire emergency measures after action report, U.S. Army Corps of Engineers, Albuquerque District.

USDA Forest Service, 2011. Las Conchas Fire Burn Severity Map, US Department of Agriculture Forest Service, Santa Fe National Forest: Santa Fe, NM.

Van Horn, D.J., Reale, J.K., Clark, A.L., Reale, C.S., O'Brien, E., 2014. Continuous water quality monitoring of the Rio Grande and Rio Chama, Submitted to: U.S. Army Corps of Engineers, Albuquerque District.

van Mantgem, P.J., Nesmith, J.C.B., Keifer, M., Knapp, E.E., Flint, A., Flint, L., 2013. Climatic stress increases forest fire severity across the western United States. Ecology Letters 16, 1151-1156.

Wagner, R.J., Mattraw, H.C., Ritz, G.F., Smith, B.A., 2006. Guidelines and standard procedures for continuous water-quality monitors: Site selection, field operation, calibration, record computation, and reporting, 1–D3 ed, U.S. Department of the Interior, U.S. Geological Survey, Reston Virginia, p. 51 + attachments.

Walterscheid, J., 2015. September 2013 Storm and Flood Assessment Report. Los Alamos National Laboratory, Los Alamos, NM.

Westerling, A.L., 2016. Increasing western US forest wildfire activity: sensitivity to changes in the timing of spring. Philosophical Transactions of the Royal Society B 371, 10.

Westerling, A.L., Gershunov, A., Brown, T.J., Cayan, D.R., Dettinger, M.D., 2003. Climate and wildfire in the western United States. Bulletin of the American Meteorological Society 84, 595.

Westerling, A.L., Hidalgo, H.G., Cayan, D.R., Swetnam, T.W., 2006. Warming and earlier spring increase western US forest wildfire activity. Science 313, 940-943.

Whitney, J.E., Gido, K.B., Hedden, S.C., Macpherson, G., Pilger, T.J., Propst, D.L., Turner, T.F., 2017. Identifying the source population of fish re-colonizing an arid-land stream following wildfire-induced extirpation using otolith microchemistry. Hydrobiologia 797, 29-45.

Whitney, J.E., Gido, K.B., Pilger, T.J., Propst, D.L., Turner, T.F., 2015a. Consecutive wildfires affect stream biota in cold- and warmwater dryland river networks. Freshwater Science 34, 000.

Whitney, J.E., Gido, K.B., Pilger, T.J., Propst, D.L., Turner, T.F., 2015b. Metapopulation analysis indicates native and non-native fishes respond differently to effects of wildfire on desert streams. Ecology of Freshwater Fish.

Williams, A.P., Abatzoglou, J.T., 2016. Recent Advances and Remaining Uncertainties in Resolving Past and Future Climate Effects on Global Fire Activity. Current Climate Change Reports 2, 1-14.

Williams, A.P., Allen, C.D., Millar, C.I., Swetnam, T.W., Michaelsen, J., Still, C.J., Leavitt, S.W., 2010. Forest responses to increasing aridity and warmth in the southwestern United States. Proceedings of the National Academy of Sciences of the United States of America 107, 21289-21294.

Wolf Engineering, 2014. Field survey cross sections and sediment delta Cochiti Lake range lines, Submitted to U.S. Army Corps of Engineers, Albuquerque District under Contract No. W912PP-09-D-0010.

Epilogue

Since 2006, the U.S. Army Corps of Engineers (USACE) has funded the U.S. Geological Survey (USGS) and the University of New Mexico (UNM) to collect continuous water quality (i.e., temperature, specific conductance (SC), dissolved oxygen (DO), pH and turbidity) data using multi-parameter sondes at five locations on the Rio Grande to assess temporal and spatial trends. During the same time-period, the Valle Caldera National Preserve (VCNP) began deploying sondes within the headwaters of the Jemez Mountains. Recognizing the importance of collecting high-frequency water quality data, a proposal was submitted to the New Mexico Experimental Program to Stimulate Competitive Research (NM EPSCoR) to develop and deploy nutrient and water quality sensors for the monitoring of stream waters in high altitude environments within the VCNP to investigate controls on water chemistry in a changing climate. This proposal was funded in 2009 and the instruments were lab tested in 2010 and field deployed in 2011.

Fortuitously, the majority of this instrumentation was in place prior to the summer of 2011 when the Las Conchas fire ignited and became the largest wildfire in New Mexico history. Recognizing the potential post-fire impacts on water quality, USACE and UNM added three additional sondes upstream of Cochiti Dam on the Rio Grande and Rio Chama to more fully assess water quality conditions within the watershed upstream and downstream of the large burn scar. These datasets provided the opportunity to assess the impacts of a major catastrophic wildfire on water quality in montane and aridland rivers with state-of-the art measurements and excellent background data along a river continuum. Combining these datasets with long-term meteorological and fish monitoring data, biological responses (i.e., whole-stream metabolism and fish community) were also evaluated prior to and following the Las Conchas fire.

In **Chapter 1,** *The effects of catastrophic wildfire on water quality along a river continuum*, the goals of the study were to; 1) evaluate water quality (turbidity, SC, and DO) before and immediately following the Las Conchas fire along an impacted river continuum (2nd through 7th order streams and rivers), and 2) assess the water quality

(turbidity, SC and DO) of a 3rd- and a 7th-order stream in a single watershed for five monsoon seasons before, during, and after the wildfire. This chapter documents the importance of streamflow pathways, geomorphology, physiochemical properties and biogeochemical processes in mediating water quality along a river continuum impacted by a major wildfire. Longer-term effects in a 3rd stream and 7th order river provide quantitative information on the initial and sustained water quality impacts of a major wildfire on streams and rivers affected by the burn scars for multiple years following disturbance. These findings highlight the need to collect water-quality data at time scales that effectively capture the ecohydrological dynamics of the watershed following a major wildfire. This chapter was published in *Freshwater Science*, as part of a special series on fire ecology.

In **Chapter 2**, *Differential responses of paired catchments to catastrophic wildfire: A multi-year study of water quality and whole-stream metabolism throughout the growing season,* the goals of the study were to; 1) assess water quality, gross primary productivity (GPP), and ecosystem respiration (ER), during the growing season for multiple years prior to the Las Conchas fire in two, nearly identical and paired headwater streams in the Jemez Mountains, 2) determine the immediate (year one), shorter-term (years two to four) and longer-term (years five and six) impacts of the wildfire on water quality and whole-stream metabolism, and 3) identify mechanisms that influence in-stream metabolic processes during pre- and post-fire conditions. Immediately following the wildfire, turbidity and specific conductance values increased substantially, and measures of whole stream metabolism declined in each of the two streams. A differential response between the two streams was observed in the shorter-term. One stream, that has tight hydrologic connections to the landscape, experienced persistently elevated turbidity and suppressed GPP and ER, likely due to light limitation. In contrast, the other stream had much lower turbidity levels and elevated GPP and ER, likely due to fertilization of stream water by nutrient-rich fire debris. By the 6th year after the fire, water quality and metabolism values returned to near pre-fire levels in both streams. This study is the first multi-year water quality and whole-stream metabolism study linked to a major wildfire. It emphasizes the need for long-term, high-frequency data, both pre- and post-fire, to accurately assess the impacts of wildfire on

ecosystem processes in aquatic environments. This chapter was submitted to *Ecosystems*, and the paper is currently undergoing peer review.

In **Chapter 3**, *The effects of water quality degradation from wildfire on downstream fish communities in an aridland river,* the goals were to 1) assess the immediate (year one) and short-term (years two to five) fish community and water quality responses at two sites on the Rio Grande (i.e., 7th order) downstream (i.e., > 20 km) of the Las Conchas fire, and 2) evaluate the effects of an extreme flood event (occurring in year three after the fire) on the fish community and water quality in a post-fire environment. During the first three years following the fire, large DO sags, but no major flood events, were documented at both sites. A differential between-site response in total abundance and fish community variables was observed. The community at the downstream site appeared to be generally unimpacted by effects from the fire. In contrast, declines in total abundance, diversity and evenness were observed post-fire in the upstream community. Following the major flood event in September of 2013, total and species-specific abundance and fish community response variables remained unchanged at the downstream site, while reductions in abundance, diversity, and evenness were observed at the upstream site. The differential post-fire and post-flood response at the two sites with similar community composition and flow regime can be attributed to the proximity and quantity of fire-impacted watersheds upstream. This study adds to the very few studies that have assessed the effects of wildfire on non-salmonid fish communities in larger rivers (≥ 5th order) downstream (i.e. ≥ 10 river-km) from burn scars. This chapter will be submitted to the *Journal of Arid Environments*.

To build upon the findings presented in this dissertation, future research should focus on topics that further improve our understanding of the effects of wildfire on aquatic ecosystems. Post-wildfire research on riverine water quality and whole-stream metabolism, including this dissertation, has focused on wildfires originating in mountainous coniferous-forested catchments in western North America. The development of long-term and high-frequency water quality networks in streams and rivers in other biomes (e.g., cerrados, savannas, rainforests, boreal forests, and arctic tundra) within fire-prone geographical regions (e.g., South America, North America,

Africa, Asia, and Australia) would allow for inter-biome comparisons. It would also allow for a comprehensive global assessment of the risks to water quality and ecosystem processes in fire-prone biomes at a global scale. To improve our understanding of how fish communities respond to poor water quality conditions post-fire, a series of mesocosm experiments could be conducted that emulate the abrupt, frequent and severe dissolved oxygen sags and large increases in suspended sediment loads observed following severe wildfires. These data will allow water resource managers to evaluate the growth and survival of young-of-year and adult fish species. Such studies would be a significant step forward in testing the impacts of fire on fish communities in a more realistic manner, as compared to the commonly used standard acute toxicity tests (ASTM 2007).

Water scarcity, water quality impairment and river biodiversity have received considerable attention recently as global threats to freshwater quality from human impacts (Jackson et al. 2001, Vörösmarty et al. 2010). We must include catastrophic wildfires as potential global threats to freshwater ecosystems and another ecological risk that must be evaluated in a changing climate (IPCC 2014). This is particularly of concern as the size and duration of wildfires and the length of the wildfire season increases (Flannigan et al. 2009, Flannigan et al. 2013).

Overall, the research in this dissertation highlights the importance of long-term ecological data collection using advanced instrumentation that can be used to evaluate the effects of a changing climate and climate-mediated disturbances on water resources. Secondly, these studies emphasize the need to collect water quality and biological data at temporal and spatial scales that more effectively capture the hydrology and water quality dynamics of landscape-scale disturbances that are becoming more common and more destructive with climate change and growing human impingement on forested lands. Thirdly, this research highlights the importance of evaluating streamflow pathways, geomorphology, physiochemical properties with biogeochemical processes, and watershed-specific hydrologic connections within their landscapes prior to and following landscape-scale disturbance.

References

ASTM. 2007. Standard Guide for Conducting Acute Toxicity Tests on Test Materials with Fishes, Macroinvertebrates, and Amphibians. West Conshohocken, PA, United States. DOI: 0.1520/E0729-96. URL: www. atsm. org.

Flannigan, M., Cantin, A. S., de Groot, W. J., Wotton, M., Newbery, A., and Gowman, L. M. 2013. Global wildland fire season severity in the 21st century. Forest Ecology and Management 294:54-61.

Flannigan, M. D., Krawchuk, M. A., de Groot, W. J., Wotton, B. M., and Gowman, L. M. 2009. Implications of changing climate for global wildland fire. International journal of wildland fire 18:483-507.

IPCC 2014. Chapter 5: Ecosystems and their goods and services. Working Group II. Impacts, adaptation and vulnerability. Cambridge University Press New York, NY.

Jackson, R. B., Carpenter, S. R., Dahm, C. N., McKnight, D. M., Naiman, R. J., Postel, S. L., and Running, S. W. 2001. Water in a changing world. Ecological applications 11:1027-1045.

Vörösmarty, C. J., McIntyre, P. B., Gessner, M. O., Dudgeon, D., Prusevich, A., Green, P., Glidden, S., Bunn, S. E., Sullivan, C. A., and Liermann, C. R. 2010. Global threats to human water security and river biodiversity. Nature 467:555.